# SODIUM ENTRY INTO SINGLE STRIATED MUSCLE FIBERS

by

Malcolm Leslie Brigden
B.Sc., University of McGill, 1968

A Thesis Submitted in Partial Fulfilment of the
Requirements for the Degree of

MASTER OF SCIENCE
in the Department of
ANATOMY

We accept this thesis as conforming to
the standard required from candidates
for the degree of Master of Science.

THE UNIVERSITY OF BRITISH COLUMBIA
October, 1969

In presenting this thesis in partial fulfilment of the requirements for an advanced degree at the University of British Columbia, I agree that the Library shall make it freely available for reference and study. I further agree tha permission for extensive copying of this thesis for scholarly purposes may be granted by the Head of my Department or by his representatives. It is understood that copying or publication of this thesis for financial gain shall not be allowed without my written permission.

Department of Anatomy

The University of British Columbia
Vancouver 8, Canada

Date Oct. 27th.

# ABSTRACT

A review of the literature on sodium distribution in muscle has been presented including the evidence for heterogeneous distribution and the possible morphological sites of localization of this sodium. Special attention was paid to influx studies on crustacean muscle. The review reveals that while there is good evidence for a heterogeneous distribution, the morphological sites and their associated concentrations of sodium remain obscure.

The experiments described in this thesis were performed on muscle fibers of the giant barnacle Balanus nubilis. Single muscle fibers of Balanus are a unique biological preparation due to their large size and ease of dissection. The major disadvantage to single fiber Balanus preparations is the extent of the extracellular space or cleft system. This cleft system contains approximately half the total fiber sodium in 6% of the fiber volume.

The purpose of these experiments was to gain a picture of $^{22}Na^{+}$ entry into these single striated muscle fibers with special emphasis on the role of the extracellular space.

A histological study revealed that the cleft system was more extensive than had been reported. From measurements made on light and electron microscope pictures it was concluded that no part of Balanus myoplasm was more than 1 - 2μ from a 0.02μ patent cleft. This study gave a picture

of the morphological pathway for $^{22}Na^{+}$ diffusion in the extracellular space.

Radioautography and radio isotope counting were two techniques used to examine $^{22}Na^{+}$ exchange between the extracellular space and the myoplasm.

Since the extracellular space had a sodium concentration of 10 times the myoplasm, the cleft system should be adequately visualized by radioautography. However, the section thickness (15μ) and the high maximum energy of $^{22}Na^{+}$ (0.540MEV) limited the resolution of the radioautograms to 15 - 17.5μ. This resolution coupled with the extent of the cleft system prevented consistent radioautographic visualization of discrete clefts.

Radioautographic analysis of fibers with minimal exposure (0.5 minutes) to $^{22}Na^{+}$ revealed a concentration gradient which could be used to define the extracellular pathway and its diffusion coefficient for $Na^{+}$. The radius of the fiber cross section was found to be a reasonable approximation of the length of the pathway and the diffusion of $^{22}Na^{+}$ in the extracellular space along the pathway was as rapid as the self diffusion of $^{22}Na^{+}$ in dilute solution.

A comparison of fibers that had spent 1.5 minutes in the $^{22}Na^{+}$ bath with similar fibers that had a 0.5 minute sucrose rinse revealed that the 0.5 minute sucrose rinse removed half of the $^{22}Na^{+}$ from the extracellular space. The 1.5 minute fibers and all fibers examined after longer periods in the $^{22}Na^{+}$ bath revealed a homogeneous grain

distribution in radioautograms. This data conflicted with the rate of $^{22}Na^{+}$ entry predicted by the 0.5 minute fibers. Inappropriate agitation of the 1.5 minute fibers was responsible for the lack of agreement.

A further radioautographic study of $^{22}Na^{+}$ influx with experimental times 5, 20, 60 and 180 minutes was analyzed quantitatively. To substantiate this radioautographic study an influx experiment was done with times 5, 10, 20, 40 and 90 minutes.

Each study demonstrated two compartments. An initial rapidly exchanging compartment with a half time of 6 - 10 minutes was identified as the extracellular space. The extracellular space contained approximately half the fiber sodium. Both studies detected a myoplasmic influx compartment which was still exchanging when the experiments were terminated. The calculated rate constant for myoplasmic exchange ($5.6 \times 10^{-3}$/minute) was in good agreement with the value of Allen and Hinke.

In conclusion, a useful technique for the radioautography of soluble substances was developed. Both a morphological and a physiological picture of the pathway for $^{22}Na^{+}$ diffusion in the extracellular space was developed. The size and half time of loading of the extracellular space was verified. The myoplasmic influx component was identified by two methods.

From these studies emerges a more comprehensive picture of the extracellular space as a pathway for diffusion

in Balanus muscle. The failure to consider this compartment in microinjection or flux studies may result in ambiguous conclusions.

# TABLE OF CONTENTS

## INTRODUCTION



## RESULTS AND DISCUSSION



## CONCLUSION

# LIST OF TABLES

# LIST OF ILLUSTRATIONS

# LIST OF FIGURES

Acknowledgements

I would like to thank my thesis supervisor, Dr. Hinke, for advice, encouragement and unlimited freedom in the pursuit of this project. In addition to arranging my stay in Vancouver, Dr. and Mrs. Friedman did everything within their power to make this research a meaningful and rewarding experience. Considerable aid in the development of the technique for soluble radioautography came from Dr. Hadfield. Drs. Webber, Spira and Slonecker provided thoughtful advice and criticism. Technical assistance was generously given by Mr. Cox and Mrs. Blackbourn. Little would have been accomplished without the assistance of Mr. Crossen in procuring supplies and apparatus. My typist, Mrs. Peaker, kindly prepared the manuscript in my absence.

# CHAPTER I

## GENERAL INTRODUCTION

The striated muscle fiber of the giant barnacle has become a valuable in vitro test object for those studies in muscle physiology and biophysics which require electrode penetrations into and chemical analysis of single fibers. Its main advantage is its unusual size (about 1 mm diameter and 3 - 4 cm long).

A major disadvantage to multifiber preparations has been the relatively large extracellular space (15 - 20%). Unfortunately this problem must still be considered with single fiber preparations. A single fiber from Balanus nubilis has an extensive cleft system which makes up about 6% of the fiber volume. This cleft system cannot be ignored when one is considering $Na^+$ or $Cl^-$ ion distribution in the muscle fiber. For example, when a single fiber is bathed in barnacle Ringer solution, containing 450 mM/L $Na^+$ and 540 mM/L $Cl^-$, this cleft system should contain about half of the total fiber sodium. Clearly the extracellular compartment can be a complicating factor in the study of ion movements and distribution in the fiber interior.

Morphologically the cleft system is profuse and branches in three dimensions through the muscle interior. Probably no part of the myoplasm is more than a few microns ($\mu$) from a branch cleft and the extracellular space.

The purpose of these experiments was to re-examine the question of $Na^+$ ion exchange between the myoplasm and the exterior of the fiber in the light of recent understanding of the cleft system as a pathway for diffusion.

In this study attention was focused on the $Na^+$ ion. The isotope $^{22}Na^+$ was used to label the pool of $Na^+$ in the bath. Penetration of a single fiber by $^{22}Na^+$ was followed by the technique of radioautography in order to attempt some correlation of $^{22}Na^+$ distribution with the morphology of the fiber cross section. In addition, the standard $^{22}Na^+$ uptake experiment was performed with emphasis on short time intervals.

The main complication in using radioautography to study the distribution of soluble ions such as sodium is translocation of the ion during the experimental procedures. However, radioautography does permit identification of a compartment which may concentrate an ion by localizing the isotope in relation to the morphology of the muscle fiber. This is valid if the distance between areas of isotope localization is not smaller than the resolution of the radioautographic technique.

Even if precise morphological localization is impossible, radioautography at short time intervals can give a visual picture of the extent of isotope penetration to the interior of the fiber. Alternatively at longer intervals, radioautograms may be analyzed quantitatively provided extreme care is taken to assure uniform processing. In this context

radioautograms can show rate of isotope entry into the fiber and therefore provide an alternative method of influx analysis. These same radioautograms can also reveal whether the entry is homogeneous.

An influx study shows the rate of isotope entry into muscle fibers. Complex or multicompartmental flux kinetics may be demonstrated. The size, rate constant, and half loading time of the compartments represented can be calculated. However, the morphological location of these compartments cannot be demonstrated.

# CHAPTER II

## LITERATURE REVIEW

### Evidence For a Heterogeneous Distribution of Sodium in Muscle

Several different experimental approaches have indicated that there exists a heterogeneous distribution of sodium in muscle. These include microelectrode studies, NMR analysis and influx-efflux data.

A comparison of values obtained by microelectrode for the activity of sodium in myoplasm with the total sodium content of the muscle fiber gives activity values lower than those of sodium solutions of equal strength. This indicates a heterogeneous distribution of intracellular sodium in muscle. In Homarus muscle, Hinke (1) found a sodium activity of 0.012 to 0.016 with a sodium concentration of 0.055 moles/kg $H_2O$. Carcinus muscle had an activity coefficient of 0.0135 and sodium concentration of 0.0516 moles/kg $H_2O$.

McLaughlin and Hinke (2) reported that a typical single muscle fiber of the giant barnacle Balanus nubilis had a sodium concentration of 0.070 moles/kg $H_2O$. The activity recorded by myoplasmic electrode for such fibers was 0.007 moles/kg $H_2O$. Lev (3) calculated the activity coefficient for $Na^+$ in the myoplasm of frog muscle to be 0.190 to 0.197. This suggested 70% of the frog muscle sodium was unavailable to

the microelectrode. Robertson (4) obtained evidence for a heterogeneous intracellular sodium distribution in lobster muscle by comparing the sodium concentration in intact muscle with the sodium concentration in fluid extracted from the muscle by a tissue press. He found 82% of the intracellular sodium was not extruded by the tissue press.

Using nuclear magnetic resonance (NMR), Cope (5) observed 72% of the muscle sodium did not contribute to the sodium spectrum. He concluded that 60% to 80% of the muscle sodium existed in a complexed state, or at least in some state other than in free solution.

Conway (6) first suggested muscle sodium was divided into several compartments as a result of influx-efflux studies on amphibian muscle. Conway and Cary (7) using the frog sartorius preparation, examined the initial rapid exchanges of sodium and potassium. They postulated a special fiber compartment larger than the extracellular space, to explain the time course of sodium loss from muscles placed in glucose solutions. The volume of the space was estimated to be 10% of fiber volume, while its sodium concentration was estimated to be 0.008 moles/kg $H_2O$.

Harris (8) after a study of the distribution of chloride ion in frog muscle postulated the existence of a small intra-fiber compartment. The compartment would be accessible to all extracellular ions and contain 15% of total cell water (12% of all volume). Such a compartment was necessary if the Donnan equilibrium was to hold for chloride ions.

Dunham and Gainer (9) recently found a non-exchangeable sodium compartment in lobster muscle. This compartment had a sodium concentration of 0.035 moles/kg $H_2O$, compared to a total myoplasmic sodium concentration of 0.090 moles/kg $H_2O$. The chloride ion was compartmentalized in a fashion similar to sodium both in terms of the kinetics of efflux and of the concentration involved.

## Location of Compartmentalized Sodium

A significant fraction of the total sodium appears complexed or compartmentalized. Where is this sodium located? Morphological studies have revealed a complex internal structure for muscle. Single muscle fibers have a number of compartments that are fluid filled, and some may be enclosed by membranes. These compartments include extracellular space, myoplasm, sarcoplasmic reticulum, nuclei and mitochondria.

The exact extent and volume of the extracellular space is under considerable debate. Numerous morphological studies have shown that transverse tubules probably open to the extracellular space by contacting the sarcolemma (10,11). Alternative evidence that the transverse tubules are open to the fiber surface is drawn from attempts to explain the high membrane capacitance of muscle fiber compared to nerve cell. Falk and Flatt (12) first suggested a major part of the capacitance of a muscle fiber resides in the tubular

membrane system. This tubular capacitance is in parallel with the surface capacitance. This requires the tubular and surface membranes to be connected in some way. Eisenberg and Gage (13) developed a glycerol soaking technique for disrupting the transverse tubular system. These authors found the muscle fiber capacitance decreased to the value predicted for a simple tube.

Zadunaisky (14) demonstrated high sodium concentration within the transverse tubules by a sodium pyroantimonate precipitation technique. This was consistent with connection of the transverse tubules to the extracellular space. However, Peachey (15) has shown this space probably occupies only 0.3% of fiber volume in frog sartorius. Thus, the potential of the transverse tubule for sodium storage is limited.

Peachey (15) concluded the sarcoplasmic reticulum represented about 13% of cell volume of which the terminal cisternae comprised 4%. Birks (16) had calculated that the sarcoplasmic reticulum occupied 10% of cell volume since the terminal cisternae contain largely solid material. Peachey (15) considered the serrated appearance of the junction between the transverse tubule and terminal cisternae to represent a low resistance path. Birks (17) took the more extreme position that an actual communication existed between transverse tubule and the terminal cisternae via microtubules.

Recently, Birks (16) has demonstrated that the sarcoplasmic reticulum changes in volume in hyper- and

hypotonic sucrose solutions. These changes in volume were linearly related with a negative slope to the reciprocal of the osmotic pressure. To explain these changes, Birks reaffirmed his contention that the sarcoplasmic reticulum is extracellular via its connection to the transverse tubules. This connection of the sarcoplasmic reticulum to the transverse tubules allows sucrose penetration. Harris (8) had considered the connection of the sarcoplasmic reticulum to the transverse tubule as possibly patent because of the close agreement of the volume of the sarcoplasmic reticulum (10% fiber volume) to the theoretical extracellular space he had postulated (12% of fiber volume).

A sarcoplasmic reticulum communicating with the extracellular fluid should have a sodium concentration much higher than the myoplasm. Zadunaisky (14) was unable to show sodium precipitation in the sarcoplasmic reticulum with his technique. However, Herlihy, Conway and Harrington (18) using a different muscle fixation procedure were successful. The muscle fibers used by Zadunaisky may have been inadequately penetrated by the pyroantimonate used for sodium precipitation.

Keynes and Steinhardt (19) have recently proposed the sarcoplasmic reticulum to be a sodium-filled membrane-bound compartment. Cope (20) has postulated non-complexed sodium in the sarcoplasmic reticulum since freezable intracellular water in single cells has been demonstrated to be located in the region of the sarcoplasmic reticulum.

These differences in water structure might reflect differences in sodium coupling.

Perhaps the most telling argument against the sarcoplasmic reticulum as a sodium reservoir is the known magnitude of its affinity for calcium. Hasselbach (21) has shown the sarcoplasmic reticulum to have a calcium transporting mechanism more efficient than any other known ion transport system. It seems unlikely that high concentrations of different cations would be sequestered in the same system.

Further evidence against the sarcoplasmic reticulum as a non-complexed sodium compartment comes from the experiments of Hinke (22) dealing with the effect of hypertonic and hypotonic solutions on single muscle fibers. These experiments indicated there was only one osmotically active compartment in single muscle fibers. This compartment was identified as the myoplasm. A sodium rich sarcoplasmic reticulum would have been detected as a second osmotically active compartment in these experiments.

The myoplasm may be the morphological site responsible for the heterogeneous distribution of sodium. Since approximately 80% of the solid material of the myoplasm is protein, it is reasonable to examine the relation of sodium to the contractile proteins. It is known that the alkali metal cations like sodium can form ion pairs with charged groups on macromolecules. Such sodium is said to be "bound".

Szent-Györgyi (23) was the first to demonstrate that extracted myosin but not actin "bound" sodium and potassium. This "binding" ability of myosin was labile and appeared to depend on the secondary and tertiary structure of the myosin molecule. More recently Lewis and Saroff (24) found extracted myosin "bound" sodium preferentially over potassium.

Fenn (25) used glycerinated fibers to examine the binding of sodium and potassium. These fibers have the contractile proteins spatially fixed in a manner similar to the living muscle fiber. The fibers "bound" sodium preferentially over potassium.

McLaughlin and Hinke (26) have pointed out that the data of Lewis and Saroff and of Fenn predict that only as much sodium would be "bound" to myosin as is free in the myoplasm (20% total fiber sodium). The rest of the fiber sodium which results in the heterogeneous distribution could be located elsewhere.

A possible explanation is that the spatial fixation of the myosin molecule in the intact fiber greatly increases its sodium "binding" capacity. This theory is supported by Szent-Györgyi's observation of the labile nature of myosin binding. It is also known that the binding capacity of ion exchange resins is enhanced when the degree of cross-linking is increased.

Nuclei remain a possible site for sodium "binding". Although evidence indicates nuclei can concentrate potassium

in preference to sodium (27), it has also been reported they contain sodium at three times the concentration of the cytoplasm (28). A similar situation exists for mitochondria. Although they have been shown to preferentially concentrate potassium over sodium (29), there is also evidence of greater internal sodium concentration in mitochondria than in the surrounding myoplasm (30).

## State of Sodium in Balanus

What is the state of sodium in Balanus and similar crustaceans? From recent influx and efflux studies on muscle fibers of Balanus nubilis, Allen and Hinke (31) found that intracellular sodium in Balanus was easily divisible into two compartments. A rapidly exchanging compartment was detectable in both influx and efflux studies and identified as free myoplasmic sodium. A slowly exchanging compartment was evident only in influx experiments. All influx experiments were corrected for the extracellular space which in Balanus accounts for over half of the total fiber sodium. The size of the rapidly exchanging compartment was about 60% of total intracellular sodium. This value agreed well with the sodium electrode myoplasmic activity measurement. The second compartment represented 40% of intracellular (20% of total fiber) sodium and exchanged very slowly. This indicated binding or compartmentalization of some sort.

In previous studies, McLaughlin and Hinke (26) estimated the average sodium concentration of a single fiber to be 0.070 moles/kg $H_2O$. The free concentration of the myoplasm was 0.010 moles/kg $H_2O$ (14% total fiber sodium) while the extracellular space accounted for 0.030 moles/kg $H_2O$ (43% total fiber sodium). The sodium content of the extracellular space was contained in 6 - 7% of total fiber volume. This left 0.030 moles/kg $H_2O$ (43% total fiber sodium) either compartmentalized in organelles in the myoplasm or "bound" to the contractile proteins. The size of this compartment as deduced by microelectrode studies (43% total fiber sodium) is thus twice as large as the slowly moving influx compartment of Allen and Hinke (31) (20% of total fiber sodium).

Thus, the state of sodium in Balanus is similar to muscle in general. There exists good evidence from flux studies and microelectrode measurements of a heterogeneous sodium distribution in Balanus. A certain fraction of the total fiber sodium appears "bound" or compartmentalized. Where in the muscle fiber is this sodium located?

In Balanus, mitochondria and nuclei occupy only a small portion of the fiber volume. The sarcoplasmic reticulum is not as extensive as in the frog. However, the sarcoplasmic reticulum would have to possess only half the volume of the extracellular space (3 - 4% of total fiber volume) to account for 20% of the total fiber sodium, (the compartment of Allen and Hinke or one half the

compartment of Hinke.) This assumes the sodium concentration of the sarcoplasmic reticulum is similar to the concentration of the extracellular space. These volume requirements (3 - 4% of the total fiber volume) are not incompatible with the electron microscope picture of the sarcoplasmic reticulum of Balanus.

In an earlier section of this review, arguments against the sarcoplasmic reticulum as a region of high sodium concentration were summarized. Thus, it is doubtful that this compartment is wholly responsible for the heterogeneous sodium distribution observed in Balanus. However, the volume of the sarcoplasmic reticulum would be adequate to explain sodium compartmentalization.

Hinke and McLaughlin (32) have postulated that the fraction of sodium in Balanus fibers inaccessible to the microelectrode is "bound" to the contractile proteins. In muscles heated to 40°C the mean sodium activity increased 130%. This was accompanied by an irreversible shortening of the fiber. The authors interpreted the increase in sodium activity as the release of "bound" sodium from binding sites on myosin. In a subsequent paper McLaughlin and Hinke (26) demonstrated a decrease in optical density of single muscle fibers when these fibers were placed in sodium free sucrose Ringers solution. It was postulated that "bound" sodium was released from myosin. The authors' final conclusion was that a minimum of 20% of fiber sodium was bound to myosin. They believed that spatial arrangements

of myosin in vivo resulted in myosin being the major sodium binding site.

Other pertinent studies are those of Shaw (33) on Carcinus muscle. The morphological organization of these muscle fibers closely resembles those of Balanus. Shaw demonstrated the uptake of $^{24}Na^{+}$ by Carcinus muscle to be exceptionally rapid. Approximately 70% of the muscle sodium (0.035 moles/kg $H_2O$) had exchanged with $^{24}Na^{+}$ from the blood in three minutes. He suggested a non-uniform sodium distribution through the muscle fibers with the bulk of the sodium in a special region probably extra-sarcoplasmic in nature. The sodium concentration of this special region would mirror that of the blood. The relatively small volume of the region would account for the fact that measurement of sodium concentration on the basis of the fiber as a whole leads to a value much lower than that of blood. The same is true for the extracellular space of Balanus; half the total fiber sodium is in the extracellular space and its concentration mirrors that of the bathing solution.

In further experiments, Shaw (33) immersed Carcinus muscles in bathing media where sodium was partially replaced by dextrose. The muscles lost half their sodium very rapidly probably from the extrasarcoplasmic regions. The myoplasmic sodium concentration fell from 0.060 - 0.080 moles/kg $H_2O$ to 0.020 - 0.023 moles/kg $H_2O$ in ten minutes in a bath having a sodium concentration of 0.027 moles/kg $H_2O$.

Caldwell (34) has observed that this latter value is close to Hinke's microelectrode value for free myoplasmic sodium in Carcinus. He concluded that after ten minutes most of the sodium remaining in the muscle is unbound and in the sarcoplasm. However, Hinke in studies on Balanus fibers placed in sodium free solutions found that sodium was removed proportionately from the "bound" and myoplasmic fractions. This resulted in the sodium content of myoplasm remaining constant. Only as a result of a microelectrode study would Caldwell's conclusion be justified.

In conclusion there is good evidence from several experimental techniques for a heterogeneous distribution of sodium in muscle. The exact morphological location of this sodium especially the "bound" or compartmentalized fraction remains obscure.

Crustaceans such as Balanus have an extensive extracellular space which equilibrates rapidly with external ions and contains at least half of the fiber sodium. A minimum of 20% of the total fiber sodium in Balanus appears to be "bound" or compartmentalized but the location of this fraction remains uncertain.

# CHAPTER III

## Barnacle Muscle Structure

### Introduction

The existence of cross striated muscle fibers of unusually large size in the barnacle Balanus nubilis was first reported by Hoyle and Smith (35). The muscle fibers occur in discrete bundles having a multiple fibrillar basal attachment to the shell and a 3 - 4mm tendon attachment to the scute. A bundle contains 30 - 40 fibers with diameters ranging from 500 - 1,500μ. There is little connective tissue between fibers and they may be separated by skilled dissection. These authors summarized the evidence that these fibers are in fact discrete single muscle cells.

The histology of individual fibers was described by Hoyle and Smith in a subsequent paper (36). The sarcolemma and its connective tissue forms a continuous ring around the circumference of the fiber and also indents deeply into the sarcoplasm. The connective tissue invaginations thin out rapidly to the point of no longer being visible with the light microscope. Clefts or channels enter the fiber from the periphery and become multibranched. They ramify through the central part of the fiber. These clefts apparently are not lined with connective tissue. When viewed in longitudinal section, long clefts running parallel to the long axis of the fiber are conspicuous but do not course for more than a

few millimeters in any instance. The basal end of a fiber has greater variability in its cleft system because of the multiple attachment to the shell. Most nuclei are situated at the periphery of the fiber subjacent to the sarcolemma. More central nuclei tend to be located on the margins of clefts.

An electron microscope description of the cleft system of Balanus was provided by Selverston (37). The clefts appear as longitudinal flattened infoldings of both plasma membrane and fibrous sheath of the fiber. The area of the cleft system effectively increases the fiber circumference by about twenty times. Selverston estimated that no portion of the contractile proteins is more than 20 - 50μ from the plasma membrane of the sarcolemma. In the barnacle, tubules arise from the sarcolemma both at the fiber surface and from the sides of the clefts. These tubules eventually form diadic contacts with the sarcoplasmic reticulum at the junction of the A and I bands.

Hoyle (38) called the branches of the clefts running to the sarcoplasmic reticulum the T system. He described the T tubules as being remarkably flattened in section. From the cleft these T tubules have only 2μ to travel to reach the most distant points of contact with the sarcoplasmic reticulum. The contacts with the sarcoplasmic reticulum are mainly diadic and are formed where the transverse, oblique or longitudinal tubules come into close relation with the sarcoplasmic reticulum. Contact points

occur along the A band in addition to those at the A - I junction. The complex between the tubule and the sarcoplasmic reticulum is without pores. Hoyle also observed wide transverse tubules making desmosone-like contacts with the Z regions where I filaments overlap between sarcomeres.

Spira (39) has shown the edges of these T tubules appear patent at the level of contact with the sarcoplasmic reticulum. The tubules are approximately 0.02μ wide at this point. In Illustration I the ferritin can be seen as black granules within the edges of the T tubule as it approaches the sarcoplasmic reticulum. The center does not appear open to ferritin. However, when horse radish peroxidase was used as a marker the entire T tubule appeared patent at the level of contact with the sarcoplasmic reticulum. Illustration 2 shows such a tubule. Note the thin layer of horse radish peroxidase coating the sides of the tubule (dark lines) while a lumen is clearly present (light center). In the light of these results, the extracellular space must be regarded as penetrating to the level where these 0.02μ tubules form diads or triads with the sarcoplasmic reticulum. The transverse tubules of amphibian muscle described by Peachey (15) appear to be analogous to these fine terminal clefts. These are 0.08 microns in diameter and patent until their termination in a triad structure.

Methods

Since the cleft system plays a major role in influx, first efforts were to further elucidate its morphology. With standard Haematoxylin and Eosin staining the brightly eosinophilic myoplasm makes it difficult to see the margins of a cleft. An effective stain was found to be aqueous Haematoxylin followed by 0.2% aqueous hydrochloric acid for differentiation. This left the cleft system and nuclei well stained but faded the cytoplasm resulting in good contrast between clefts and cytoplasm. As in all subsequent experiments, care was taken to obtain sections from the middle of fibers.

A series of electron micrographs of Balanus was obtained from Dr. A. Spira.

Results and Discussion

The low, medium and oil immersion photographs of Balanus reveal the complexity of the branching of the cleft system. Illustration 3 is a low power photomicrograph. Note the large clefts which run from the edge of the fiber and their closely associated nuclei. From these, smaller clefts branch. These are not connected to the surface. They may have associated nuclei. Illustration 4 is a high dry photomicrograph. Here three smaller clefts with nuclei surround a triangular area of myoplasm approximately 80$\mu$ across.

Illustration 5 is an oil immersion photomicrograph

of one side of the same area. A large number of small clefts are seen. Although larger clefts seem patent these small clefts appear without visible lumen. These large clefts are seen to branch forming smaller clefts. Overall there is a complicated array of branching and ramification from larger to smaller and smaller clefts. The smallest clefts in this photomicrograph probably represent the clefts from which the T tubules are seen to branch in the electron micrographs. These clefts as seen in both the light and electron microscope, have the same dimensions (0.2 - 0.3μ). Measurements on this photomicrograph reveal no part of myoplasm more than 2 - 3μ from a 0.3μ cleft. This is a much smaller distance than that reported by Selverston.

Illustrations 6 and 7 are electron micrographs of a fiber cut in cross section. The bar in the lower corner is 1μ in length. In both photographs there is a 0.2 - 0.3μ cleft. In electron micrographs the clefts appear to consist of electron dense material that stains similarly to basement membrane. This is consistent with experiments by Allen (40) which demonstrated oil could not enter the cleft system. From this cleft a branch cleft (T tubule) leads to a triad. The length of this T tubule is between 1 - 2μ as stated by Hoyle. Thin sheets of sarcoplasmic reticulum surround each myofibril. T tubules contact this sarcoplasmic reticulum at diads and triads at the perimeter of the myofibrils. Since A, I and Z bands are seen in the same transverse section, the banding of adjacent myofibrils

is not always in phase.

Illustration 8 is an electron micrograph of a longitudinal sectioned fiber. The bar is 1μ in length. The triad terminations of the T tubules with the sarcoplasmic reticulum are found along the full length of the A and I bands. Only in the region of the Z band are no terminations seen. Mitochondria are located between myofibrils but are not numerous.

By examining the location of the diad and triad terminations of the T tubules in relation to the myofibrils it is possible to estimate the distance of any part of the myoplasm from the extracellular space. A single myofibril appears to have triad terminations on all sides of the perimeter and along the full length except for a small area immediately under the Z band. Myofibrils are most frequently quadrangular in cross section. One diameter is usually 1 - 2μ while the other is 3 - 4μ. It is reasonable to conclude that no part of the myoplasm is more than 1 - 2μ from the extracellular space. In the area of the Z band, however, the distance may be somewhat greater.

In conclusion, the muscle fiber has a complex cleft system extending from the surface and dividing extensively in three dimensions through the muscle interior to the extent that no part of the myoplasm or contractile proteins is more than 1 - 2μ from the cell membrane. This is not unique to Balanus or to invertebrate muscle. For

example, it has been demonstrated that no part of mammalian cardiac myoplasm is more than 2 - 3$\mu$ from the extracellular space (41).

Illustrations 1 and 2

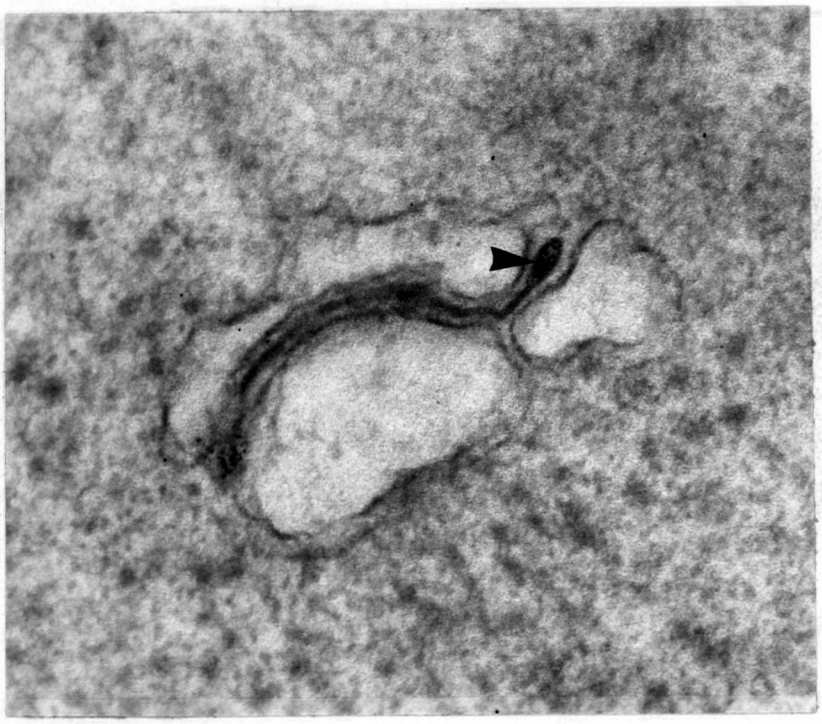

An electron micrograph of a T tubule.
Note the ferritin (black granules) in the edges of the T tubule as it terminates in close relationship to the sarcoplasmic reticulum as a triad. The center of the T tubule does not appear to be patent to molecules the size of ferritin. Magnification 88,000 x

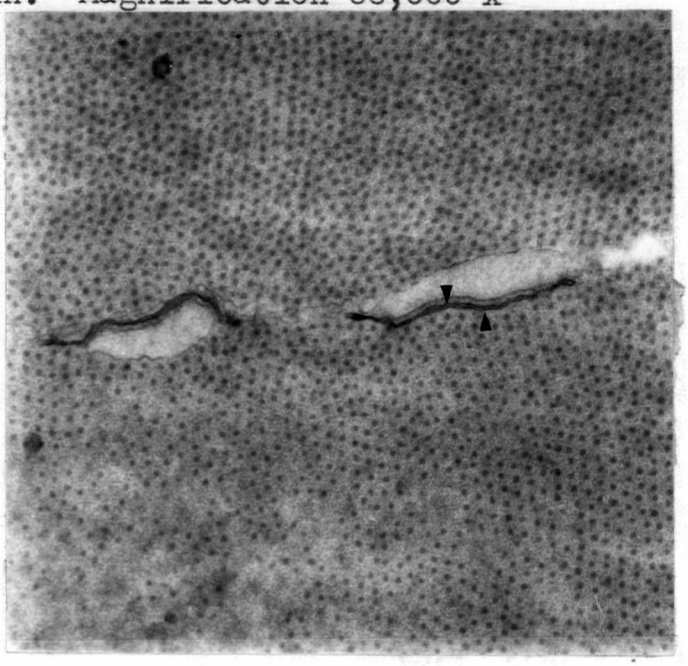

An electron micrograph of a T tubule.
Note horse radish peroxidase coating both sides of the T tubule (arrows) as it meets the sarcoplasmic reticulum.
Unstained material. Magnification 34,300 x

Illustrations 3 and 4

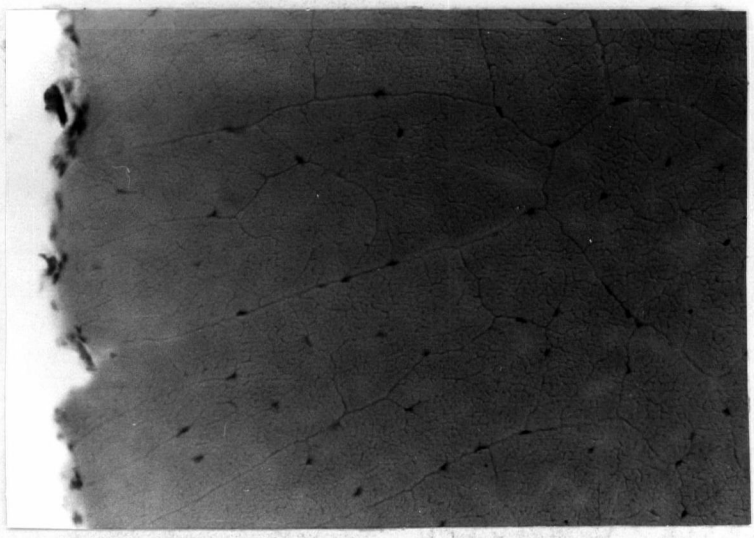

A photomicrograph of a fiber cut in cross section.
Large clefts extend from the surface of the fiber and have closely associated nuclei. From these larger clefts, smaller clefts are seen to branch.
Magnification 75 x

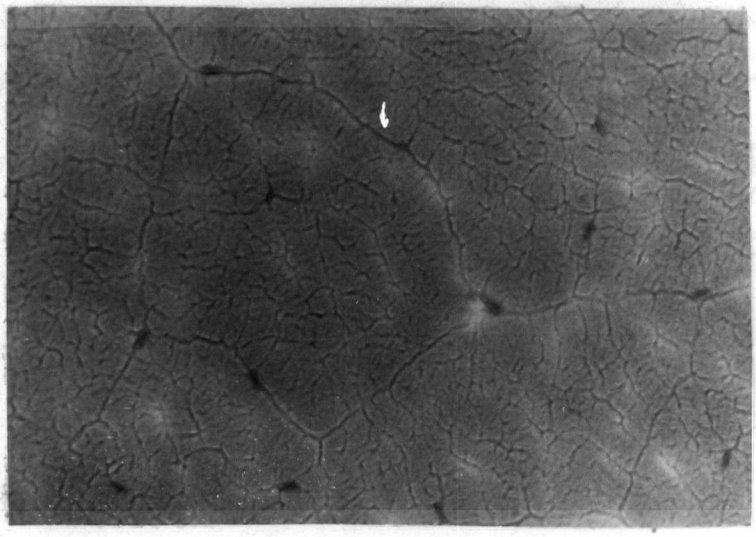

A photomicrograph of a fiber cut in cross section.
Three large clefts define a triangular area of myoplasm. Many smaller clefts are seen in the center of this area.
Magnification 370 x

Illustration 5

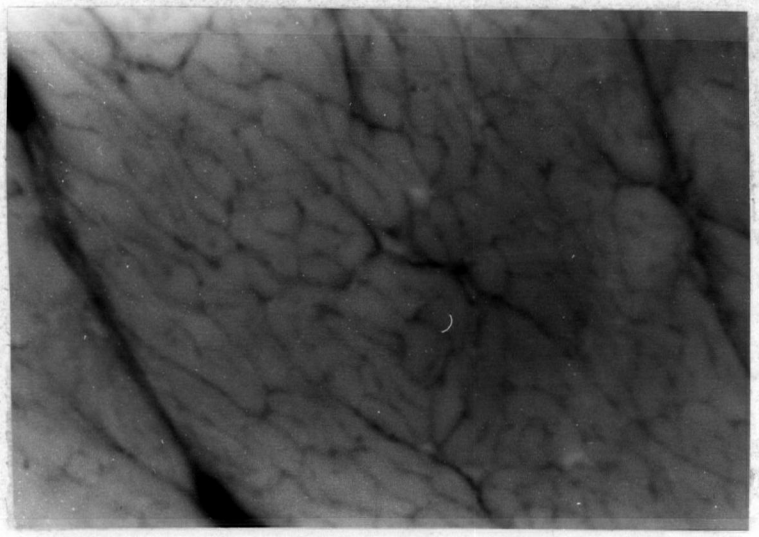

A photomicrograph of a fiber cut in cross section. Note divisions and ramifications of the clefts from a larger cleft at the side and within the myoplasm. Larger clefts can be seen subdividing to progressively smaller clefts.
Magnification 1,800 x

Illustration 6

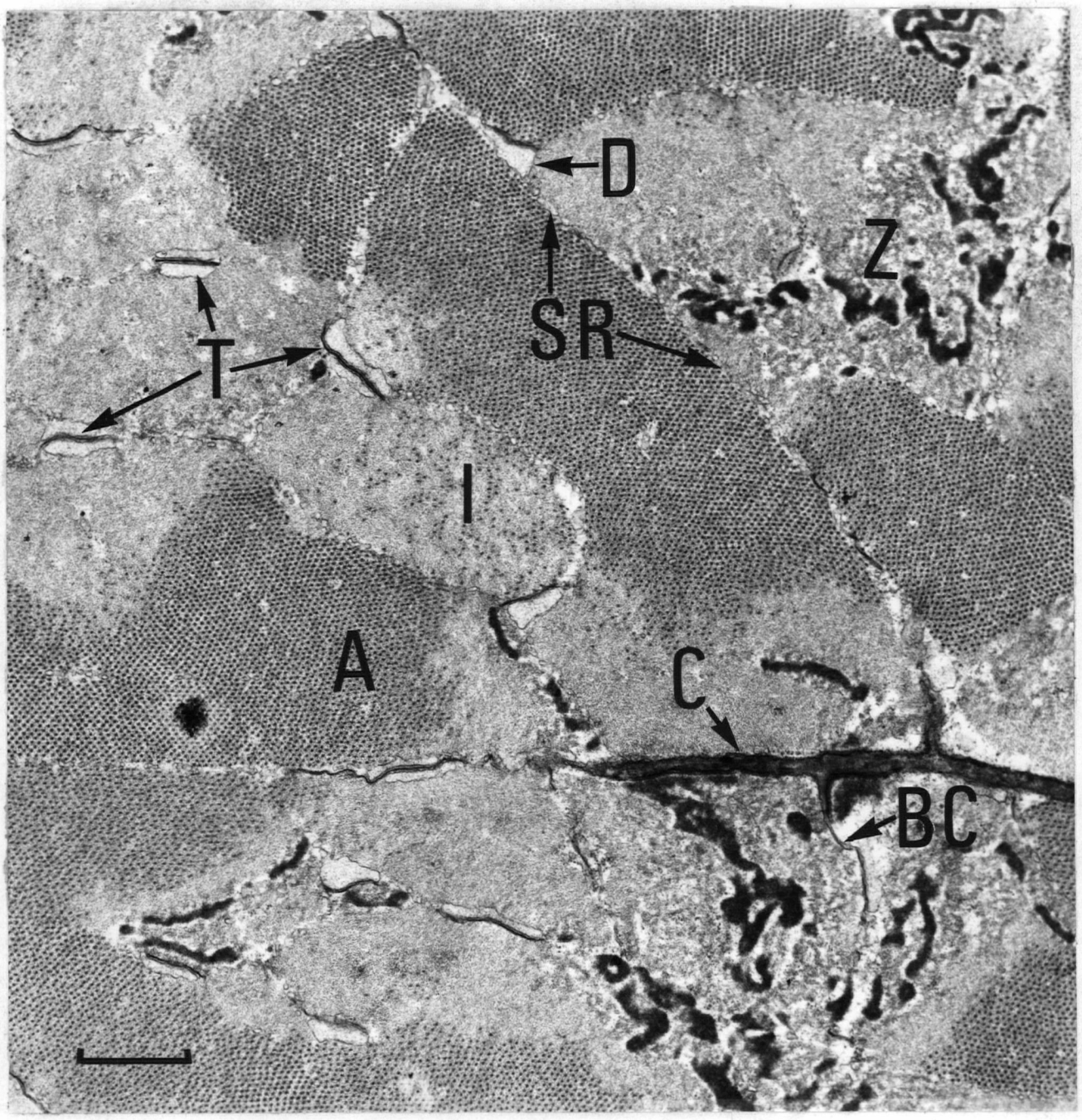


An electron micrograph of a fiber cut in cross section. A T tubule (BC) branching from a cleft (C) leads to a diad structure. The sarcoplasmic reticulum (SR) surrounds individual myofibrils as a thin fenestrated sheet. T tubules are in close relation to the sarcoplasmic reticulum at diads (D) and triads (T) at the perimeter of the myofibrils. Banding of adjacent myofibrils is not in phase: A, I and Z bands are seen in the same section. (A) (I) (Z).
Scale, Bar = 1μ. Magnification 18,200 x

Illustration 7

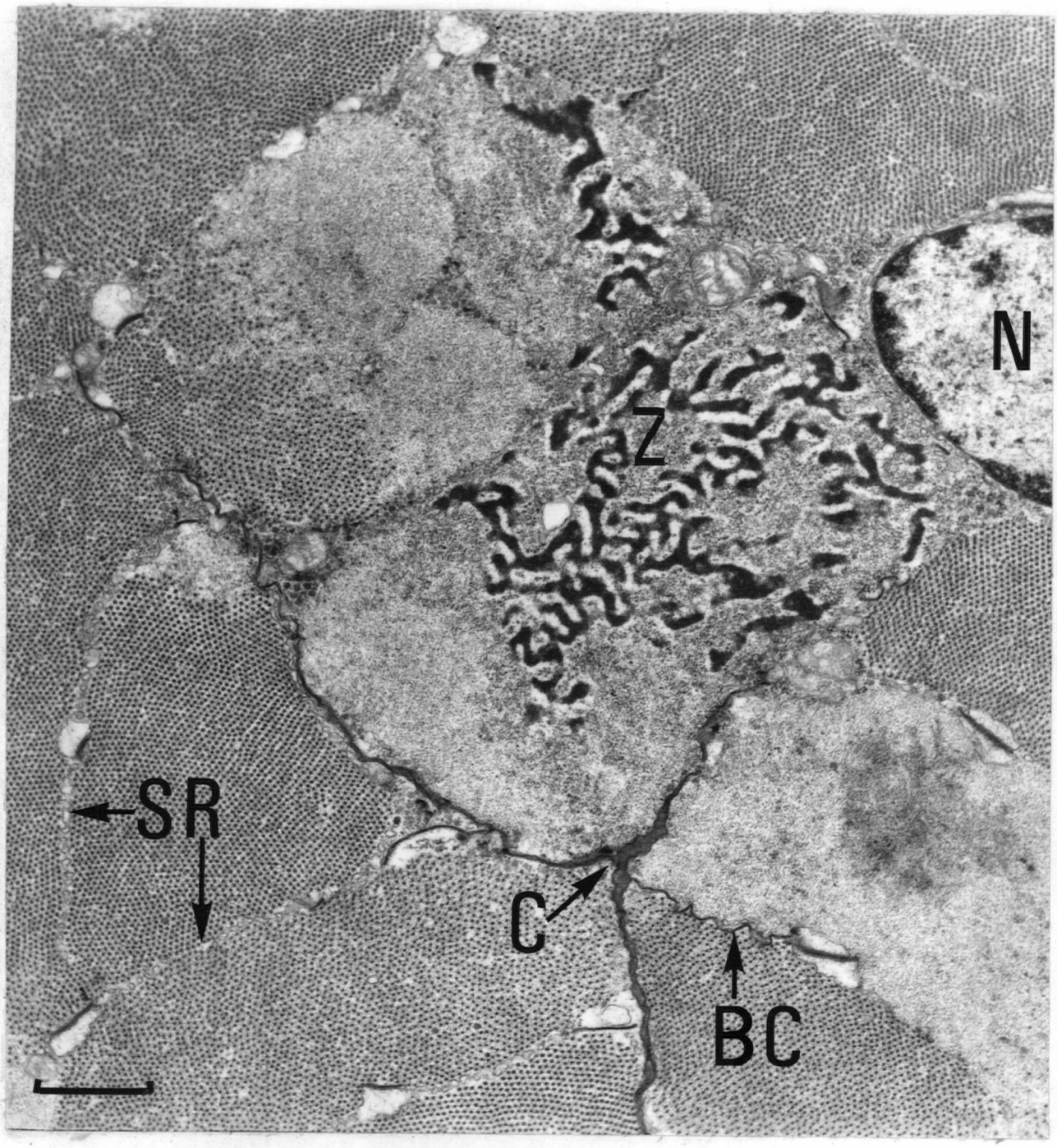


An electron micrograph of a fiber cut in cross section. A T tubule (BC) branching from a cleft (C) leads to a triad structure. The sarcoplasmic reticulum (SR) surrounds individual myofibrils as a thin fenestrated sheet. T tubules (unlabelled) are in close relation to the sarcoplasmic reticulum at diads and triads at the perimeter of the myofibrils. Banding of adjacent myofibrils is not in phase: A, I (unlabelled) and Z bands (Z) are seen in the same section. A nucleus is seen (N).
Scale, Bar = 1μ. Magnification 18,200 x

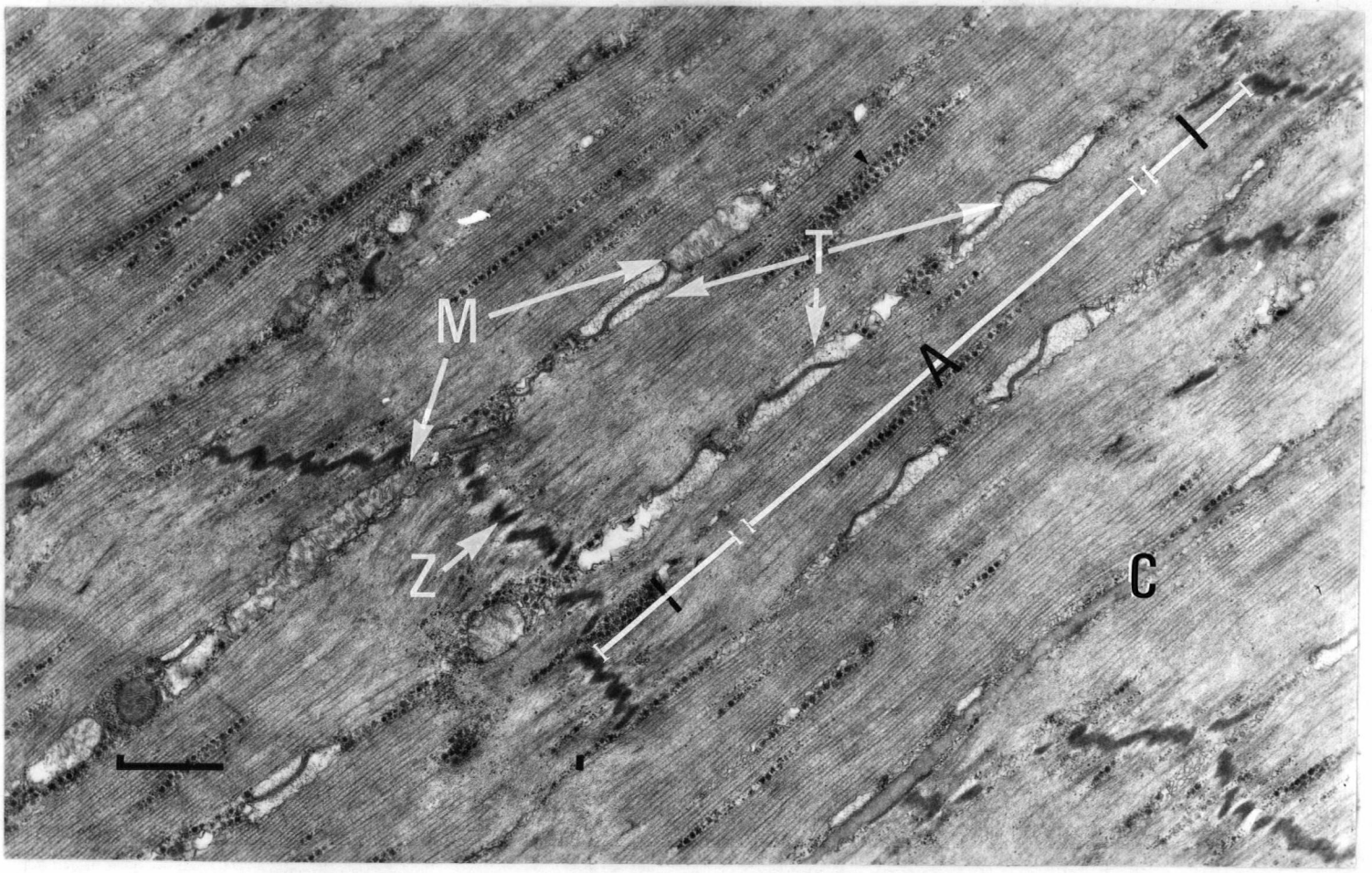


An electron micrograph of a longitudinally sectioned fiber. A cleft (C) and mitochondria (M) lie between myofibrils. Glycogen is abundant within myofibrils (small arrow). A full sarcomere is labelled from Z line to Z line (Z). The A and I bands of this sarcomere are marked. Note that the triad terminations (T) of the T tubules are present along the full length of the A and I bands. None are seen in the region of the Z line. The Z lines appear fenestrated allowing communication of the I bands of adjacent sarcomeres.
Scale, Bar = 1μ Magnification 14,500 x

Illustration 8

# CHAPTER IV

## Radioautographic Studies of $^{22}Na^{+}$ Influx

### Introduction

#### General Theory and Terminology

Radioautography may be defined as a method for locating radioactive substances by the use of modified photographic techniques. Radioautographs may be used in a quantitative as well as in a qualitative manner providing procedures are rigorously standardized to prevent variability.

#### Latent Image Formation

The photographic material used in this study was Kodak A.R.-10 stripping film, a 5μ layer of emulsion on a 10μ layer of gelatin base. When light or ionizing radiation strikes a silver bromide (AgBr) crystal in the emulsion, the crystal is made susceptible to conversion to metallic silver by the developer. In photographic terms, the emulsion has a latent image which can be converted to a true image by development.

A variety of physical and biological agents may cause latent image formation in the emulsion. Physical agents include mechanical pressure, heat, light and ionizing radiation. Manual pressure can produce finger prints on radioautographs. Any radioautographic technique must guard against undue pressure between section and emulsion during the mounting process. This will cause inappropriate latent

image formation (pressure artifacts). A part of the background of any radioautograph is caused by thermal agitation which results in random latent image formation in the emulsion.

Biological materials used in radioautograms may cause the production or destruction of latent images. These processes are respectively called positive and negative chemography. Chemography depends on the diffusion of molecules from the specimen into the emulsion and the reaction of these molecules with the silver halide crystals. The rates of both of these processes are temperature dependent. The production of latent images by ionizing radiation is temperature independent. Exposing radioautographs at about -20°C should discriminate against chemography. The amount of chemography may vary from experiment to experiment and within the same experiment. One series of sections may be affected by chemography or it may vary from area to area in the same section. Rogers (42) has found negative chemography to be the single most consistent problem in a wide variety of radioautographic studies.

Latent images may spontaneously revert over long periods of time. This process is called latent image fade. It occurs as a random process and is only significant when exposures are for several months.

In conclusion, care must be taken to prevent inappropriate latent image formation in the emulsion. Light and mechanical pressure must be avoided. During

exposure the emulsion should be cooled to avoid thermal background and chemography. Exposure should be as short as possible to avoid latent image fade. Controls should be used to detect the presence of positive or negative chemography.

Resolution

Resolution of radioautographs is usually defined as the distance from the tissue section edge (source) where the grain density is one half the value directly over the tissue section edge. Pelc (43) has shown for such high energy isotopes as $^{22}Na^{+}$ the best theoretical resolution is equal to one half the thickness of the emulsion and section. Thus for the experiments to be described with five microns of emulsion and a fifteen micron section, the best theoretical resolution is ten microns. Any substantial increase in this value implies isotope translocation at some point in the radioautographic procedure. Factors effecting the resolution in decreasing order of importance include the distance between the section and emulsion, the isotope used, the thickness of the section, the thickness of the emulsion, the length of exposure, the size of the emulsion silver halide crystals and the sensitivity of the emulsion.

An isotope emits beta particles over a wide spectrum of energies. The path of the particles is unpredictable with many direction changes. Sodium-22 emits a positron which behaves like a high energy beta particle until it ends its brief existence by annihilating an orbital

electron giving off two quanta of gamma rays. With high energy isotopes the maximum energy of the particles is increased. Silver grains are produced at greater distances from the tissue section edge by higher energy beta particles and the resolution is poorer. The great value of tritium in radioautography is the low maximum energy of the particles emitted (0.018 MEV).

Separating tissue section and emulsion will have more effect on resolution than altering any other parameter. When the section is in direct contact with the emulsion the distance to grains immediately under the section is much smaller than the distance to grains at some distance from the section edge. If source and emulsion are separated by a thin layer of inert material, grains at some distance from the section edge are the same distance from the section as grains under the section. Grains in the two areas now have equal probabilities of being hit by beta particles and the resolution decreases.

The thickness of the section is a special case of separating the section from the emulsion. A section may be regarded as a series of layers. In effect the lower layers separate the upper layers from the emulsion. The resolution of the entire section is a composite of the resolutions of all the layers. This resolution is poorer than the resolution of a single layer in direct contact with the emulsion.

The effect of increasing the emulsion thickness is similar to the effect of increasing the section thickness. With a thin emulsion layer in direct contact with section the grain density falls off rapidly from the section edge. As the emulsion thickness is increased the grain density does not fall off abruptly. This effect of emulsion thickness on resolution depends on the maximum energy of the particles emitted. With tritium the maximum track length of the most energetic particle is 3μ. Increasing the emulsion thickness beyond 3μ will not change the resolution. For higher energy isotopes the emulsion thickness is critical.

The longer exposure continues the greater the probability of multiple hits by beta particles of silver grains immediately under the section. Multiple hits are less likely for grains several microns away from the section. If exposure is long term, the increase in grain density immediately under the section will not be proportional to the increase in grain density several microns away from the section. For long exposures multiple hits can decrease resolution in this manner.

The smaller the size of the silver halide crystal in the emulsion, the more closely the position of the developed grain corresponds to the trajectory of the particle. This will result in a small improvement in resolution. If the emulsion is relatively insensitive, the highest energy beta particles will only produce latent

images at some distance from the section. This will result in poor resolution. This is a minor factor since isotopes emit beta particles over a wide spectrum of energies and emulsions can be selected for various sensitivities.

Efficiency

Efficiency has been defined for radioautographs as the number of grains produced in the volume of emulsion under the source per radioactive disintegration in the source. Major factors influencing efficiency are energy of the beta particles emitted, thickness of the emulsion and thickness of the source.

The lower the energy of the beta particle emitted, the less the chance of the particle reaching the emulsion due to self absorption in the section. This means isotopes like tritium (0.018 MEV) with low energy beta particles tend to have low efficiencies. On the other hand, the lower the energy of the beta particles that reach the emulsion, the higher the probability of these particles causing grain formation in the emulsion. This means isotopes of high energy like $^{22}Na^{+}$ (0.54 MEV) tend to have low efficiencies since particles may pass completely through the emulsion without causing latent image formation. This is especially true of particles over 0.500 MEV. Herz's (44) tabulation of grains produced in A.R.-10 per beta particle emitted to the emulsion for different isotopes, ranged from 2 grains per particle for carbon-14 (0.155 MEV) to 0.8 grains per particle for phosphorus-32 (1.7 MEV).

As the thickness of the section is increased, self absorption of particles by the specimen increases. A maximum point is reached where increasing the thickness of the section no longer produces an increase in the latent images of the emulsion. At this point the section is said to be infinitely thick. When the section is sufficiently thin for self absorption to be minimal it is said to be infinitely thin. At infinite thickness self absorption by the section makes the number of latent images formed in the emulsion proportional to the isotope concentration of the specimen but independent of its absolute amount. The thickness of sections used in these experiments (15μ) probably represents infinite thickness for $^{22}Na^{+}$. These radioautographs, when treated quantitatively, are proportional to the concentration of the isotope in the section, but are not an accurate reflection of the absolute amount. The extent to which self absorption decreases the efficiency depends on the energy of the isotope. Hendler (45) has shown that for carbon-14 (0.155 MEV) and 10μ sections, 30% of the beta particles do not reach the emulsion. Tritium (0.018 MEV) represents the extreme case, where self absorption is the single most important factor in efficiency.

For high energy isotopes like $^{22}Na^{+}$, increasing the thickness of the emulsion will increase the efficiency of the radioautographs. Thickness of the emulsion is the critical factor for quantitative work with high energy beta emitters if any comparison is to be made between

specimens. Liquid emulsions produce a variable thickness for each batch of slides prepared. This was a major factor in deciding to use A.R.-10 stripping film which Kodak claims to vary only 10% from the 5μ thickness.

There are few reliable estimates of efficiency in the literature. For calculating the approximate exposure time and the minimum quantity of isotope needed, Rogers (46) has estimated that for a 5 micron emulsion layer and a 5 micron section thickness, $^{22}Na^{+}$ produced 20 to 30 grains in the emulsion for a hundred disintegrations in the specimen.

Previous Techniques for Soluble Radioautography

Consider the problems posed by the radioautography with the highly soluble ion $^{22}Na^{+}$. What is needed are thin tissue sections in which ion migration is inhibited during preparation. This migration can occur within the section itself or later at the interface between the emulsion and tissue. The loss of only small amounts of radioactivity to solvents or embedding media in a radioautographic procedure may seem tolerable. However, this implies redistribution of the label within the tissue. A step which has loss of radioactivity from the specimen is invalidating.

The classical histological techniques of fixation, dehydration and wax embedding seem perfectly suited to extract labelled material. They are clearly inadequate. The same is true for any technique involving the overlaying of wet emulsion. Stumpf and Roth (47) have pointed out that fixation refers to the denaturation of proteins and does not

necessarily imply binding, trapping or immobilizing of compounds administered as tracers. Kaminski (48) found with various fixatives the amount of radioactivity lost in fixation varied from 25 - 90% for phosphorus-32 to 4 - 20% for iodine-131. Fixation may remove not only the tracer substance but significant amounts of tissue as well. Merriam (49) reported that 10% formaldehyde fixation extracted 4% of the total protein of muscle and 6% of the total protein of liver. Even formaldehyde vapour fixation has been demonstrated to be capable of producing isotope translocation (47).

To date, rapidly freezing tissue in isopentane made viscous by liquid nitrogen seems the only certain way to immobilize ions. Appleton (50) has detected no radioactivity in liquid isopentane used to freeze tissue samples containing high concentrations of $^{22}Na^{+}$. Trump et al (51) reported localized disruptions of the cellular membranes following the rapid freezing of tissues in viscous isopentane. This could allow the rapid influx of extracellular material or the escape of cellular constituents. However, Smith (52) has shown membrane injury occurs following ice crystal formation, and therefore after freezing has taken place. Further movement of compounds within the tissue would be restricted by the extreme rapidity of the freezing. Trump et al (51) demonstrated the central part of a tissue block 5 x 3 x 1mm reached -175°C within six seconds after immersion in viscous isopentane.

Proceeding from frozen tissue several approaches have been tried. Wilske and Ross (53) took small frozen sections and freeze dried them. These freeze dried sections were fixed in formaldehyde vapour, and then embedded in epon. Thin sections were cut with a glass knife and were dipped in liquid emulsion. The technique achieved good results with labelled aspirin. However, translocation of the highly soluble ion $^{22}Na^{+}$ could occur during the epon embedding or when the sections were floating in the boat of the glass knife.

Cutting frozen sections in a cryostat does ensure that no translocation occurs. Unfortunately cryostat sections are not as satisfactory as those prepared by wax embedding. Minute ice crystals may have formed during the freezing of the tissue giving a moth-eaten appearance to the sections at high magnifications. Sections are fragile and frequently may have tears or wrinkles.

Ullberg (54) first suggested polyvinyl chloride backed tape to pick up sections and to press them onto emulsion coated slides. Dissolving the tape in acetone was necessary at the end of exposure before development could proceed. Rabinow and Barry (55) modified this technique by leaving the sections on the tape to freeze dry overnight in the cryostat. The following day sections were mounted at room temperature by pressing the polyvinyl tape against emulsion coated slides. Difficulty in removing the tape and lack of good section histology on removal of the tape

make these procedures cumbersome.

The sandwich technique was first described by Kinter, Leape and Cohen (56). They simply placed frozen sections between a glass slide and an emulsion coated slide. The technique was later modified by coating the non-emulsion slide of the sandwich with Saran F-120 (Dow Chemicals)(57). This was an attempt to prevent adhesion of the section to the glass slide at the termination of exposure. In both experiments it was noted that permitting the section to thaw for only one second before contacting the emulsion allowed translocation of the label and prevented isotope localization to specific cellular structures. Although these authors reported no pressure artifacts, Stumpf and Roth (47) found such artifacts a major hazard of the sandwich technique.

Horowitz and Finichel (58) coated the non-emulsion slide of the sandwich with teflon spray. These authors noted pressure artifacts and positive chemography in their radioautographs. Unfortunately they did not utilize controls to check the extent or consistency of these artifacts in their procedure. Roberts, Ciofalo and Martin (59) picked sections up on teflon slides. These sections were freeze dried at low pressure and then used to prepare a sandwich. The complications reported by these authors were pressure artifacts and difficulty in maintaining contact between section and emulsion on removal of the teflon slide.

In summary, sandwich techniques appear promising

since they allow no opportunity for translocation of the label. However, section adherence to the wrong slide at the end of exposure and pressure artifacts are major complications.

In a recent paper Stumpf and Roth (47) evaluated a number of methods for treating frozen sections. Sections were cut only 0.5 - 1μ thick at -70°C using a special cryostat and a glass knife. The following procedures were examined:

(1) frozen sections were cut, freeze dried and mounted at room temperature by gentle manual pressure between teflon support and emulsion coated slide (a clamping technique previously used was rejected due to the production of pressure artifacts);

(2) frozen sections were cut, mounted on thawed glass slides and dipped in liquid emulsion;

(3) tissue sections were freeze dried, fixed in the vapour phase, embedded in epoxy and dipped in liquid emulsion (similar to Wilske and Ross);

(4) tissue sections were fixed in formalin, embedded in paraffin and dipped in liquid emulsion.

Method (1) gave good localization of the label with no evidence of translocation. Methods (2), (3) and (4) showed diffusion of the label and loss of tissue radioactivity. Several of these techniques with obvious loss or translocation of the label gave reproducible results. Thus, reproducibility of results is no criterion for accurate

localization. In some sections excellent labelling of the lumen of a blood vessel was accompanied by spread or loss of isotope from adjacent structures. Therefore differential loss of activity can occur from adjacent sites in the same section.

In a subsequent paper, Stumpf, Roth and Brown (60) utilized the first method to determine the location of three labelled extracellular space markers (inulin, mannitol, sulphate) in the superior cervical sympathetic and nodose ganglia of cats. Except for a small quantity of intraneuronal activity there was good localization of these markers to the extracellular space.

The method of Stumpf and Roth shows promise but is technically difficult. Thin freeze dried sections have the consistency of fine powder and good histological preservation is difficult. The possibility of translocation or sublimation of the label in the freeze drying of tissue must be considered.

To date the most promising technique in its simplicity and reliability is that of Appleton (61). He cut frozen sections in darkness with safe light illumination. To facilitate mounting a temperature differential was maintained between tissue section and coverslip by storing the coverslips in a separate container at -10°C. Mounting was accomplished by touching a chilled coverslip coated with A.R.-10 stripping film to the section on the cryostat blade at -20°C. Appleton concluded that neither freeze substitution in absolute ethanol at dry ice temperature nor vacuum

dehydration at low temperature showed any advantage over the storage of sections at -25°C. In any case, sections are probably rapidly dehydrated even at -25°C.

In a subsequent paper Appleton (62) examined the resolving power of his technique for $^{22}Na^{+}$ and A.R.-10 stripping film at different temperatures. The best theoretical resolution was 5μ. The resolution achieved was 9 - 13μ, or 4 - 8μ greater than the theoretical resolution. Appleton concluded that if this difference was caused by diffusion it was occurring over the short distance of 5μ. The optimum exposure temperature for A.R.-10 was found to be -25°C by examining the sensitivity of the film at various temperatures. At lower temperatures the sensitivity of the emulsion decreased but the background did not. At the higher temperature of -10°C unmistakable artifacts occurred under the sections. These artifacts were probably due to positive chemography which is temperature dependent. Appleton's background for A.R.-10 and $^{22}Na^{+}$ was 1.4 - 2.4 grains/100$\mu^2$.

## Methods

### Preparation of A.R.-10 Stripping Film

All preparatory steps were carried out three feet from a Wratten series 2 safelight. The film is packaged with its gelatin layer mounted on glass. Squares of film were cut with a scalpel and gently stripped off the glass. These squares of film were placed in a water bath with the

emulsion side of the film facing upwards. The cut sections of film floated on the bath, imbibed water and swelled. Two percent by volume glycerol was added to the bath, following the recommendation of Rogers (46). This maintained the gelatin in a pliable state and allowed the subsequent adhesion between section and emulsion to be firm. After three minutes in the bath the film (emulsion side up), was picked up on a slide which was coated previously with gelatin. The slide plus film was placed in a light-tight box containing silica gel and allowed to dry overnight. Dried slides were stored in light-tight boxes at -25°C.

Freezing and Mounting of Muscle Fibers

All muscle fibers used in radioautographic experiments were frozen by immersion in viscous isopentane (-155°C) cooled by liquid nitrogen (-196°C). Although freezing probably takes place instantaneously, fibers were left in the freezing mixture for 30 seconds before transfer to the cryostat (I.E.C. International Harris Cryostat, Model C.T.D.) for sectioning at -25°C. This cryostat was modified so the temperature sensing probe was at the blade level rather than at the cryostat bottom. When in the cryostat, fibers were handled only with chilled instruments. Cylindrical sections 3mm long were cut from the center of the muscle fibers and mounted on the microtome chuck.

The method of mounting these muscle cylinders on the chuck is critical to the whole procedure. If the tissue is allowed to thaw while sitting in a drop of mounting

media translocation of the label will occur. A thick slush of carboxymethyl cellulose as recommended by Ullberg (54) was found to be superior to water or to dilute gelatin as a mounting media. This material is insoluble in water. The water carboxymethyl cellulose slush must be stirred immediately before use since no lasting suspension will form. Once a drop of the slush is deposited by Pasteur pipette the carboxymethyl cellulose tends to settle out and water can be suctioned back into the pipette.

Mounting was accomplished in two stages. First the frozen cylinder of muscle was taken with precooled forceps and applied to a drop of carboxymethyl cellulose which was almost solidly frozen on the chuck. If the section sank more than 1mm into the drop it was discarded as unsuitable for subsequent steps. Fortunately a drop blanches as it freezes on the chuck so the proper moment for application of the muscle can be gauged. In the second stage the chuck with drop and section was turned sideways in order to inspect the mounting of the fiber cylinder. Carboxymethyl cellulose was applied to the sides of the lower 2mm of the fiber cylinder using the deposition-suction method. Sections were taken only from the top 1mm of the muscle cylinder. This was the only part of the cylinder which had not contacted mounting medium.

Only with such an approach is there reasonable hope of no translocation occurring in the top millimeter of the fiber cylinder. This assumption is justified since

thawing has not been visually detected and mounting media has not contacted the top 1mm of the muscle cylinder.

The Technique for Radioautography

The technique used for radioautography was a modification of Appleton's technique (61). Slides coated with stripping film (emulsion side up) were used rather than coverslips because of their large mass. Cooled slides require more heat to thaw than do cooled coverslips. Thus the risk of accidentally thawing sections is less with cooled slides than with coverslips. Another advantage is that slides are much easier to handle than coverslips under safe-light conditions. It was found to be difficult to consistently store slides at a higher temperature in a separate container (-15°C). A special plexiglass cryostat shelf was built and slides were stored at cryostat temperature (-25°C).

An arrangement of a safe-light and a mobile pole type of tungsten light was utilized to allow sectioning in normal light. Five to six sections were cut at -25°C and the tungsten light switched off by simple overhead reach. Since the safe-light was left continuously on, it adequately illuminated the cryostat blade three feet away. A slide was now extracted from the slide storage box on the cryostat shelf. The previously cut sections were brushed from the cryostat blade with a fine camel's hair brush onto this slide held below and parallel to the blade. Next, the slide with the sections resting on the emulsion was manipulated to ensure uniform application of the sections to the

emulsion. Now the slide with sections firmly adherent to the emulsion was placed in the second light tight box. Then the box was taped shut, sealed in an air tight plastic bag and quickly transferred to the deep freeze (Viking Vertical Model V6305) for storage at -25°C.

Appleton (63) has subsequently converted to a similar routine and no longer cuts sections under safelight illumination.

The manipulation to ensure adhesion for the duration of exposure consisted of gently pushing the sections against the emulsion with a teflon plunger. This plunger was constructed from the standard I.E.C. suction cup and a 1 inch square of teflon. Control slides with non-radioactive specimens revealed that no significant pressure artifacts resulted from this procedure. However, it was impossible to consistently apply the same pressure to a series of slides. Thus, non uniform treatment of slides and tissue deformation were potential problems. In the final technique, slides with the brushed on sections were inverted onto a 4 inch square of teflon. The square of teflon was held for convenience by silicon grease to the top of a slide box. This procedure created a temporary sandwich with emulsion, sections and teflon sheet as the layers. The advantage of this final procedure is uniform gentle contact pressure ensured by the fact that only the weight of the slide presses the sandwich together. Rogers (42) considers his variable success with the Appleton technique is due to the failure to achieve uniform contact between section and emulsion.

Appleton (63) did not experience any significant loss of sections from the emulsion with long term exposures even up to one year. The loss of sections from the emulsion was a major problem in the course of the development of the technique reported here. The steps of the technique essential to the prevention of this loss of sections were the addition of glycerol to the water bath prior to the preparation of film and the inversion of emulsion and sections onto teflon during the mounting procedure. Also, for storage it seemed advantageous to utilize gravity as a positive factor in adhesion. Accordingly slides were placed in the storage box so that the emulsions with adherent sections all faced the same direction. To utilize gravity, boxes were stored on end rather than flat.

Treatment and Processing at the Termination of Exposure

Fixation

All solutions used in fixation and processing were kept at 19°C to prevent swelling of the gelatin emulsion leading to detachment of the section. Preliminary experiments indicated that the most suitable exposure time was 7 days. At the end of exposure slides were removed from the deep freeze and thawed for 2 minutes under a safe-light. The thawed slides were immersed in 70% ethanol for 10 seconds in order to prevent negative chemography due to diffusion of soluble enzymes during processing (Darzynkiewicz)(64). After drying at room temperature in air for 15 minutes fixation was continued for 5 minutes in 4% buffered formaldehyde (phosphate buffer PH7.4). Slides were then washed for

10 minutes in water.

Development

A.R.-10 has an optimum development time of 5 - 6 minutes for maximum specimen grains with minimum background. However the grain counting procedure allowed for a maximum of 40 - 50 grains/100$\mu^2$ of emulsion. This grain level was achieved in the longest labelled specimens at 4 minutes. Thus 4 minutes was the development time used. Slides were placed in Kodak D-19 developer for exactly 4 minutes with agitation 5 times at 1 minute intervals. A water stop bath was used for 30 seconds. Next slides were fixed in Kodak F-24 fixer (nonhardening) for 6 minutes with agitation at 1 minute intervals. Slides were then placed in water for 10 minutes and normal lighting resumed.

Staining and Mounting

The staining procedure was as follows:

Harris Haematoxylin diluted 1.3 with water . . 15 minutes
Wash in water 19°C . . . . . 30 seconds
Differentiate in 0.2% aqueous HCl. . . . . 20 seconds
Blue in water 19°C . . . . . 10 minutes
Eosin 1% aqueous . . . . . 20 seconds
Wash in water 19°C . . . . . 30 seconds

Slides were than processed through graded alcohols to xylene. The coverslip was mounted with Permount. When the mount had hardened, excess film was removed from the back of the slide with a razor blade.

Grain Counting Procedures

Grains were counted at a 1,000 power with a Bausch and Lomb binocular microscope (research model). Grain counts were performed with aid of a 70μ square grid subdivided into 49 smaller squares (10μ sides).

Two types of grain counting procedures were performed. In the first type the grid was moved across the longest diameter of the fiber cross section to determine a grain density profile. Since the average fiber cross section is 1,000 - 1,500μ in diameter, a minimum of 15 - 20 grid positions were necessary to traverse a cross section. At each grid position a diagonal row of seven $100\mu^2$ squares was counted. In this way, the full 70μ width of the grid was represented. The direction of the diagonal was altered for each new grid position to allow random sampling. The average background was removed from each grid position by subtracting the number of grains associated with a grid diagonal of emulsion away from the specimen.

The second type of grain count was for resolution. For this determination the edge of section is considered a point source. The grid was located with the first line of $100\mu^2$ squares on the tissue edge; the other squares extending out into the emulsion. Counting the seven squares in each row gave the variation in response of the emulsion as a function of the distance from the source edge.

Photography

In photographing radioautographs the stained tissue

section tends to obscure the silver grains since the section sits on top of the emulsion. The major photographic problem is that grains are located throughout the thickness of the emulsion with such a high energy isotope as $^{22}Na^{+}$. Thus it is impossible to have both grains and tissue section in focus in one photograph using ordinary transmitted light illumination. With darkfield illumination the silver grains appear as light specks on a dark background since they scatter light. The tissue section absorbs light and is dark.

The solution was to take two photographs using both dark field and transmitted illumination. A Nikon binocular microscope (Model SKE) equipped with a Zeiss Automatic Camera was used. The grains were focused with dark field illumination and an exposure of 1 - 1.5 minutes was made with Adox KB-14 film. The darkfield condensor was removed and the tissue section sharply focused utilizing normal transmitted illumination. A second exposure was made without movement of the tissue section. Thus, the area of the tissue section photographed was the same for both exposures. By comparing the darkfield photomicrograph (grains in focus) with the transmitted light photomicrograph (section in focus) the relation of the grains to the cellular morphology may be examined.

Experimental

Barnacle muscle fibers were maintained in barnacle Ringer's solution (In M/litre 0.450 $Na^{+}$, 0.008 $K.^{+}$, 0.020 $Ca^{++}$, 0.010 $Mg^{++}$, 0.518 $Cl^{+}$, 0.025 Tris) at 2°C. Barnacle Ringer

was used for all labelled and unlabelled solutions in influx experiments.

Two basic radioautographic influx experiments were done. One was a quantitative influx study utilizing times 5, 20, 60 and 180 minutes. The second was a study of the shortest possible times in which $^{22}Na^{+}$ penetration of the fiber can be detected by the radioautographic technique.

For this latter study single fibers were left attached to the baseplate and handled in the following manner. A 1 cm loop of number 4 surgical silk was tied to the fiber tendon. The fiber was momentarily suspended in air from a hook attached to a micromanipulator. A 10 ml vial of labelled Ringer's solution (specific activity 100 $\mu$c/ml) was positioned on a platform jack immediately below the baseplate of the fiber. The suspended fiber was momentarily immersed in the labelled Ringer's solution by raising the jack. After removal the fiber was immediately frozen by thrusting it into viscous isopentane. The procedure, from immersion in the bath to freezing, was conducted either at 0.5 minutes or 1.5 minutes. Some of the 1.5 minute fibers were washed for 0.5 minutes in isotonic sucrose before freezing. Three radioautographs each with 5 cross sections were prepared from each fiber.

For the quantitative study a group of eight fibers from the depressor muscle was dissected apart leaving the baseplate attachment intact. This fiber and baseplate preparation was submerged in $^{22}Na^{+}$ labelled Ringer's solution

(specific activity 100μc/ml) at 2°C. At periods of 5, 20, 60 and 180 minutes, 1 - 2 fibers were taken from the bath, rinsed for 0.5 minutes in isotonic sucrose, and then quickly frozen in viscous isopentane. Three radioautographs each with 5 cross sections were prepared from each fiber.

For both types of influx experiments, one radioautograph was prepared with non-radioactive fiber sections as a control for detection of positive chemography. Also one normal radioautograph with radioactive tissue sections was "fogged" by exposing it to room light. This slide was the control for negative chemography.

Results

Table XI shows the average background was 1.5 grains/100$\mu^2$ for a total area of 1.2 x $10^6\mu^2$ counted.

The data for the resolution study is in Tables I, II, III and IV. In addition, Figures 1, 2, 3 and 4 show the resolution obtained with different time intervals of fiber immersion in isotope. The response of the emulsion to ionizing radiation is plotted as a function of the distance from the section edge. Zero is the section edge. Plus distances extend on the emulsion under the section and minus distances are on the emulsion away from the section edge. For the numerical value of resolution, the background is subtracted from the number of grains over the section edge and the result divided by two. This value in grains is indicated by the horizontal dashed line on the

graph. The distance (μ) associated with this half value of grains is the resolution. This value is indicated by the vertical dashed line. The resolution values obtained range from 17.5μ at five minutes to 15μ at 180 minutes. Thus, slightly better resolution was achieved with the longer fiber immersion.

Illustrations 9 to 14 are photomicrographs of the short term influx fibers. These photographs show higher grain density per unit area than were detected in the grain counts. This is due to the fact that grains just below the limits of visibility with transmitted light appear with darkfield illumination. Grain counts made under dark field lighting conditions would be proportional to those made with transmitted light. All photomicrographs are taken with darkfield lighting conditions unless otherwise indicated.

The grain count results for the short term experiment are given in Tables V, VI, and VII. The grain counts were plotted as a function of the distance from the cross section edge in Figure 5. Zero is the section edge. Plus distances extend on the emulsion under the section. Minus distances extend on the emulsion away from the section edge. The left half of the graph from 0 to 140 is a resolution curve similar to Figures 1, 2, 3 and 4. Each curve was fitted to a resolution of 17.5μ on this left half of the graph (the largest resolution number found experimentally). Each experimental point represents the mean from 3 - 6 cross sections from each of 3 fibers taken from one barnacle.

The right half of the graph from 0 to 700μ is one half a cross section diameter, since the average fiber cross section was 1500μ in diameter. The three curves are labelled according to the time interval from immersion to freezing. Only the 0.5 minute graph appears to change significantly along the fiber radius. This curve falls from approximately 30 grains/100$\mu^2$ to 3 grains/100$\mu^2$ in a distance of 400μ along the cross section diameter. This distance represents about .27 of the cross section diameter or .54 of the cross section radius. The 1.5 minute graph shows a straight line representing about 20 grains/100$\mu^2$. The 1.5 minute graph with 0.5 minute rinse graph is lower than the 1.5 minute graph. It is a straight line representing approximately 5 grains/100$\mu^2$,

An analysis of variance for one of the cross sections represented by these curves is given in Tables VIII, IX and X. This analysis shows there is a very significant difference (1% level) between the experimental points of curve (1). There is no significant difference at the 5% level between the experimental points of curves (2) and (3).

Illustrations 15 to 24 are photomicrographs of the long term influx fibers. A dark field and a transmitted light microphotograph is provided for each time interval. An examination of the relationships of the clefts and nuclei in a pair of photomicrographs reveals that they are pictures of the same area of the tissue section. By relating

specific areas of the darkfield to the transmitted light microphotograph the relationship of the silver grains to the cleft system may be examined.

In some areas of various darkfield photomicrographs grains are arranged in straight line or circular patterns. When these areas of patterned grains are related to the transmitted light photomicrograph a cleft of the same shape may be visible. Thus, these grain patterns probably represent areas of myoplasm with $^{22}Na^{+}$ containing clefts. The grain density of the darkfield photographs is seen to increase steadily from the 5 to the 180 minute fibers.

The grain count values for the long term influx experiment are tabulated in Table XI. Each value for a fiber represents the average value of two to three cross sections. For each cross section approximately 15 - 20 grid counts were made as has been described. Each grid count comprised seven $100\mu^2$ areas counted. Each fiber value thus represents the mean of 3 x 15 x 7 or 300 to 400, $100\mu^2$ areas counted. These fiber values were plotted semilogarithmically against time in Figure 6.

This graph shows the influx as determined by radioautography was divisible into two phases. There was an initial rapid phase representing the extracellular space. Half of the sodium content of this compartment had entered by ten minutes. Therefore the half time of this compartment was ten minutes. The size of this compartment

was estimated by extrapolating the portion of the curve for the slow compartment to t = 0. No absolute statement as to compartment size can be made as the radioautographs are only proportional to the amount of radioactivity present in the specimens. The reason is tissue specimens were cut at infinite thickness. The compartment size has 67% of grains present at 180 minutes. This implies that of all the labelled sodium present at 180 minutes, over one half had filled the extracellular space.

The more slowly exchanging compartment was still exchanging at 180 minutes when the experiment was terminated. It was not possible to calculate a rate constant for this compartment but the slope of the line was 0.08 compared to 1.5 for the slope of the line for the rapid compartment. The slower compartment must represent myoplasmic exchange.

Grain density profile data for the long-term radioautographs is given in Tables XII, XIII, XIV and XV. These grain counts relate the grain density to the distance from the cross section edge. This data is plotted in Figure 7. Zero is the section edge and positive distances extend on the emulsion under the section. Minus distances extend on the emulsion away from the section edge. The left half of the curve from 0 - 140 is a resolution curve similar to Figure 5. The point in the curves at 17.5μ on this side of the graph is fixed. This means each curve has a fitted resolution of 17.5μ. This is justified since 17.5μ was the largest experimental resolution detected. Each experimental point

is the average of 3.5 cross sections representing 3 fibers from the same barnacle. The right half of the graph from 0 - 700μ is a section of radius since the average fiber cross section was 1,500μ in diameter. The four curves are labelled according to time spent in isotope prior to freezing. The five minute plot shows a straight line representing about 7.5 grains/100$\mu^2$. The twenty minute plot is a straight line signifying approximately 20 grains/100$\mu^2$. The sixty minute plot is a straight line representing about 30 grains/100$\mu^2$. The 180 minute plot is also a straight line signifying approximately 40 grains/100$\mu^2$.

Justification for these values as straight line plots comes from the analysis of variance in Tables XVI, XVII and XVIII. These analyses represent a cross section diameter for three different 5 minute fibers of three different barnacles. In each case the F test is not significant. This means there is no significant difference between the means of grids counted at different points on the cross section diameter. To put it another way, the variation between grid counts does not differ from the normal variation within a grid count. All grid counts belong to the same population. Therefore there is a homogeneous distribution of grains across a fiber cross section. Since this was true at 1.5 and 5 minutes, no analysis of variance was done for the longer fiber times.

The slides with non-radioactive sections did not reveal any significant grain concentrations under the

specimens. This means positive chemography was not occurring to any extent. It also implies that the technique did not produce pressure artifacts which were masked in the radioactive specimens. The slides with radioactive specimens "fogged" by exposure to light gave no indication of negative chemography. There was no fading of the emulsion under the section and the emulsion remained uniformly "fogged".

Discussion

The range of background found (1.4 to 1.7 grains/$100\mu^2$) and the mean background (1.5 grains/$100\mu^2$ agrees favourably with Appleton's (61) background values for $^{22}Na^+$ and A.R.-10 (1.4 to 2.4 grains/$100\mu^2$). This implies adequate precautions against inappropriate latent image formation. It indicates light proof during preparation, mounting, exposure and processing of the radioautographs.

Table XIX shows the calculated efficiency to be 13%. This is somewhat lower than the value predicted by Rogers (20 - 30%). However Roger's (46) value was for an infinitely thin specimen ($5\mu$). Self absorption by the thicker specimens ($15\mu$) probably is the major factor in the variation.

The resolution obtained (15 - $17.5\mu$) exceeds the theoretical resolution ($10\mu$) by values similar to Appleton's (61) (4 - $8\mu$) for $^{22}Na^+$. If diffusion is taking place during the technique it only occurs over a distance of 5 - $7.5\mu$. This implies the technique developed is comparable to Appleton's in its usefulness for the radioautography

of soluble substances. No translocation occurs because if it did the resolution would be in the vicinity of 70μ as detected by Appleton for his unsuccessful methods.

The cleft system has a sodium concentration (0.450 M/kg $H_2O$), approximately ten times the myoplasm (0.040 M/kg $H_2O$). Because of this concentration difference it was originally hoped to visualize the clefts by radioautography as discrete structures in relation to the myoplasm. This proved rarely possible. The grain patterns observed in Illustrations 17 and 19 probably represent discrete clefts.

The morphological study revealed no part of the myoplasm more than 1 - 2μ from a patent cleft. Thus to consistently resolve clefts from myoplasm, a radioautographic technique must have a resolution of 1μ. Otherwise, grains produced over the myoplasm by isotope actually in the clefts results in a homogeneous grain distribution over both cleft and myoplasm.

The profusion of the cleft system in three dimensions means it is possible for the cleft-cleft distance to be smaller than the cleft-myoplasm distance. Thus, to be visualized, the cleft must be immediately adjacent to the emulsion to allow optimum resolution and sufficiently far from other clefts to prevent crossfire effects.

To allow visualization of the clefts, there must be sufficient $^{22}Na^{+}$ (grains) to present a pattern. However, if the grains are too numerous the pattern will be obscured.

Once the myoplasmic loading is unmasked by the saturation of the extracellular space (20 minutes), the increasing loading of the myoplasm will tend to obscure the clefts. Thus, the rarity of the visualization of clefts as discrete structures can be explained both on the basis of the transient nature of the optimum conditions for the observation and in terms of the limits imposed by the resolution.

The fact that the resolution improved with the longer duration of fiber immersion in isotope can be explained on the basis of grain counts. When counting 40 grains/100$\mu^2$ over a section edge the presence or absence of one grain will have less effect on the resolution calculation than when the number is 8 grains/100$\mu^2$.

The short term radioautographic study illustrates the rapidity with which isotope enters the extracellular space. At 0.5 minutes the $^{22}Na^+$ was distributed on a gradient traversing half the fiber radius.

Table XX is a comparison of the experimental distance along the fiber radius the $^{22}Na^+$ had diffused from the section edge (r) to the calculated theoretical distance the isotope had diffused to have the observed concentration at 0.5 minutes (x). The equation of Crank (65) is used for these calculations. The use of this equation presumes that diffusion of $^{22}Na^+$ in the extracellular space is a non-steady state of one dimensional diffusion from a source of fixed concentration. The value of the diffusion coefficient used for sodium is for self diffusion in dilute solutions.

Therefore, these calculations also assume diffusion of $^{22}Na^{+}$ in the extracellular space is equivalent in rate to self diffusion in dilute solutions.

The close agreement in Table XX between the observed experimental distance (r) and the theoretical calculated distance (x) indicates both of the assumptions are rational. Diffusion of $^{22}Na^{+}$ in the extracellular space follows a relatively straight pathway towards the fiber center. Thus the radius of the fiber cross section is a reasonable approximation of this pathway. The increasing deviation of the experimental distance (r) from the theoretical distance (x) as the fiber center is approached is plausible. The results also indicate that diffusion of $^{22}Na^{+}$ in the extracellular space is equivalent in rate to diffusion in dilute solutions.

Table XXI is a calculation based on the 0.5 minute curve. It supplies information on the geometry of the pathway for extracellular diffusion of $^{22}Na^{+}$. The equations of Bull (66) were utilized. These equations relate the experimental ratio of the $^{22}Na^{+}$ concentrations at the section edge and at a given distance along the fiber radius to the fiber surface area for $^{22}Na^{+}$ entry.

The calculations show approximately 60% of the fiber surface is theoretically involved in $^{22}Na^{+}$ entry of the extracellular space. This implies the cleft system should occupy at least half of the fiber surface. This is not completely incompatible with the morphology. Examination of an area of the edge of the fiber cross section in

Illustration 3 reveals the clefts comprise at least 20%. These clefts do not all deeply penetrate the fiber. The calculation may be in error by a factor of two to three.

Table XXII is a calculation utilizing the equation of Crank (65) and based on the 0.5 minute curve. This calculation reveals 6.11 minutes is required for the concentration of $^{22}Na^{+}$ in the fiber center to reach half the concentration of $^{22}Na^{+}$ at the section edge. This value is in good agreement with the half time for loading of the extracellular space calculated for the long term radioautographic experiment (10 minutes). The result of the movement of this quantity of $^{22}Na^{+}$ to the center would be 15 grains/100$\mu^2$ of emulsion under the center of the cross section. The grain value under the center of the five minute cross sections in the long term radioautographic study was half of this predicted value (7.6 grains/100$\mu^2$). This emphasizes that the sucrose rinse must remove about half the $^{22}Na^{+}$ from the extracellular space.

In summary, these secondary calculations based on the data for the 0.5 minute grain density profile curve provide a comprehensive picture of $^{22}Na^{+}$ diffusion in the extracellular space. The path of entry for $^{22}Na^{+}$ is the cleft system which theoretically occupies over 50% of the fiber surface area. The radius of the fiber is a reasonable approximation of the $^{22}Na^{+}$ diffusion pathway. Diffusion of $^{22}Na^{+}$ is as rapid in the extracellular space as in dilute solutions. The time required for the $^{22}Na^{+}$ concentration of

the fiber center to reach half the concentration of the fiber edge is approximately 6 minutes.

The 1.5 minute grain density profile curve is suspect since the grain count at the periphery of the fiber cross section (20 grains/100$\mu^2$) is lower than the grain count for the 0.5 minute curve (30 grains/100$\mu^2$). A possible explanation is that the 0.5 minute fibers and the 1.5 minute fibers are from different barnacles.

These 1.5 minute fibers without sucrose rinse showed a homogeneous isotope distribution. This is difficult to explain since six minutes should be required for the center of the fiber to reach one half the isotope concentration of the edge of the fiber. This calculated time value thus predicts a nonhomogeneous $^{22}Na^+$ distribution for 1.5 minute cross sections although the tracer gradient would be less marked than for the 0.5 minute fibers. Again, the origin of these 1.5 minute fibers from a different barnacle than the 0.5 minute fibers may be responsible. Another possibility is agitation or contracture of the 1.5 minute fibers. These fibers spent a full minute longer in the isotope bath than the 0.5 minute fibers and would be more susceptible to agitation. Agitation is postulated because of its known effect on the 1.5 minute fibers with sucrose rinse.

The 0.5 minute sucrose rinse should result in a heterogeneous distribution in the 1.5 minute fibers if the kinetics were the same as for the loading of the 0.5 minute fiber. The homogeneity of the 1.5 minute fiber with sucrose

rinse may be explained in terms of different kinetics. The influx is an exchange diffusion with no manipulation of the fiber. The rinse process is a diffusion into a sodium free isotonic sucrose solution with vigorous fiber agitation. This vigorous agitation probably disperses whatever $^{22}Na^{+}$ gradient the rinse creates in the fiber. Similarly inappropriate agitation while in the bath or during handling could account for the homogeneous distribution of the 1.5 minute fibers without rinse.

The 1.5 minute fibers without sucrose rinse were equivalent in grains to the 20 minute fibers of the long term experiment (approximately 20 grains/100$\mu^2$). When 1.5 minute fibers were washed for 0.5 minutes in isotonic sucrose their grain value was homogeneous representing 5 grains/100$\mu^2$. This change from 20 grains/100$\mu^2$to 5 grains/100$\mu^2$ implies that 0.5 minute sucrose rinse washes away at least half of initial fiber $^{22}Na^{+}$. This is supported by experimental results of Hinke (67). He found Balanus fibers without a 0.5 minute sucrose rinse had a sodium concentration of 90 - 120 moles/kg $H_2O$. Following the sucrose rinse this value was 60 - 70 moles/kg $H_2O$, or approximately 50% of the initial concentration. The fact the grain value of the 1.5 minute fibers with rinse is similar to the 5 minute fibers with rinse also support the concept that much of the initial $^{22}Na^{+}$ is washed out.

It is known that the extracellular space takes twenty minutes to load. The twenty minute fibers would have

the same amount of $^{22}Na^{+}$ removed from the extracellular space by the rinse as other fibers with different durations of $^{22}Na^{+}$ exposure. The grain value of the twenty minute fibers after the removal of this amount of $^{22}Na^{+}$ was 20 grains/100$\mu^2$. Thus the extracellular space fills in such a manner that the 0.5 minute rinse no longer removes a large fraction of the label. In other words, there is a portion of the extracellular space that loads progressively and is inaccessible to the half minute rinse. This was noted by Hinke (67) who demonstrated prolonging the sucrose rinse beyond 0.5 minutes did not remove appreciably more sodium from the fiber. It is tempting to postulate the small terminal clefts and T tubules represent this component of the extracellular space. The sodium which the rinse removes is in the larger clefts.

The long term influx study identified the loading of the extracellular space as an initial rapid phase. The half time of this compartment was ten minutes and it contained about half the fiber sodium. This is in good agreement with previous work by Hinke (68). The more slowly changing compartment had a smaller slope and was still exchanging when the experiment was terminated. This is compatible with unmasking of the myoplasmic exchange following the saturation of the cleft system. A similar interpretation was given to experimental results by Allen and Hinke (31). It was unfortunate this graph derived from radioautographs did not allow absolute calculations of the amount of sodium

in each compartment. To determine this and to substantiate the radioautographic plot it was decided to perform an influx experiment emphasizing the shorter time intervals.

This influx experiment would have no subtraction for the extracellular space since the radioautographic study made no correction for this compartment.

The profile analysis curves for the long term experiment reveal homogeneous distribution at each time interval. The time required for the $^{22}Na^{+}$ concentration of the fiber center to reach half the concentration of the fiber edge is 6 minutes. The sucrose rinse probably destroyed the small $^{22}Na^{+}$ gradient that would exist in the five minute fibers. Longer times would have a homogeneous distribution of $^{22}Na^{+}$ in the extracellular space. The amount of variation between experimental points is small but these are fibers from the same barnacle. Generally in grain counting procedures (see Table XI) the amount of variation between barnacles was much greater than the amount of variation between fibers of the same barnacle.

TABLE I

Data for 5 Minute Resolution Curve

Barnacle C Fiber 1 Section b

Grain Counts Within a Grid Line

grains/100$\mu^2$

| Grid Line Number | 1 | 2 | 3 | 4 | 5 | 6 | 7 |
|---|---|---|---|---|---|---|---|
| Distance of Grid Line from Section Edge ($\mu$) | 0 | 10 | 20 | 30 | 40 | 50 | 60 |
| | 16 | 7 | 4 | 4 | 2 | | |
| | 13 | 9 | 5 | 3 | 1 | | |
| | 16 | 11 | 5 | 3 | 2 | | |
| | 8 | 9 | 4 | 2 | 2 | - | - |
| | 13 | 6 | 5 | 3 | 2 | | |
| | 9 | 8 | 4 | 3 | 1 | | |
| | 10 | 7 | 3 | 3 | 3 | | |
| Mean and S.E. | 12.1 ± 1.1 | 8.1 ± .6 | 4.3 ± .3 | 3 ± .2 | 1.9 ± .3 | | |

Background 1.5 grains/100$\mu^2$

Resolution Grain Value $\frac{12.1 - 1.5}{2}$ = 5.3 grains

Figure 1

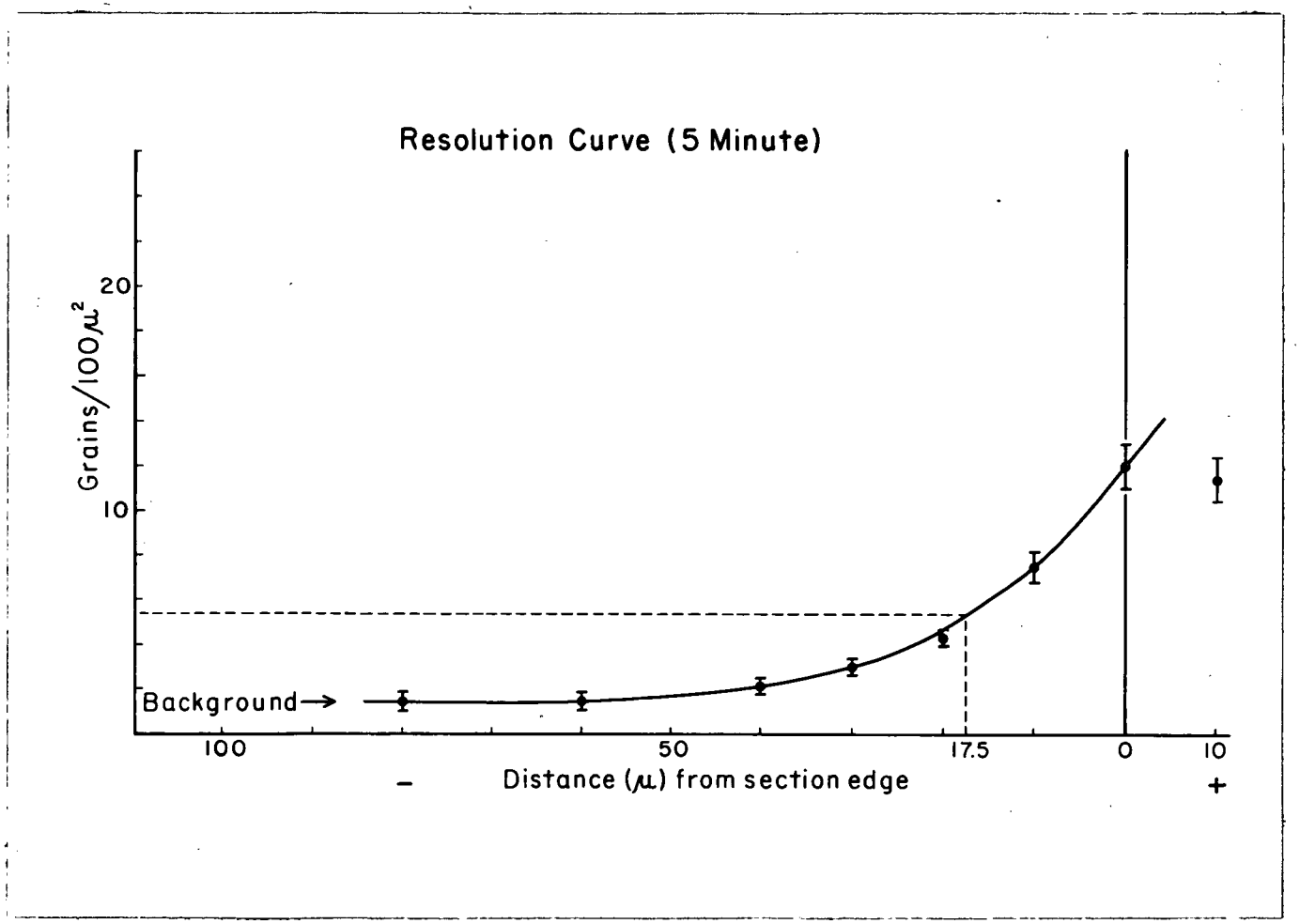
Resolution Curve (5 Minute)
Grains/100μ²
20
10
Background
100
50
17.5
0
10
−
Distance (μ) from section edge
+

TABLE II

Data for 20 Minute Resolution Curve

Barnacle C Fiber 1 Section b

Grain Counts Within a Grid Line

grains/100$\mu^2$

| Grid Line Number | 1 | 2 | 3 | 4 | 5 | 6 | 7 |
|---|---|---|---|---|---|---|---|
| Distance of Grid Line from Section Edge ($\mu$) | 0 | 10 | 20 | 30 | 40 | 50 | 60 |
| | 24 | 10 | 8 | 6 | 3 | 2 | 1 |
| | 17 | 7 | 9 | 6 | 3 | 1 | 2 |
| | 17 | 20 | 9 | 5 | 4 | 2 | - |
| | 14 | 15 | 7 | 6 | 2 | 2 | 1 |
| | 23 | 14 | 8 | 5 | 4 | 3 | 1 |
| | 19 | 13 | 10 | 7 | 3 | 1 | 1 |
| | 28 | 16 | 7 | 5 | 3 | 4 | 3 |
| Mean and S.E. | 20.3 ± 1.7 | 13.6 ± 1.4 | 8.3 ± .4 | 5.7 ± .3 | 3.2 ± .3 | 2.1 ± .3 | 1.3 ± .3 |

Background 1.4 grains/100$\mu^2$

Resolution Grain Value $\frac{20.3 - 1.4}{2}$ = 9.4 grains

Figure 2

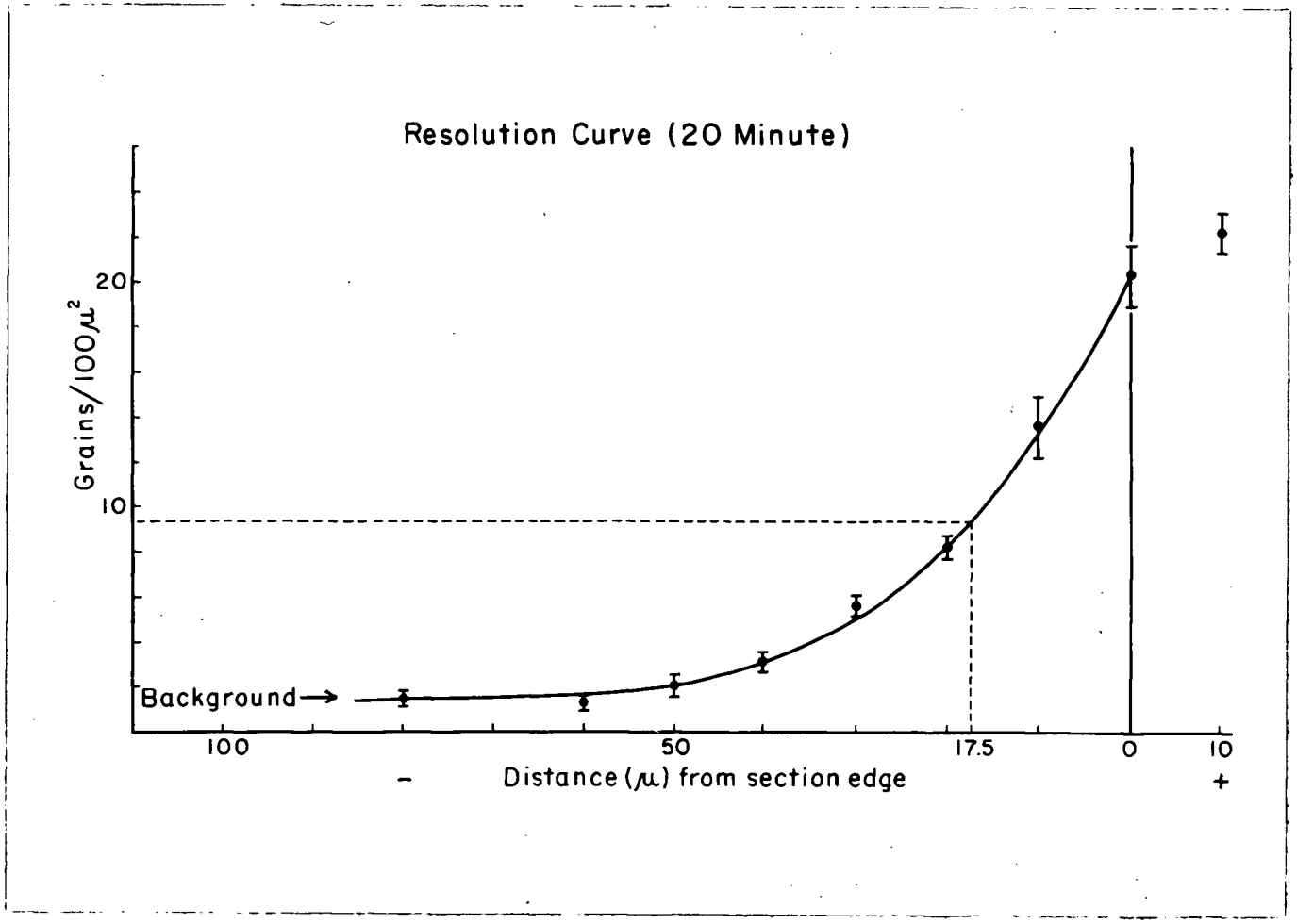
Resolution Curve (20 Minute)
Grains/100μ²
20
10
Background
100
50
17.5
0
10
−
Distance (μ) from section edge
+

TABLE III

Data for 60 Minute Resolution Curve

Barnacle B Fiber 2 Section b

Grain Counts Within a Grid Line

grains/100$\mu^2$

| Grid Line Number | 1 | 2 | 3 | 4 | 5 | 6 | 7 |
|---|---|---|---|---|---|---|---|
| Distance of Grid Line from Section Edge ($\mu$) | 0 | 10 | 20 | 30 | 40 | 50 | 60 |
| | 13 | 15 | 7 | 5 | 2 | | |
| | 26 | 17 | 19 | 7 | 3 | | |
| | 33 | 14 | 7 | 3 | 2 | | |
| | 30 | 14 | 11 | 8 | 4 | | |
| | 23 | 18 | 12 | 5 | 3 | | |
| | 30 | 20 | 13 | 7 | 2 | | |
| | 31 | 17 | 11 | 4 | 4 | | |
| Mean and S.E. | 26.6 ± 2.4 | 16.4 ± .8 | 11.4 ±1.4 | 5.6 ±.6 | 2.9 ± .3 | | |

Background 1.8 grains/100$\mu^2$

Resolution Grain Value $\frac{26.6 - 1.8}{2}$ = 12.4 grains

Figure 3

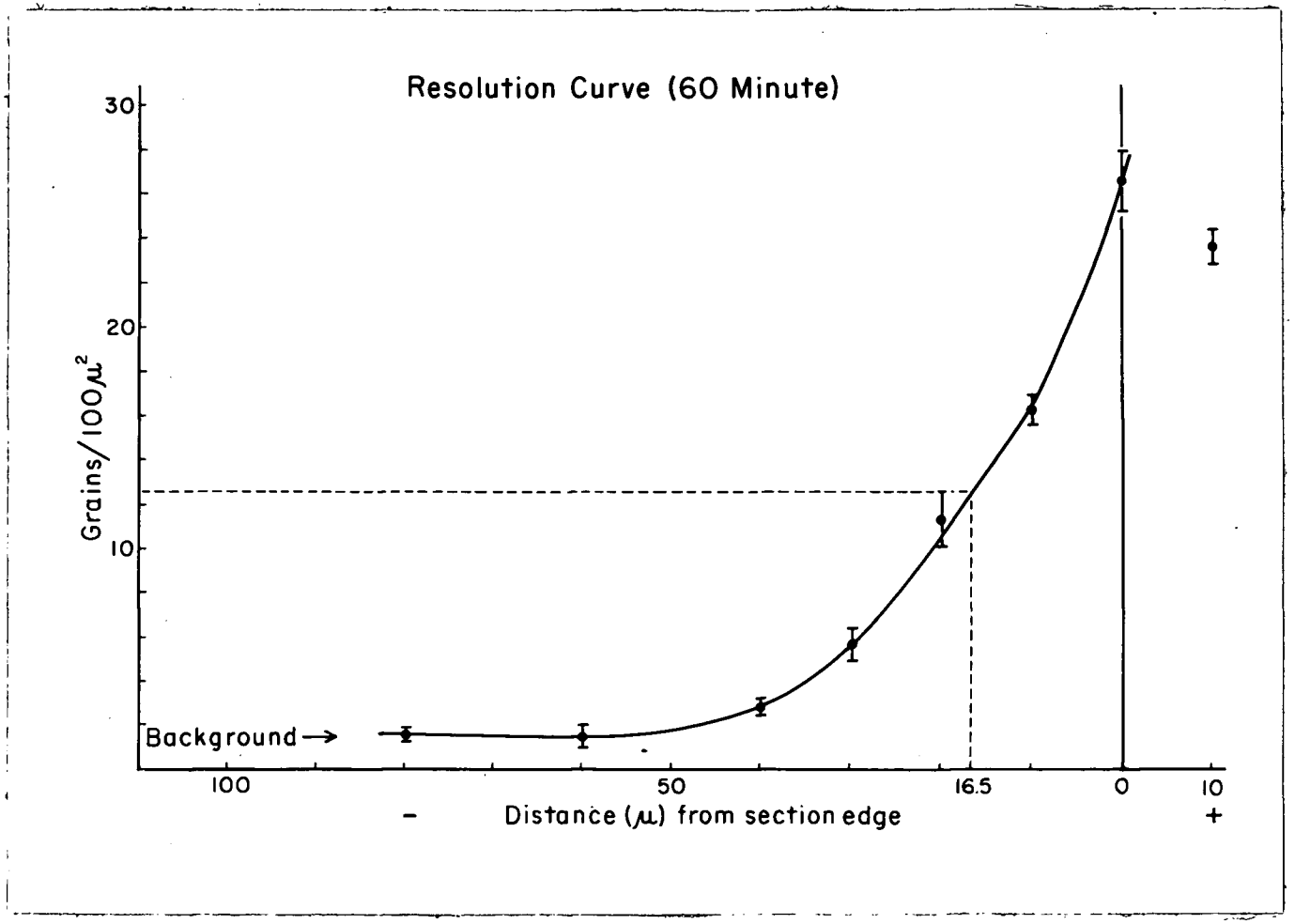
Resolution Curve (60 Minute)
Grains/100μ²
30
20
10
Background →
100
50
16.5
0
10
−
Distance (μ) from section edge
+

TABLE IV

Data for 180 Minute Resolution Curve

Barnacle A Fiber 2 Section a

Grain Counts Within a Grid Line

grains/100$\mu^2$

| Grid Line Number | 1 | 2 | 3 | 4 | 5 | 6 | 7 |
|---|---|---|---|---|---|---|---|
| Distance of Grid Line from section Edge ($\mu$) | 0 | 10 | 20 | 30 | 40 | 50 | 60 |
| | 50 | 28 | 20 | 6 | 6 | | 1 |
| | 42 | 24 | 13 | 7 | 5 | | 2 |
| | 44 | 29 | 15 | 9 | 4 | | 2 |
| | 49 | 34 | 15 | 5 | 5 | | 2 |
| | 46 | 30 | 18 | 10 | 3 | | 1 |
| | 35 | 27 | 21 | 8 | 5 | | 2 |
| | 42 | 19 | 12 | 7 | 4 | | 2 |
| Mean and S.E. | 44 ± 1.8 | 27.3 ± 1.7 | 16.3 ± 1.2 | 7.4 ± .6 | 4.6 ± .4 | | 1.7 ± .2 |

Background 1.5 grains/100$\mu^2$

Resolution Grain Value $\frac{44 - 1.5}{2}$ = 21.2 grains

Figure 4

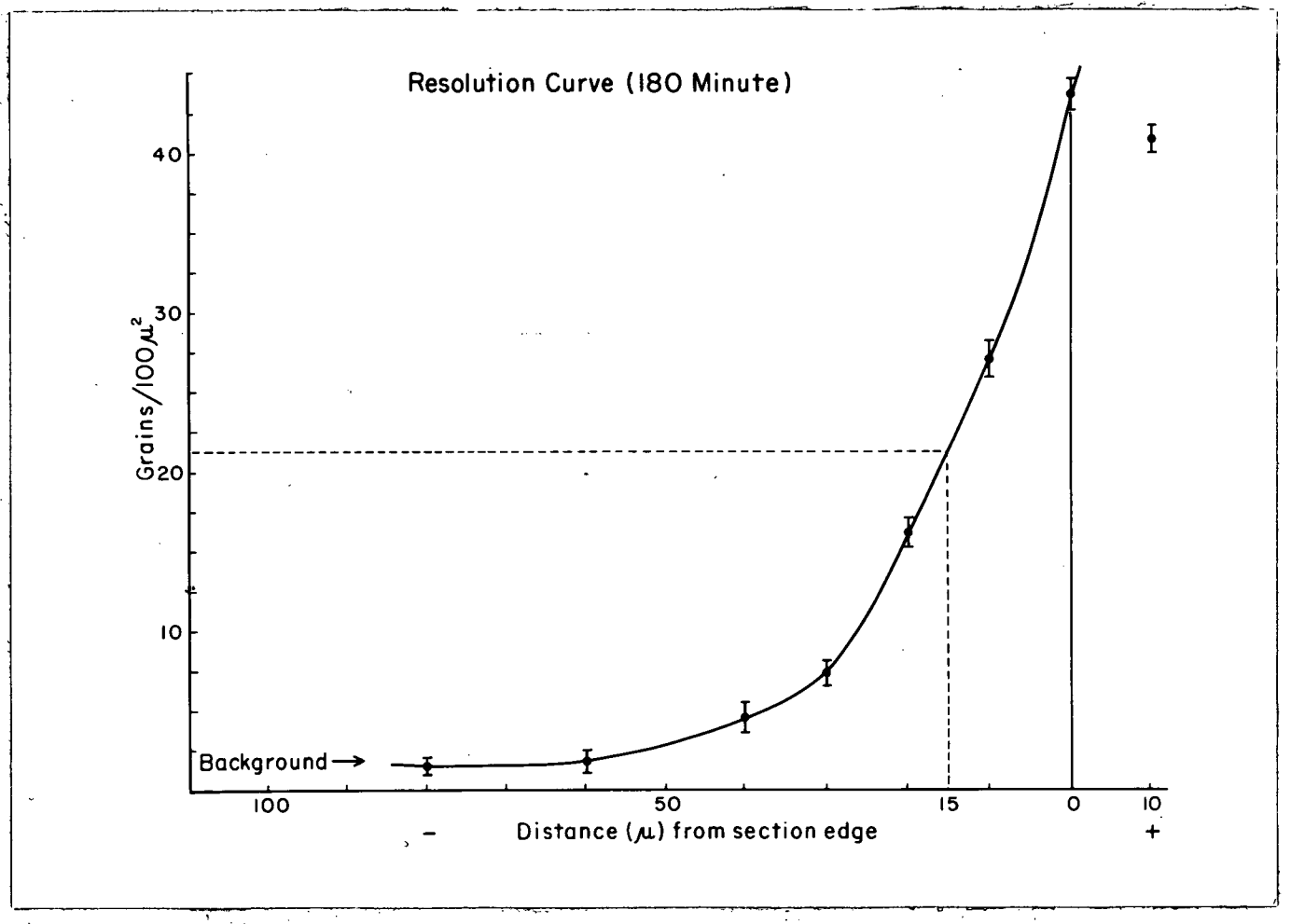
Resolution Curve (180 Minute)
Grains/100μ²
40
30
20
10
Background
100
50
15
0
10
−
Distance (μ) from section edge
+

Illustrations 9 and 10

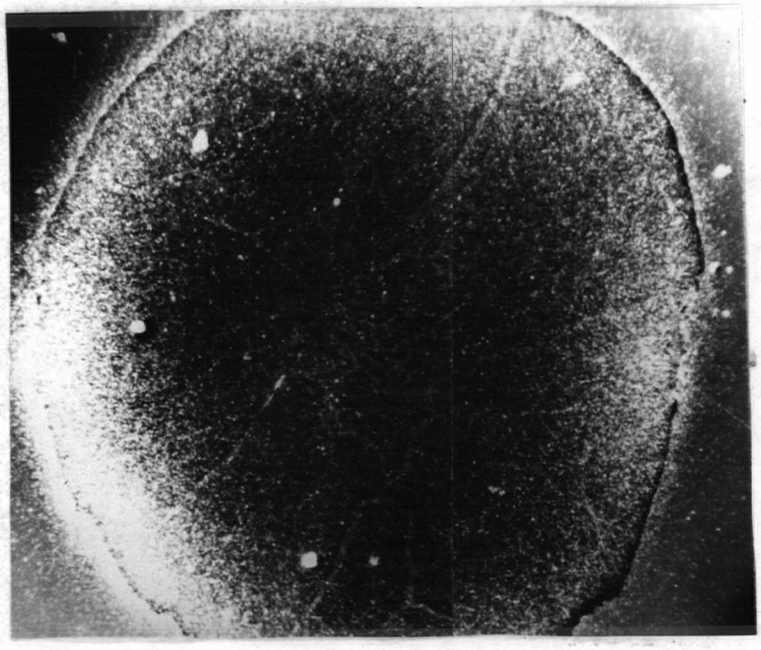

A photomicrograph of a 0.5 minute fiber cross section. The periphery is heavily labelled. This labelling extends inward approximately half of the fiber radius.
Magnification 90x

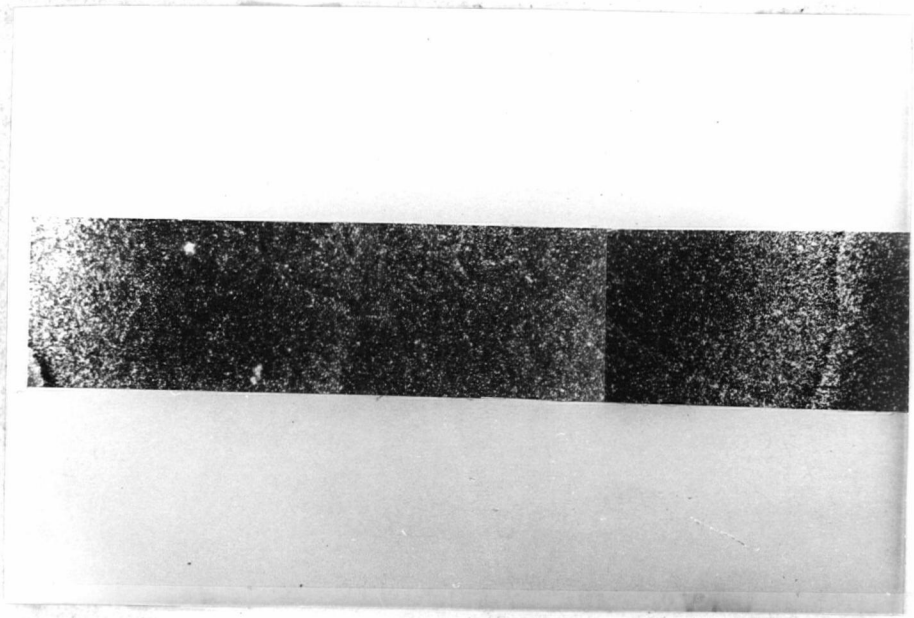

A photomicrograph of the same 0.5 minute fiber cross section taken along the axis of the fiber diameter. Note the heavy peripheral labelling.
Magnification 220 x

Illustrations 11 and 12

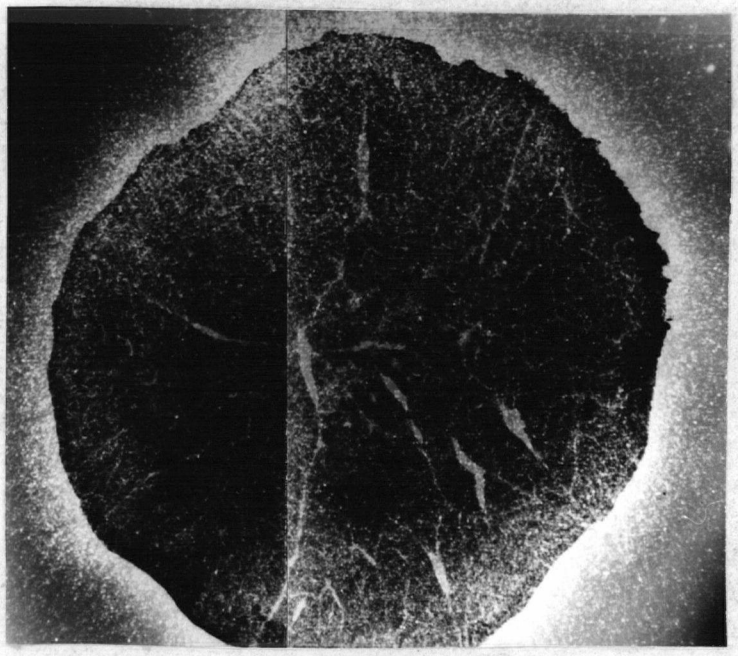

A photomicrograph of a 0.5 minute fiber cross section. Note that the periphery is heavily labelled. This labelling has decreased to background levels at the fiber center. Magnification 90 x

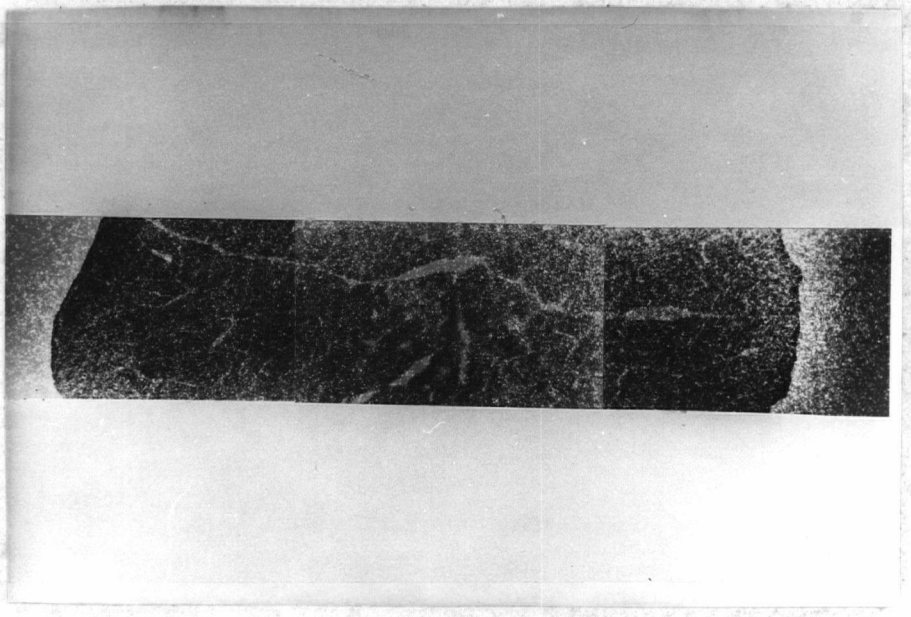

A photomicrograph of the same 0.5 minute fibers taken along the axis of the fiber diameter. Magnification 220 x

Illustrations 13 and 14

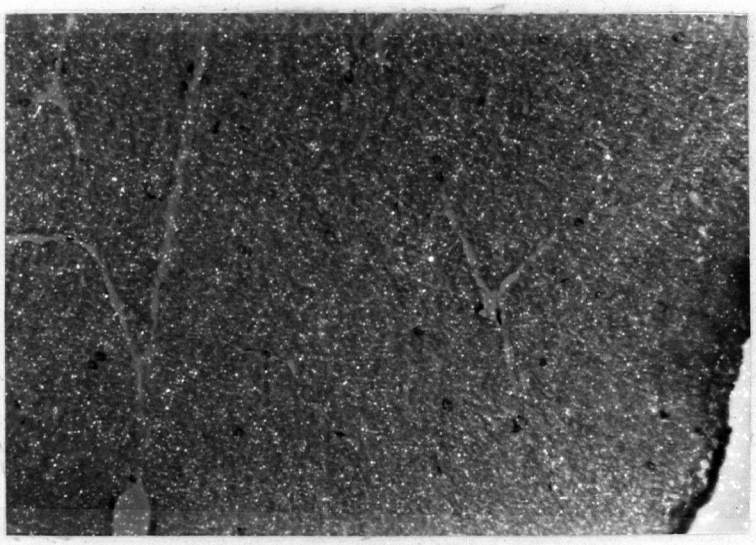

A photomicrograph of an area of a cross section from a 1.5 minute fiber with a 0.5 minute sucrose rinse. The grain density is low. The silver grains appear homogeneously distributed.
Magnification 185 x

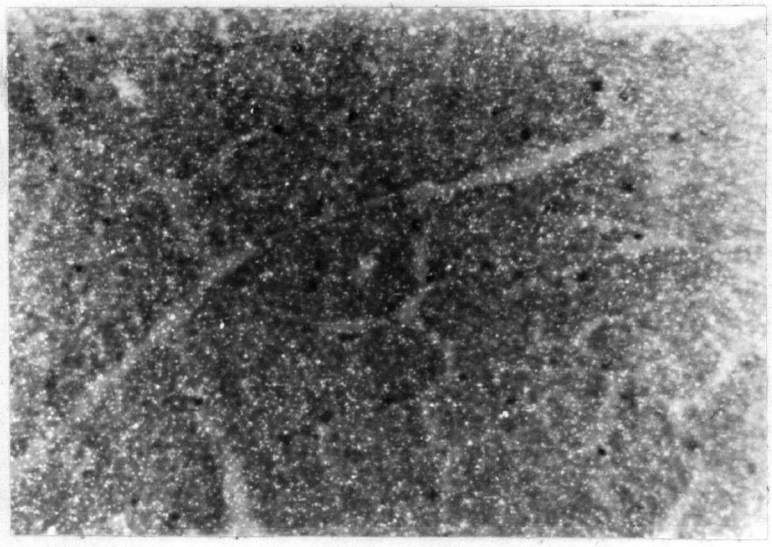

A photomicrograph of a 1.5 minute fiber cross section. Contrast the grain density to the lower density shown in Illustration 13. This difference in grain density represents $^{22}Na^{+}$ removed by the sucrose rinse. The label appears homogeneously distributed.
Magnification 185 x

TABLE V

Data for Grain Density Profile Graph

0.5 Minute Fibers

Mean Grid Grain Density

grains/100$\mu^2$

| Distance ($\mu$) of grid from section edge | CS1 | CS2 | CS3 | CS4 | CS5 | CS6 | Average & S.E. |
|---|---|---|---|---|---|---|---|
| 0 | 27. | 27.1 | 29. | 30.6 | 34.1 | 34.2 | 30.3 ± 1.2 |
| 70 | 22.3 | 21.6 | 26.3 | 19.9 | 26.7 | 28.4 | 24.2 ± 1.3 |
| 140 | 17.1 | 15. | 19.3 | 15.1 | 24.3 | 21.8 | 18.8 ± 1.4 |
| 210 | 10.9 | 14. | 11.1 | 12.1 | 14.6 | 19.7 | 13.7 ± 1.2 |
| 280 | 5.1 | 6.7 | 7.1 | 7.9 | 7.3 | 6.9 | 6.8 ± .4 |
| 350 | 4. | 5.9 | 5.1 | 5.4 | 4.7 | 6.1 | 5.2 ± .3 |
| 420 | 2.9 | 4.4 | 3.6 | 3.3 | 2.6 | 3.9 | 3.5 ± .3 |
| 490 | 2.3 | 3.9 | 3.6 | 3.4 | 2.1 | 2.7 | 3.0 ± .3 |
| 560 | 2. | 3.3 | 2.1 | 2.7 | 2.3 | 2.4 | 2.5 ± .2 |
| 630 | 1.9 | 3.4 | 2.4 | 2.6 | 1.7 | 2.7 | 2.5 ± .2 |
| 700 | 2. | 1.6 | 2.6 | 2.8 | 3.3 | 2.4 | 2.4 ± .2 |

TABLE VI

Data for Grain Density Profile Graph

1.5 Minute Fibers

Mean Grid Grain Density

Grains/100$\mu^2$

| Distance ($\mu$) of grid from section edge | CS1 | CS2 | CS3 | Average & S. E. |
|---|---|---|---|---|
| 0 | 18.3 | 21.8 | 21.7 | 20.6 ± 1 |
| 70 | 22.3 | 19. | 23.1 | 21.5 ± 1 |
| 140 | 20.4 | 20.8 | 18.6 | 19.9 ± .6 |
| 210 | 19.8 | 19.3 | 21.2 | 20.1 ± .5 |
| 280 | 22.1 | 20.1 | 20.9 | 21.0 ± .5 |
| 350 | 22.2 | 19.4 | 20.4 | 20.7 ± .7 |
| 420 | 21.1 | 19.3 | 19.1 | 19.8 ± .5 |
| 490 | 19.6 | 18. | 19.7 | 19.1 ± .5 |
| 560 | 19.4 | 17.9 | 21.6 | 19.6 ± .9 |
| 630 | 19.7 | 19. | 18.5 | 19.1 ± .5 |
| 700 | 19.2 | 22.1 | 20.7 | 20.7 ± .6 |

TABLE VII

Data for Grain Density Profile Graph

1.5 Minute Fibers

.5 Minute Rinse

Mean Grid Grain Density

grains/100$\mu^2$

| Distance ($\mu$) of grid from section edge | CS1 | CS2 | CS3 | Mean & S.E. |
|---|---|---|---|---|
| 0 | 5. | 4.9 | 4.1 | 4.7 ± .3 |
| 70 | 5.1 | 4. | 4.3 | 4.5 ± .3 |
| 140 | 5.4 | 4.5 | 6.2 | 5.3 ± .4 |
| 210 | 5.7 | 4.6 | 6.7 | 5.6 ± .5 |
| 280 | 7. | 4.7 | 3.9 | 5.2 ± .8 |
| 350 | 4.7 | 5. | 4.9 | 4.9 ± .3 |
| 420 | 4.7 | 5.1 | 4.9 | 4.9 ± .2 |
| 490 | 5.4 | 4.9 | 5.8 | 5.4 ± .2 |
| 560 | 5.7 | 5.1 | 4.9 | 5.2 ± .2 |
| 630 | 6.3 | 3.7 | 5.1 | 5.0 ± .6 |
| 700 | 5.3 | 4.6 | 5.9 | 5.2 ± .3 |

Figure 5

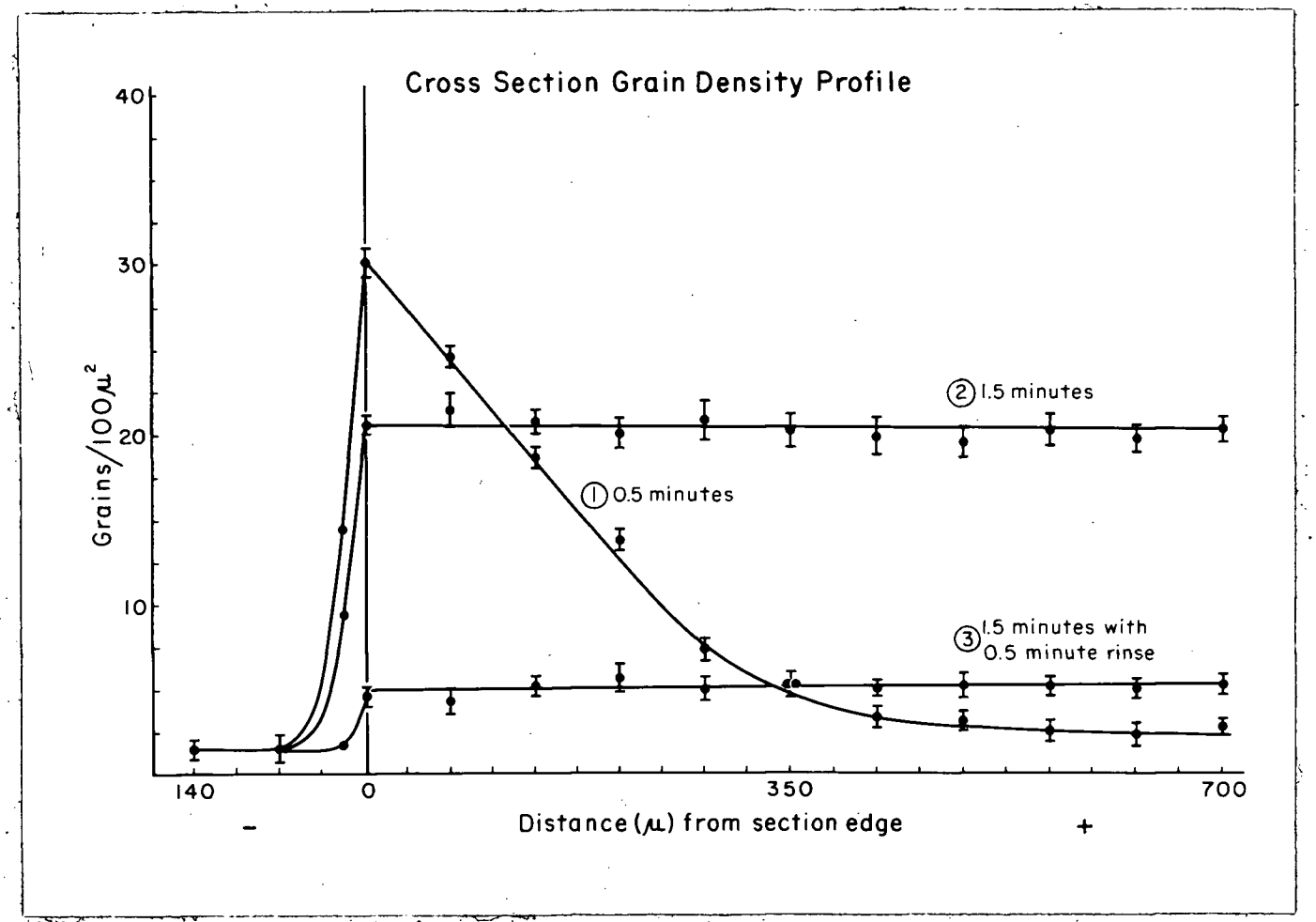
Cross Section Grain Density Profile
Grains/100μ²
40
30
20
10
140
0
350
700
Distance (μ) from section edge
-
+
② 1.5 minutes
① 0.5 minutes
③ 1.5 minutes with
0.5 minute rinse

TABLE VIII

Analysis of Variance for Grain Density Profile

A 0.5 Minute Cross Section

Grain Counts Within Grid Position

grains/100$\mu^2$

| Distance ($\mu$) of grid position from section edge | 0 | 70 | 140 | 210 | 280 | 350 | 420 | 490 | 560 | 630 |
|---|---|---|---|---|---|---|---|---|---|---|
| | 35 | 28 | 18 | 12 | 9 | 6 | 4 | 3 | 3 | 4 |
| | 32 | 33 | 24 | 24 | 8 | 8 | 3 | 2 | 3 | 3 |
| | 37 | 27 | 25 | 16 | 3 | 6 | 5 | 4 | 2 | 3 |
| | 33 | 25 | 22 | 17 | 6 | 5 | 4 | 2 | 3 | 2 |
| | 35 | 26 | 22 | 16 | 6 | 5 | 4 | 3 | 1 | 2 |
| | 34 | 32 | 22 | 22 | 7 | 6 | 4 | 4 | 3 | 4 |
| | 36 | 28 | 22 | 20 | 9 | 7 | 3 | 1 | 2 | 3 |
| Mean | 34.6 | 28.4 | 21.9 | 18.1 | 6.9 | 6.1 | 3.9 | 2.7 | 2.4 | 3 |
| Degrees of freedom | 6 | 6 | 6 | 6 | 6 | 6 | 6 | 6 | 6 | 6 |

| Source of Variation | Degrees of Freedom | Sum of Squares | Mean Square | F. Ratio |
|---|---|---|---|---|
| Between grid positions | 9 | 8,958.91 | 995.43 | 228.7** |
| Within grid positions | 60 | 256.86 | 4.35 | |
| Total | 69 | 9,215.77 | | |

F (9,60 degrees of freedom) must be greater than 2.72 to be significant at the 1% level.

TABLE IX

An Analysis of Variance for Grain Density Profile

A 1.5 Minute Cross Section

Grain Counts Within Grid Position
grains/100$\mu^2$

| Distance ($\mu$) of grid position from section edge | 0 | 70 | 140 | 210 | 280 | 350 | 420 | 490 | 510 | 630 |
|---|---|---|---|---|---|---|---|---|---|---|
| | 17 | 23 | 17 | 18 | 16 | 23 | 21 | 16 | 18 | 21 |
| | 16 | 20 | 20 | 19 | 23 | 24 | 19 | 21 | 23 | 21 |
| | 18 | 26 | 20 | 19 | 21 | 19 | 23 | 18 | 21 | 18 |
| | 17 | 19 | 23 | 16 | 25 | 19 | 25 | 19 | 20 | 16 |
| | 20 | 21 | 15 | 18 | 23 | 21 | 25 | 16 | 19 | 18 |
| | 19 | 25 | 23 | 26 | 24 | 23 | 22 | 25 | 19 | 19 |
| | 21 | 22 | 25 | 23 | 23 | 26 | 17 | 22 | 20 | 18 |
| Mean | 18.3 | 22.3 | 20.4 | 19.9 | 22.1 | 22.2 | 21.8 | 19.6 | 20 | 18.7 |
| Degrees of freedom | 6 | 6 | 6 | 6 | 6 | 6 | 6 | 6 | 6 | 6 |

| Source of Variation | Degrees of Freedom | Sum of Squares | Mean Square | F. Ratio |
|---|---|---|---|---|
| Between grid positions | 9 | 137.77 | 15.31 | 2.02 NS |
| Within grid positions | 60 | 453.71 | 7.56 | |
| Total | 69 | 591.48 | | |

F (9, 60 degrees of freedom) must be greater than 2.04 to be significant at the 5% level.

TABLE X

Analysis of Variance for Grain Density Profile

A 1.5 Minute Cross Section
With 0.5 Minute Wash

Grain Counts Within Grid Position
grains/100$\mu^2$

| Distance ($\mu$) of grid position from section edge | 0 | 70 | 140 | 210 | 280 | 350 | 420 | 490 | 560 | 630 |
|---|---|---|---|---|---|---|---|---|---|---|
| | 10 | 4 | 5 | 6 | 5 | 6 | 5 | 5 | 5 | 6 |
| | 6 | 6 | 4 | 7 | 7 | 8 | 6 | 5 | 6 | 8 |
| | 4 | 5 | 5 | 7 | 6 | 5 | 5 | 7 | 3 | 6 |
| | 5 | 4 | 4 | 6 | 5 | 7 | 7 | 8 | 7 | 7 |
| | 3 | 5 | 6 | 5 | 7 | 5 | 4 | 5 | 6 | 5 |
| | 6 | 4 | 7 | 5 | 6 | 4 | 4 | 4 | 7 | 6 |
| | 5 | 5 | 5 | 4 | 4 | 3 | 5 | 5 | 6 | 6 |
| Mean | 5.6 | 4.6 | 5.1 | 5.7 | 5.6 | 5.4 | 5.1 | 5.6 | 5.7 | 6.2 |
| Degrees of freedom | 6 | 6 | 6 | 6 | 6 | 6 | 6 | 6 | 6 | 6 |

| Source of Variation | Degrees of Freedom | Sum of Squares | Mean Square | F. Ratio |
|---|---|---|---|---|
| Between grid positions | 9 | 11.42 | 1.27 | .70 NS |
| Within grid positions | 60 | 108.07 | 1.80 | |
| Total | 69 | 119.49 | | |

F (9, 60 degrees of freedom) must be greater than 2.04 to be significant at the 5% level.

Illustrations 15 and 16

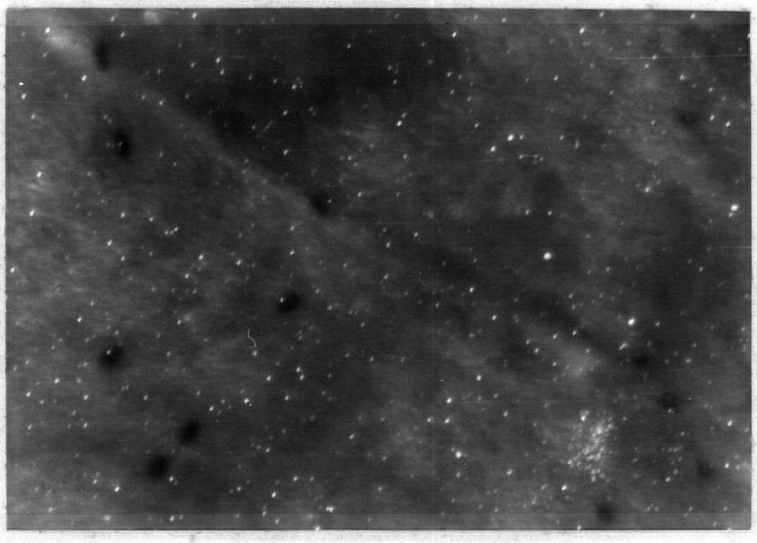

A photomicrograph of an area of a 5 minute fiber cross section. Note the low grain density. The grains are homogeneously distributed.
Magnification 370 x

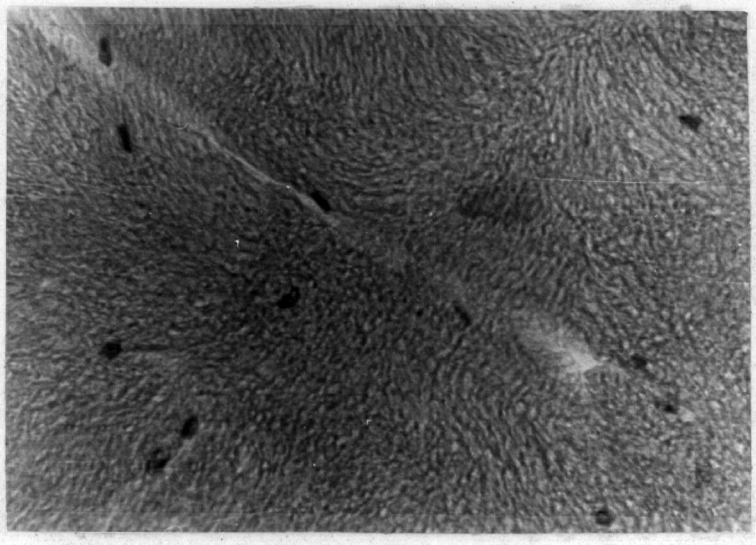

A photomicrograph of the same area taken with transmitted light.
Magnification 370 x

Illustrations 17 and 18

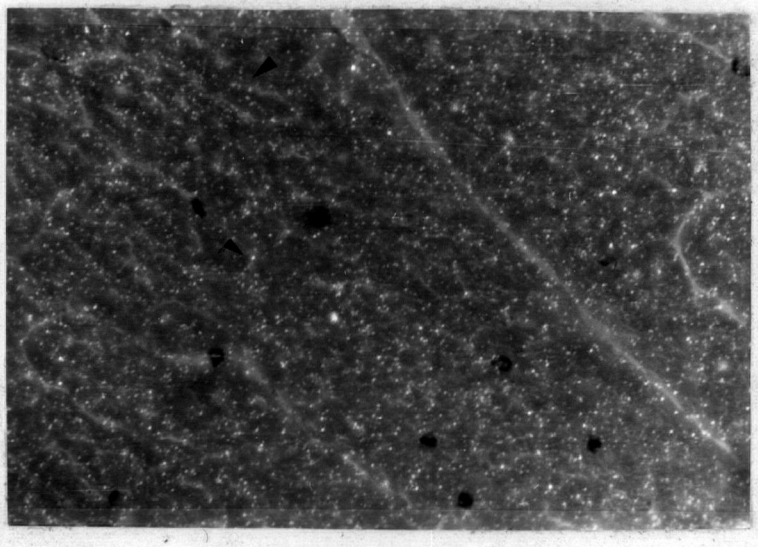

A photomicrograph of an area of a 5 minute fiber cross section. The grain density is higher than the grain density of the 5 minute fiber in Illustration 15. The arrows demonstrate the straight line type of grain pattern.
Magnification 370 x

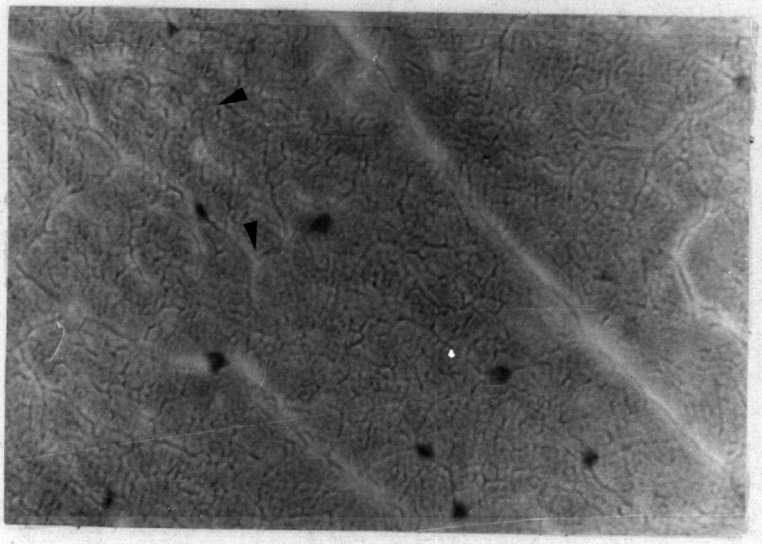

A photomicrograph of the same area taken with transmitted light. The arrows illustrate the clefts to which the patterned labellings correspond.
Magnification 370 x

Illustrations 19 and 20

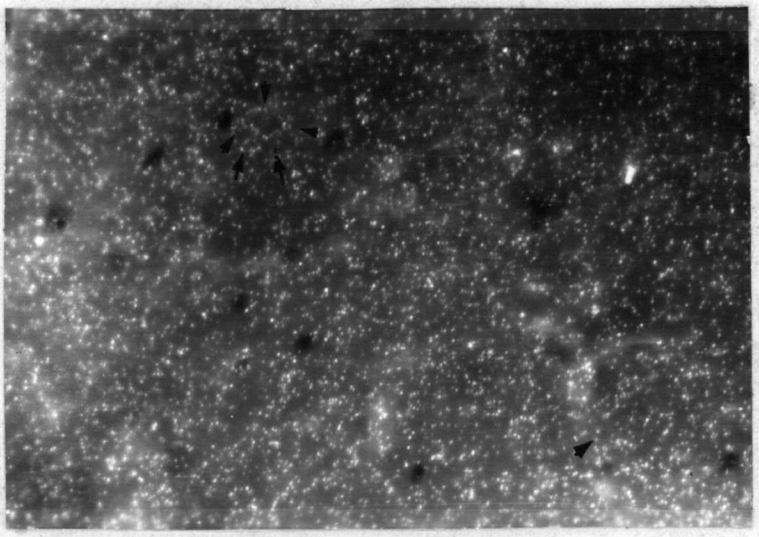

A photomicrograph of an area of a 20 minute fiber cross section. The clustered arrows indicate two of the circular type of grain patterns in close proximity to a nucleus. The single arrow demonstrates a straight line grain pattern.
Magnification 370 x

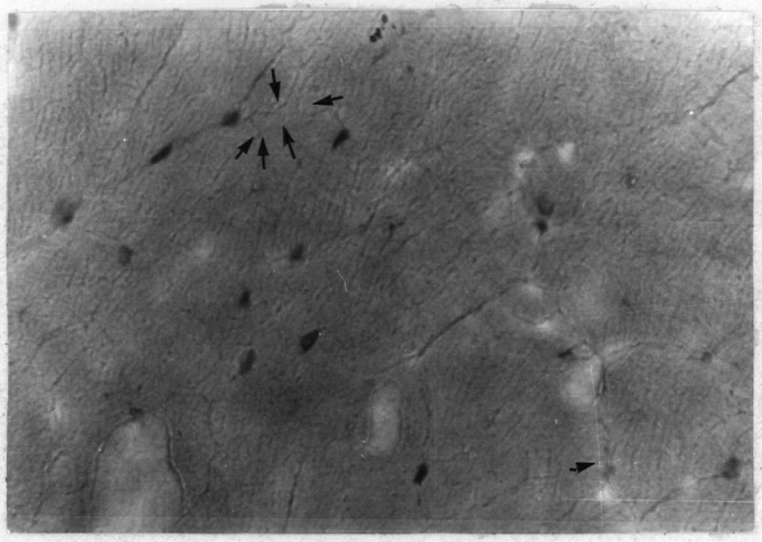

A photomicrograph of the same area taken with transmitted light. Note the circular clefts at the side of the nucleus which correspond to the grain pattern visible in the darkfield photograph (clustered arrows). The single arrow demonstrates the cleft which corresponds to the straight line grain pattern.
Magnification 370 x

Illustrations 21 and 22

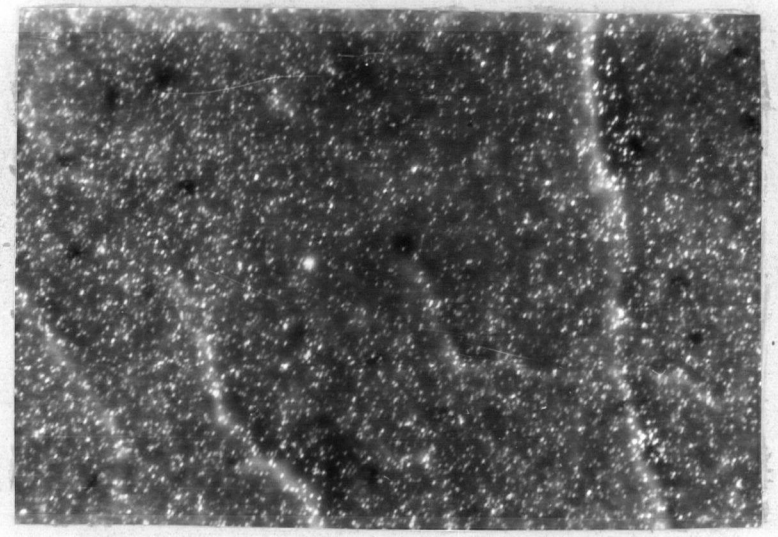

A photomicrograph of an area of a 60 minute fiber cross section. The grain density has increased in comparison with the 20 minute fiber cross section.
Magnification 370 x

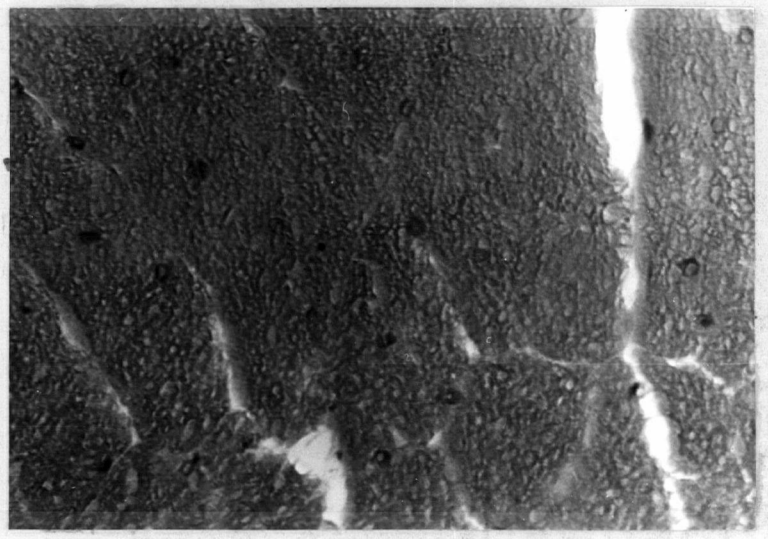

A photomicrograph of the same area taken with transmitted light. Ice crystal damage probably caused by the freezing in isopentane has "pock marked" this section to some extent.
Magnification 370 x

Illustrations 23 and 24

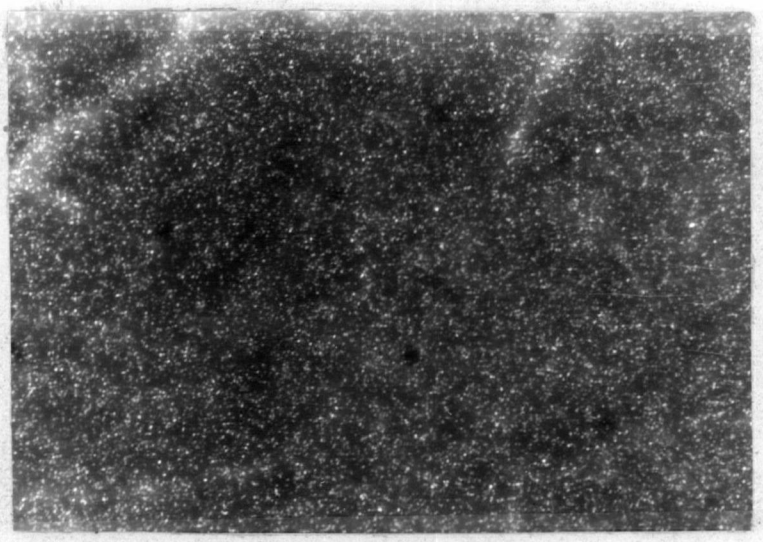

A photomicrograph of an area of a 180 minute fiber cross section. The grain density is at a maximum, obscuring any possible grain patterns.
Magnification 370 x

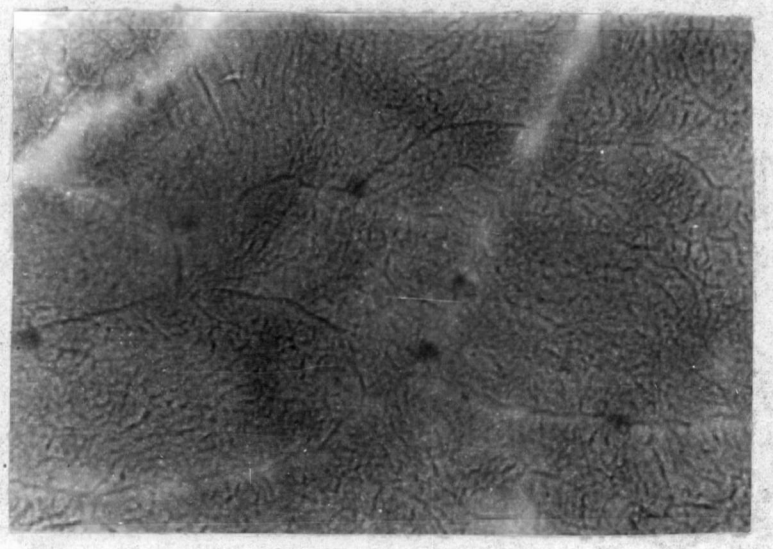

A photomicrograph of the same area taken with transmitted light.
Magnification 370 x

TABLE XI

Grain Counts

| Time (Mins.) | Fiber No. | Mean Cross Section Grid Count grains/100$\mu^2$ | | | | Average Background grains/100$\mu^2$ |
|---|---|---|---|---|---|---|
| | | C.S.a | C.S.b | C.S.c | Ave. | |
| 5 | 1-A | 6.3 | 5.8 | 6.0 | 6.0 | 1.3 |
| | 2-A | 6.2 | 5.2 | 4.8 | 5.4 | 2.6 |
| | 1-B | 10.6 | 8.8 | 10.6 | 10.0 | 1.5 |
| | 2-B | 7.1 | 6.8 | 7.3 | 7.1 | 1.5 |
| | 1-C | 6.0 | 8.4 | 9.6 | 8.0 | 1.3 |
| | 2-C | 8.2 | 6.2 | 8.4 | 7.6 | 1.5 |
| | 1-D | 6.3 | 8.3 | - | 7.3 | 1.4 |
| | 2-D | 7.6 | 7.2 | - | 7.4 | 1.3 |
| | 3-D | 8.9 | 8.3 | - | 8.6 | 1.7 |
| | 1-E | 7.3 | 7.0 | - | 7.2 | 1.5 |
| | 2-E | 9.8 | 7.9 | - | 8.9 | 1.5 |
| Mean and Standard Error | | | | | 7.6 ± 0.4 | |
| 20 | 1-A | 15.4 | 16.1 | 15.8 | 15.8 | 1.6 |
| | 2-A | 19.2 | 17.0 | 17.9 | 18.0 | 1.2 |
| | 1-B | 19.4 | 22.0 | 16.6 | 19.3 | 1.6 |
| | 2-B | 22.0 | 21.3 | 20.2 | 21.2 | 1.5 |
| | 1-C | 26.4 | 23.0 | 19.5 | 23.0 | 1.5 |
| | 2-C | 22.8 | 19.9 | 21.3 | 21.3 | 1.2 |
| | 1-D | 21.7 | 21.4 | - | 21.6 | 1.7 |
| | 2-D | 21.2 | 20.1 | - | 20.7 | 1.2 |
| | 1-E | 24.2 | 25.6 | - | 24.9 | 1.6 |
| | 2-E | 26.4 | 25.8 | - | 26.1 | 1.4 |
| | 3-E | 26.1 | 25.9 | - | 26.0 | 1.6 |
| Mean and Standard Error | | | | | 21.6 ± 0.9 | |

TABLE XI cont'd

Grain Counts

| Time (Mins.) | Fiber No. | Mean Cross Section Grid Count grains/100$\mu^2$ | | | | Average Background grains/100$\mu^2$ |
|---|---|---|---|---|---|---|
| | | C.S.a | C.S.b | C.S.c | Ave. | |
| | 1-A | 30.0 | 30.6 | - | 30.3 | 1.8 |
| | 2-A | 27.2 | 27.5 | - | 27.4 | 1.3 |
| | 1-B | 34.1 | 31.1 | 30.6 | 31.9 | 1.5 |
| | 2-B | 30.6 | 34.7 | 30.8 | 32.0 | 1.7 |
| | 1-C | 27.8 | 31.5 | 32.2 | 30.5 | 1.3 |
| 60 | 2-C | 31.2 | 29.0 | 32.0 | 30.7 | 1.6 |
| | 1-D | 26.2 | 29.9 | - | 28.1 | 1.5 |
| | 2-D | 30.4 | 29.9 | - | 30.2 | 1.6 |
| | 1-E | 36.4 | 35.0 | - | 35.7 | 1.6 |
| | 2-E | 34.9 | 34.5 | - | 34.7 | 1.6 |
| Mean and Standard Error | | | | | 31.2 ± 0.8 | |
| | 1-A | 38.7 | 34.5 | - | 36.6 | 2.3 |
| | 2-A | 39.5 | 36.8 | - | 38.2 | 1.7 |
| 180 | 1-B | 46.3 | 49.9 | 53.7 | 50.0 | 1.7 |
| | 1-C | 45.0 | 38.4 | 38.2 | 40.5 | 1.3 |
| | 1-D | 37.8 | 34.8 | - | 36.3 | 1.4 |
| | 1-E | 40.1 | 40.8 | - | 40.5 | 1.6 |
| Mean and Standard Error | | | | | 40.4 ± 1.9 | |

Figure 6

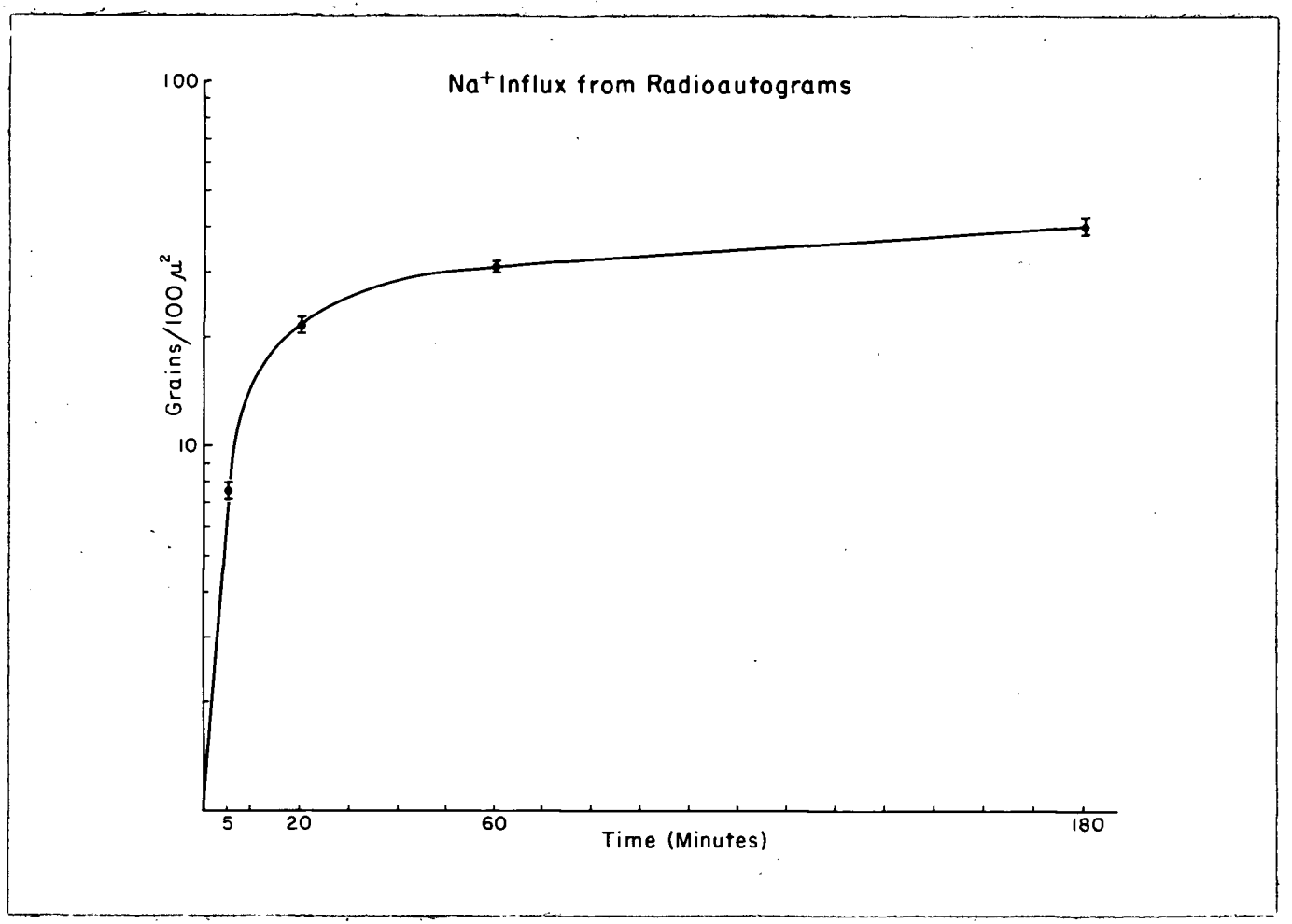
Na+ Influx from Radioautograms
100
10
Grains/100 μ²
5
20
60
180
Time (Minutes)

TABLE XII

Data for Grain Density Profile Graph

5 Minute Fibers

Mean Grid Grain Density

grains/100$\mu^2$

| Distance ($\mu$) of grid from section edge | CS1 | CS2 | CS3 | CS4 | CS5 | Mean & S.E. |
|---|---|---|---|---|---|---|
| 0 | 7.1 | 7.9 | 7.1 | 8.3 | 7.3 | 7.5 ± .3 |
| 70 | 7.9 | 5.6 | 6.7 | 8.1 | 6.7 | 7.0 ± .4 |
| 140 | 6.1 | 6.6 | 6.6 | 9.1 | 7.9 | 7.3 ± .4 |
| 210 | 6.6 | 7.4 | 6.9 | 8.7 | 8.1 | 7.5 ± .3 |
| 280 | 7. | 9. | 6.7 | 7.9 | 7.3 | 7.6 ± .4 |
| 350 | 5.7 | 6.7 | 8. | 7.6 | 7.9 | 7.1 ± .4 |
| 420 | 6.4 | 8.7 | 7.3 | 9.4 | 8.4 | 8.0 ± .4 |
| 490 | 6.6 | 8.3 | 6.9 | 9. | 7.9 | 7.7 ± .4 |
| 560 | 7.1 | 7.9 | 10.4 | 8.6 | 7.9 | 8.4 ± .5 |
| 630 | 7.6 | 8.6 | 7.1 | 8.6 | 8. | 8.0 ± .3 |
| 700 | 8.1 | 6.1 | 7.6 | 7.6 | 8.7 | 7.6 ± .4 |

TABLE XIII

Data for Grain Density Profile Graph

20 Minute Fibers

Mean Grid Grain Density

grains/100$\mu^2$

| Distance ($\mu$) of grid from Section edge | CS1 | CS2 | CS3 | CS4 | CS5 | Mean & S.E. |
|---|---|---|---|---|---|---|
| 0 | 18.3 | 18. | 18.7 | 18. | 20.9 | 18.8 ± .5 |
| 70 | 18.9 | 17.9 | 21.6 | 20.4 | 16.4 | 19.0 ± .8 |
| 140 | 17.9 | 19.7 | 17.3 | 18.1 | 21.4 | 18.9 ± .7 |
| 210 | 19.5 | 19.1 | 20. | 17.6 | 17.1 | 18.7 ± .5 |
| 280 | 20. | 18. | 19.6 | 18.6 | 18.3 | 18.9 ± .3 |
| 350 | 19.3 | 17.3 | 19.7 | 16.1 | 20.3 | 18.5 ± .7 |
| 420 | 19.4 | 17.1 | 20.5 | 18.7 | 16.2 | 18.4 ± .6 |
| 490 | 17. | 18.1 | 20. | 19.6 | 18. | 18.6 ± .5 |
| 560 | 16.6 | 19.1 | 20.9 | 19.6 | 19.4 | 19.1 ± .6 |
| 630 | 15.3 | 18.5 | 21.4 | 18.3 | 19.9 | 18.7 ± .9 |
| 700 | 20.3 | 18.5 | 21.4 | 17.4 | 18.6 | 19.2 ± .6 |

TABLE XIV

Data for Grain Density Profile Graph

60 Minute Fibers

Mean Grid Grain Density

grains/100$\mu^2$

| Distance ($\mu$) of grid from section edge | CS1 | CS2 | CS3 | CS4 | Mean & S.E. |
|---|---|---|---|---|---|
| 0 | 30.6 | 31.6 | 29.3 | 28.0 | 29.9 ± .7 |
| 70 | 29.1 | 27. | 32.9 | 32. | 30.3 ± 1.2 |
| 140 | 26.7 | 26. | 32.9 | 32. | 29.4 ± 1.2 |
| 210 | 30.3 | 28.9 | 30.7 | 32.3 | 30.6 ± .6 |
| 280 | 29.4 | 29.8 | 31.7 | 31.9 | 30.7 ± .6 |
| 350 | 29.3 | 29.9 | 33.1 | 30.6 | 30.7 ± .7 |
| 420 | 27.9 | 26.8 | 31.9 | 32.5 | 29.7 ± .8 |
| 490 | 30.9 | 29.8 | 31.2 | 28.7 | 30.1 ± .5 |
| 560 | 29.9 | 27.8 | 31.3 | 30.5 | 29.9 ± .6 |
| 630 | 27.5 | 26.3 | 31.9 | 33.1 | 29.7 ± 1.2 |
| 700 | 29.3 | 32.9 | 30.9 | 28.6 | 30.4 ± .8 |

TABLE XV

Data for Grain Density Profile Graph

180 Minute Fibers

Mean Grid Grain Density

grains/100$\mu^2$

| Distance ($\mu$) of grid from section edge | CS1 | CS2 | CS3 | CS4 | Mean & S.E. |
|---|---|---|---|---|---|
| 0 | 37.0 | 40.4 | 39.6 | 38.8 | 39.0 ± .6 |
| 70 | 41.5 | 37.7 | 40. | 38.4 | 39.4 ± .6 |
| 140 | 37.7 | 39.3 | 36.7 | 39.9 | 38.4 ± .6 |
| 210 | 38.4 | 40.9 | 38.7 | 39.7 | 39.4 ± .5 |
| 280 | 43. | 39.6 | 38. | 40.9 | 40.4 ± .9 |
| 350 | 39.7 | 37.1 | 43.1 | 38.3 | 39.6 ± .1 |
| 420 | 41.3 | 36.6 | 43.4 | 41.7 | 40.7 ± 1.3 |
| 490 | 41. | 41.7 | 37. | 40.6 | 40.1 ± .9 |
| 560 | 40.5 | 38.7 | 39. | 37.4 | 38.9 ± .6 |
| 630 | 39.4 | 41.9 | 38.1 | 40.7 | 40.0 ± .7 |
| 700 | 42.8 | 38.5 | 37.3 | 39.5 | 39.5 ± .8 |

Figure 7

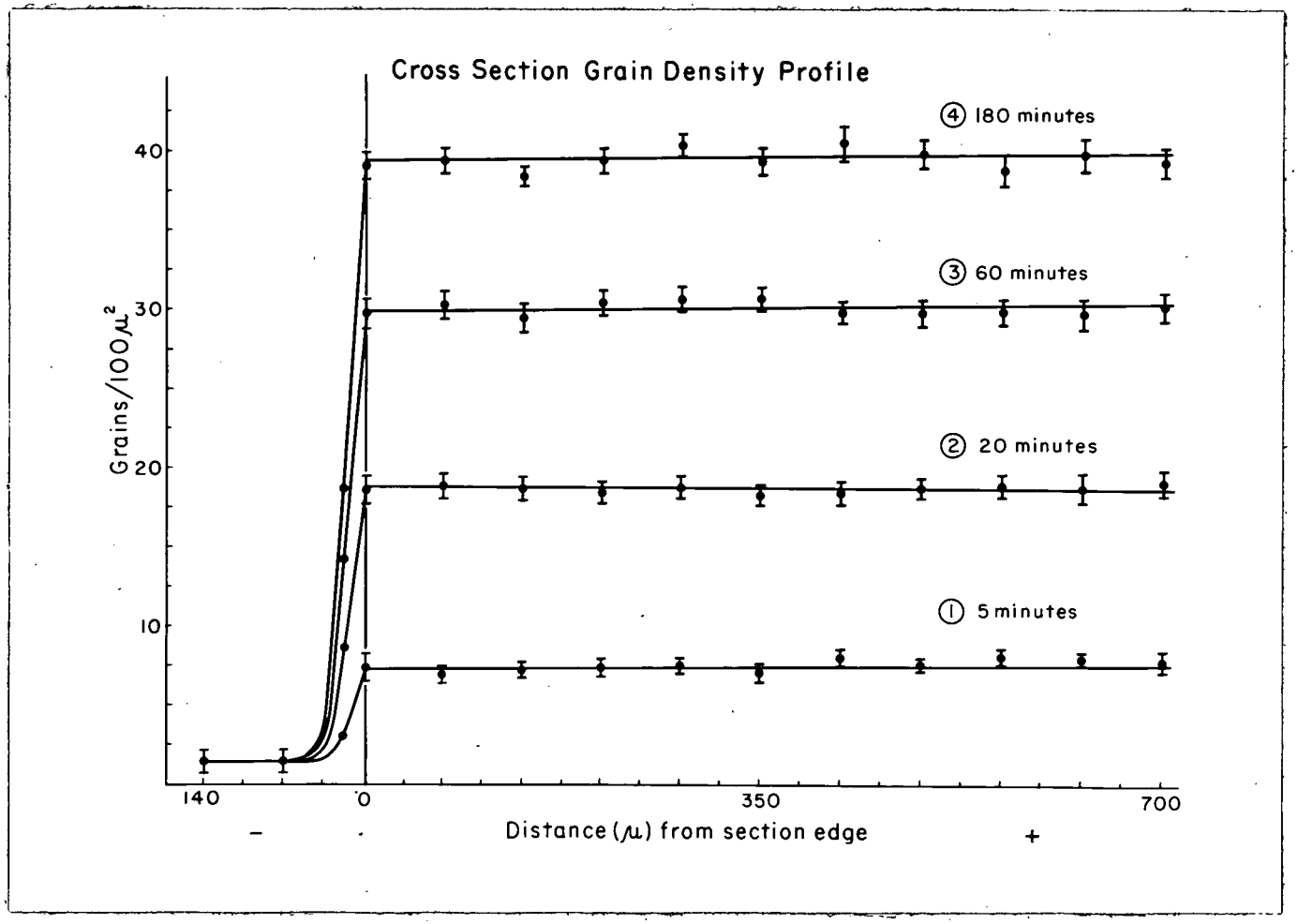
Cross Section Grain Density Profile
④ 180 minutes
③ 60 minutes
② 20 minutes
① 5 minutes
Grains/100μ²
40
30
20
10
140
0
350
700
−
Distance (μ) from section edge
+

TABLE XVI

Analysis of Variance for 5 Minute Cross Section

Barnacle B Fiber 1 Cross Section b

Grain Counts Within Grid Position
grains/100$\mu^2$

| Distance ($\mu$) of grid position from section edge | 0 | 70 | 140 | 210 | 280 | 350 | 420 | 490 | 560 | 630 | 700 | 770 | 840 | 910 | 980 | 1050 | 1120 | 1190 |
|---|---|---|---|---|---|---|---|---|---|---|---|---|---|---|---|---|---|---|
| | 16 | 15 | 12 | 7 | 9 | 7 | 9 | 10 | 13 | 5 | 7 | 13 | 10 | 13 | 16 | 9 | 9 | 10 |
| | 7 | 11 | 9 | 7 | 13 | 7 | 10 | 10 | 10 | 9 | 9 | 6 | 17 | 7 | 8 | 12 | 18 | 16 |
| | 12 | 12 | 10 | 9 | 15 | 8 | 12 | 6 | 7 | 10 | 12 | 13 | 5 | 11 | 15 | 14 | 9 | 9 |
| | 11 | 11 | 11 | 12 | 9 | 13 | 8 | 11 | 13 | 7 | 19 | 8 | 12 | 9 | 12 | 13 | 11 | 11 |
| | 10 | 10 | 10 | 10 | 9 | 12 | 7 | 13 | 12 | 9 | 11 | 7 | 11 | 6 | 11 | 16 | 10 | 9 |
| | 10 | 9 | 8 | 11 | 7 | 10 | 7 | 11 | 8 | 6 | 11 | 11 | 6 | 8 | 11 | 10 | 15 | 7 |
| | 16 | 6 | 5 | 6 | 6 | 6 | 11 | 7 | 7 | 5 | 10 | 10 | 18 | 6 | 11 | 10 | 9 | 14 |
| Mean | 11.7 | 10.6 | 9.3 | 8.9 | 9.7 | 9 | 9.1 | 9.7 | 10 | 7.3 | 11.3 | 9.7 | 9.9 | 8.6 | 12 | 12 | 11.6 | 10.9 |
| Degrees of freedom | 6 | 6 | 6 | 6 | 6 | 6 | 6 | 6 | 6 | 6 | 6 | 6 | 6 | 6 | 6 | 6 | 6 | 6 |

| Source of Variation | Degrees of Freedom | Sum of Squares | Mean Square | F. Ratio |
|---|---|---|---|---|
| Between grid positions | 17 | 204.92 | 12.05 | 1.45 NS |
| Within grid positions | 108 | 896.57 | 8.03 | |
| Total | 125 | 1,101.49 | | |

F (17, 108 degrees of freedom) must be greater than 1.66 to be significant at the 5% level.

TABLE XVII

Analysis of Variance for 5 Minute Cross Section

Barnacle C Fiber 2 Cross Section b

Grain Counts within Grid Position
grains/100$\mu^2$

| Distance ($\mu$) of grid position from section edge | 0 | 70 | 140 | 210 | 280 | 350 | 420 | 490 | 560 | 630 | 700 | 770 | 840 | 910 | 980 | 1050 | 1120 | 1190 |
|---|---|---|---|---|---|---|---|---|---|---|---|---|---|---|---|---|---|---|
| | 7 | 7 | 7 | 10 | 11 | 7 | 8 | 8 | 8 | 9 | 10 | 8 | 8 | 9 | 8 | | | |
| | 8 | 7 | 7 | 7 | 7 | 11 | 9 | 10 | 5 | 10 | 10 | 14 | 12 | 8 | 6 | | | |
| | 7 | 5 | 6 | 10 | 10 | 8 | 9 | 6 | 10 | 7 | 9 | 11 | 5 | 8 | 8 | - | - | - |
| | 4 | 9 | 7 | 8 | 9 | 8 | 10 | 7 | 7 | 6 | 7 | 9 | 6 | 8 | 9 | | | |
| | 5 | 11 | 9 | 5 | 8 | 9 | 10 | 6 | 6 | 8 | 7 | 6 | 7 | 7 | 7 | | | |
| | 8 | 9 | 7 | 6 | 7 | 9 | 11 | 8 | 7 | 9 | 8 | 7 | 8 | 10 | 7 | | | |
| | 5 | 5 | 7 | 5 | 7 | 7 | 9 | 8 | 8 | 9 | 5 | 7 | 7 | 10 | 9 | | | |
| Mean | 6.3 | 7.6 | 7.2 | 7.3 | 8.4 | 8.4 | 9.4 | 7.6 | 7.3 | 8.3 | 8 | 8.9 | 7.6 | 8.6 | 7.7 | | | |
| Degrees of freedom | 6 | 6 | 6 | 6 | 6 | 6 | 6 | 6 | 6 | 6 | 6 | 6 | 6 | 6 | 6 | | | |

| Source of Variation | Degrees of Freedom | Sum of Squares | Mean Square | F. Ratio |
|---|---|---|---|---|
| Between grid positions | 14 | 60.21 | 4.30 | 1.47 NS |
| Within grid positions | 90 | 260.83 | 2.93 | |
| Total | 104 | 321.04 | | |

F (14, 90 degrees of freedom) must be greater than 1.75 to be significant at the 5% level.

TABLE XVIII

Analysis of Variance for 5 Minute Cross Section

Barnacle A Fiber 1 Cross Section c

Grain Counts within Grid Position
grains/100$\mu^2$

| Distance ($\mu$) of grid position from section edge | 0 | 70 | 140 | 210 | 280 | 350 | 420 | 490 | 560 | 630 | 700 | 770 | 840 | 910 | 980 | 1050 | 1120 | 1190 |
|---|---|---|---|---|---|---|---|---|---|---|---|---|---|---|---|---|---|---|
| | 6 | 8 | 5 | 7 | 9 | 6 | 6 | 9 | 10 | 8 | 6 | 8 | 11 | 12 | 4 | 6 | 7 | |
| | 6 | 10 | 5 | 6 | 7 | 5 | 6 | 7 | 8 | 9 | 7 | 9 | 10 | 11 | 7 | 7 | 7 | |
| | 10 | 9 | 4 | 7 | 5 | 7 | 12 | 6 | 7 | 6 | 9 | 6 | 6 | 6 | 8 | 8 | 7 | - |
| | 7 | 7 | 5 | 6 | 9 | 4 | 7 | 5 | 4 | 7 | 10 | 5 | 8 | 8 | 11 | 9 | 5 | |
| | 9 | 6 | 5 | 5 | 7 | 6 | 6 | 8 | 8 | 11 | 5 | 6 | 5 | 7 | 8 | 6 | 5 | |
| | 5 | 10 | 6 | 4 | 5 | 7 | 9 | 7 | 7 | 8 | 12 | 7 | 10 | 6 | 8 | 9 | 4 | |
| | 7 | 5 | 10 | 8 | 7 | 9 | 12 | 7 | 6 | 8 | 8 | 12 | 11 | 7 | 7 | 7 | 7 | |
| Mean | 7.1 | 7.9 | 5.7 | 6.1 | 7 | 6.3 | 8.3 | 7 | 7.1 | 8.1 | 8.1 | 7.6 | 8.7 | 8.1 | 7.6 | 7.4 | 6 | |
| Degrees of freedom | 6 | 6 | 6 | 6 | 6 | 6 | 6 | 6 | 6 | 6 | 6 | 6 | 6 | 6 | 6 | 6 | 6 | |

| Source of Variation | Degrees of Freedom | Sum of Squares | Mean Square | F. Ratio |
|---|---|---|---|---|
| Between grid positions | 16 | 86.64 | 5.41 | 1.44 NS |
| Within grid positions | 102 | 382.86 | 3.75 | |
| Total | 118 | 469.50 | | |

F (16, 102 degrees of freedom) must be greater than 1.75 to be significant at the 5% level.

TABLE XIX

Calculation of Efficiency of Radioautograms

Measurements of average fiber cross section r = 750μ = .075 cm
thickness = 15μ = .0015 cm

Volume of average fiber cross section

= (3.14 x .075 cm x .075 cm x .0015 cm)

= $2.65 \times 10^{-5}$ cc

Area of average fiber cross section = (3.14 x 750μ x 750μ)

= $1.77 \times 10^{6}\mu^2$

Average fiber is 75% water

Average fiber cross section has (.75 x $2.65 \times 10^{-5}$cc)$H_2O$

= $1.99 \times 10^{-5}$gm $H_2O$

= $1.99 \times 10^{-8}$Kg $H_2O$

Average fiber sodium concentration is .070 M/Kg.$H_2O$

Average fiber cross section ($1.99 \times 10^{-8}$Kg $H_2O$ x $7 \times 10^{-2}$M Na)

= $1.39 \times 10^{-9}$M Na

At 180 minutes 78% fiber sodium has exchanged.

So the average 180 minute cross section has
($1.39 \times 10^{-9}$M Na x .78

= $1.08 \times 10^{-9}$M Na exchanged

The average 180 minute fiber cross section
after 1 week exposure has 40 grains/100$\mu^2$

or ($4 \times 10^{-1}$ grains/$\mu^2$ x $1.77 \times 10^{6}\mu^2$)

= $7.08 \times 10^{5}$ grains total

TABLE XIX cont'd

Calculation of Efficiency of Radioautograms

Bath has 100 $\mu c/ml$ of $^{22}Na^{+}$

Bath has $4.5 \times 10^{-4}$M Na/ml

So $4.5 \times 10^{-4}$M Na has 100 $\mu c$ $^{22}Na^{+}$

1 M Na has $2.22 \times 10^{5} \mu c$ $^{22}Na^{+}$

The average 180 minute fiber cross section contains

$(1.08 \times 10^{-9}$M Na $\times 2.22 \times 10^{5} \mu c/M\ ^{22}Na^{+}$

$= 2.4 \times 10^{-4} \mu c$ $^{22}Na^{+}$

1 $\mu c = 3.2 \times 10^{9}$ disintegrations per day

$= 2.24 \times 10^{10}$ disintegrations per week (dpw)

The average 180 minute fiber cross section has

$(2.24 \times 10^{10}$(dpw/$\mu c$) $\times 2.4 \times 10^{-4} \mu c)$

$= 5.38 \times 10^{6}$ disintegrations in a week

The average 180 minute fiber cross section has produced

$7.08 \times 10^{5}$ grains in a week

So the efficiency is $\frac{7.08 \times 10^{5}}{5.38 \times 10^{6}}$ grains/disintegration = 13%

The theoretical efficiency according to Rogers 20 - 30%

TABLE XX

Grain counts are per $100\mu^2$.
The tissue section is assumed to be uniformly thick.
So Grain counts per $100\mu^2$ also represent grain counts for a fixed volume.

The extracellular space represents 5% of fiber volume.
The extracellular space is assumed to be equally distributed through the fiber cross section.
So grain counts per $100\mu^2$ also represent grain counts for a fixed volume of the extracellular space.

The number of grains per $100\mu^2$ is proportional to the amount of $^{22}Na^+$ within $100\mu$ of tissue.
So grain counts per $100\mu^2$ also represent the concentration of $^{22}Na^+$ for a fixed volume of the extracellular space.

So grain counts per $100u^2$ may be used as relative concentrations of $^{22}Na^+$ present in the extracellular space at the location of the area the count represents.

A solution to Fick's Law for one dimentional diffusion in the non steady state from a source of fixed concentration is given by Crank (65).

$$C = Co \ \mathrm{erfc} \ \frac{x}{2\sqrt{Dt}}$$

where
Co is the concentration of $^{22}Na^+$ in the extracellular space at the fiber surface.
This represents the source of fixed concentration
= 30.3 grains/$100\mu^2$ - 1.5 grains/$100\mu^2$
= 28.8 grains/$100\mu^2$

C is the concentration of $^{22}Na^+$ in the extracellular space at distance x from the fiber cross section edge at time t.

t is the time for diffusion.
= 30 seconds.

x is the distance the concentration C of $^{22}Na^+$ has moved from the plane of Co at time t.

D is the diffusion coefficient for $^{22}Na^+$.
The value used is for self diffusion in dilute solutions.
= $1.48 \times 10^{-5} cm^2 sec^{-1}$.

erfc is the error function of x

r is the actual (experimental) distance along the fiber radius of the concentration C of $^{22}Na^+$.

TABLE XX - cont'd

Table of values for the calculated distance (x) and the experimental distance (r) the concentration (C) of $^{22}Na^{+}$ moves from the plane of Co.

| r ($\mu$) | C* grains/100$\mu^2$ | C/Co | $z = \frac{x}{2\sqrt{Dt}}$ | x ($\mu$) | x/r |
|---|---|---|---|---|---|
| 70 | 22.7 | 0.79 | 0.19 | 80 | 1.14 |
| 140 | 17.3 | 0.60 | 0.37 | 156 | 1.11 |
| 210 | 12.5 | 0.435 | 0.55 | 232 | 1.10 |
| 280 | 5.3 | 0.184 | 0.94 | 396 | 1.41 |
| 350 | 3.7 | 0.129 | 1.075 | 453 | 1.29 |
| 420 | 2. | 0.0695 | 1.285 | 452 | 1.29 |
| 490 | 1.5 | 0.052 | 1.375 | 580 | 1.18 |

* all values of C and Co corrected for background of 1.5 grains/100$\mu^2$. The values of C and Co are taken from Table XXI.

Sample calculation.

C = 22.7 grains/100$\mu^2$ when x = 80$\mu$ and t = 30 seconds

$C = Co \ \text{erfc} \ \frac{x}{2\sqrt{Dt}}$

C/Co = .079, the error function of x.

The value of x associated with this value of the error function is obtained from error function tables. It is 0.19.

$$\frac{x}{2\sqrt{Dt}} = 0.19$$

$$x = 1.9 \times 10^{-1} \times 2\sqrt{Dt}$$

$$x = \sqrt{cm^2/sec.sec}$$

$$x = 1.9 \times 10^{-1} \times 2 \times \sqrt{1.48 \times 10^{-5} \times 30}$$

$$= 1.9 \times 10^{-1} \times 2 \times 2.11 \times 10^{-2}$$

$$= 8.02 \times 10^{-3} cm$$

$$= .00802 \ cm$$

$$= 80.2\mu$$

TABLE XXI

A calculation of the theoretical percent of fiber surface area involved in $^{22}Na^{+}$ influx.

Bull (66) gives equations

(1) $\ln \frac{\Delta C}{\Delta Co} = -\beta Dt$ and (2) $\beta = \left(\frac{1}{V_1} - \frac{1}{V_2}\right) \frac{A}{h}$

where $\Delta Co = Co - C$ at $t = o$
$\Delta C = Co - C$ at $t = t$
and C is measured at x in both cases.

Co is the concentration of $^{22}Na^{+}$ in the extracellular space at the fiber surface.
This represents the source of fixed concentration.
= 28.8 grains/100$\mu^2$

C is the concentration of $^{22}Na^{+}$ in the extracellular space at distance h from the fiber cross section edge at time t.
= 4.8 grains/100$\mu^2$.

t is the time for diffusion.
= 30 seconds.

h is the distance the concentration C of $^{22}Na^{+}$ has moved from the plane of Co at time t.
= 380$\mu$
= .038cm

D is the diffusion coefficient for $^{22}Na^{+}$.
The value used is for self diffusion in dilute solutions.
= $1.48 \times 10^{-5} cm^2 sec^{-1}$.

$V_1$ is the volume of the $^{22}Na^{+}$ bath.
= 10 ml.

$V_2$ is the volume of the fiber.
= $\pi r^2 h$
= $3.14 \times .075cm \times .075cm \times 3cm$
= $5.3 \times 10^{-2}$ml.

A is the area of the fiber surface involved in the diffusion.

$\beta$ is a constant.

TABLE XXI cont'd

Substituting in equation (1)

$$2.3 \log \frac{24}{28.8} = -\beta\, 30 \times 1.48 \times 10^{-5}$$

$$\beta = \frac{0.184}{30 \times 1.48 \times 10^{-5}}$$

$$\beta = 415$$

$$\beta = \left(\frac{1}{V_1} - \frac{1}{V_2}\right) \frac{A}{h}$$

$$415 = \left(\frac{1}{10} - \frac{1}{5.3 \times 10^{-2}}\right) \frac{A}{.038}$$

$$A = \frac{.038 \times 415}{19}$$

$$A = 0.83 cm^2$$

Surface area of fiber = $2\pi rh$
= $2 \times 3.14 \times .075cm \times 3cm$
= $1.41 cm^2$

Percent of fiber surface area involved in $^{22}Na^+$ influx.

$$= \frac{0.83}{1.41} = 59\%$$

TABLE XXII

A calculation of the time required for the $^{22}Na^{+}$ concentration at the fiber center (C) to equal half the $^{22}Na^{+}$ concentration at the fiber edge (Co).

Equation $C = Co\ \text{erfc}\ \frac{x}{2\sqrt{Dt}}$

where C, Co erfc, x, D and t are as defined in Table XXI,

$C = 1/2\ Co$ at $x = .07$cm (average cross section radius)

$C/Co = .5$, the error function of x.

The value of x associated with this value of the error function is obtained from error function tables. It is 0.475.

$$\frac{0.07}{2\sqrt{Dt}} = 0.475$$

$$\sqrt{Dt} = \frac{.07}{2 \times .475}$$

$$= \frac{7 \times 10^{-2}}{9.5 \times 10^{-1}}$$

$$= 7.37 \times 10^{-2}$$

$$Dt = 5.43 \times 10^{-4}$$

$$cm^2/sec \quad t = cm^2$$

$$t = \frac{5.43 \times 10^{-4}}{1.48 \times 10^{-5}}$$

$$= 3.67 \times 10^{1} \text{ seconds}$$

$$= 6.11 \text{ minutes.}$$

# CHAPTER V

## Influx of $^{22}Na^{+}$

### Introduction

The long term radioautographic study revealed two compartments. An initial rapid compartment was identified as the extracellular space. The more slowly exchanging compartment representing myoplasmic exchange of $^{22}Na^{+}$ was still exchanging when the experiment was terminated. Unfortunately the graph derived from the radioautographs did not allow calculation of the amount of $^{22}Na^{+}$ in each compartment. To determine this and verify the radioautographic plot an influx experiment was performed utilizing short time intervals.

### Methods

The total time period for influx was 90 minutes. Twenty fibers were dissected but left with their baseplate attachments intact. These fibers and baseplate were submerged in 30 ml of $^{22}Na^{+}$ labelled Ringers solution of activity 2µc/ml. At 5, 10, 20, 40 and 90 minutes four fibers were cut from the baseplate, removed from the bathing solution, rinsed for thirty seconds in isotonic sucrose solution, gently blotted and placed in a preweighed stoppered bottle. The wet weight of these fibers was determined and they were left to dry for 12 - 18 hours. After determination of the dry weight, fibers were digested in nitric acid for 12 - 18 hours, neutralized with ammonia and diluted up to 10 ml.

Half of this solution was used for counting and half was used for sodium analysis (Unicam S.P.900 flame spectrophotometer). Sample blanks were analyzed with each group of fibers to correct for sodium contamination from solutions and from pyrex weighing bottles.

Sample counting was performed on a Nuclear Chicago automatic gamma well counting system (Model 958). A single channel gamma radiation analyzer (Model 8725) measured gamma radiation over a 0.3MEV range centered at 1.28MEV, the principal peak of $^{22}Na^{+}$. Background correction was made for all samples and care was taken to ensure constant sample geometry.

Results

Table XXIII gives sample influx data for a barnacle and Table XXIV shows the specific activity of the bath. Table XXV shows the specific activities of fibers and the percent labelling that had occurred at various times. No correction for the extracellular space was made since none was made in the radioautographic study. This data was plotted semilogarithmically against time in Figure 8. This graph shows the influx of $^{22}Na^{+}$ into the fiber was clearly divisible into two phases. The half time of loading for the initial rapid phase was six minutes. The size of this first compartment was estimated by extrapolating the portion of the curve for the slow compartment to t = 0. This initial rapid compartment contained 44% of total fiber sodium.

The more slowly exchanging compartment had a rate constant of $5.6 \times 10^{-3}$/minute. This compartment was still exchanging when the experiment was terminated at 90 minutes. At this time 70% of total fiber sodium had exchanged.

Discussion

The initial rapidly exchanging compartment with half time of six minutes and containing 44% of total fiber sodium represents the extracellular space. McLaughlin and Hinke (26) concluded the extracellular space of an average fiber contained 0.030moles/kg $H_2O$ sodium (43% of total fiber sodium), so good agreement exists for the sodium content of the extracellular space. The half time determined for this compartment lies midway between the half time for the rapidly exchanging compartment detected in the radioautographic study (10 minutes) and the half time for sodium washout of the extracellular space into sodium free sucrose Ringers (3 minutes) as detected by Hinke (68). The lower value of Hinke can be explained on the basis of the half minute sucrose wash prior to ion analysis removing sodium and making the half time shorter than in reality. For influx studies the opposite effect occurs. After an influx of five minutes a half minute sucrose wash tends to decrease the amount of labelled sodium in the fiber and make the half time of loading of the extracellular space longer than in reality. The radioautographic study had fewer experimental points to allow sharp separation of the slow and fast compartments

resulting in a longer estimation of half time.

The more slowly exchanging compartment represents sodium exchange with the myoplasm. The rate constant for this compartment ($5.6 \times 10^{-3}$/minute) is in good agreement with the rate constant for myoplasmic exchange calculated by Allen and Hinke (31) ($8.45 \times 10^{-3}$/minute). The same authors concluded 50% of the myoplasmic sodium had exchanged at 90 minutes. McLaughlin and Hinke (26) have stated in the average fiber the extracellular space has 43% of total fiber sodium (0.03 moles/kg $H_2O$). If one assumes the extracellular space is fully loaded at twenty minutes, the data of Allen and Hinke (31) would predict 72% of total fiber sodium exchanged at 90 minutes. When the experiment was terminated at 90 minutes, 71% of sodium had exchanged.

In making a comparison of the influx curve (Figure 8) with the curve obtained by quantitative radioautography (Figure 6) the following should be noted. Both curves reveal a fast and slow compartment. The calculated half times for the initial extracellular space compartment are similar. Both studies demonstrate the extracellular space contains approximately 50% of fiber sodium which can be mobilized in 20 minutes. The slower myoplasmic component was still exchanging at the termination of both experiments. Absolute comparisons at experimental points cannot be made between curves since the curve obtained by radioautography was proportional to the concentration of radioactivity that was present in the specimens but independent of the

absolute amount. This is due to the fact that the tissue sections for the radioautographs were cut at infinite thickness.

TABLE XXIII

BARNACLE C

Influx data

| Time (Min.) | Fiber No. | % Water | Fiber water Kg x $10^{-5}$ | Sodium Concentration M x $10^{-2}$ | Total Fiber Sodium M x $10^{-7}$ | Counts | Fiber Specific Activity counts/ mole x $10^{+9}$ |
|---|---|---|---|---|---|---|---|
| | 1-C | 75.7 | 3.1 | 7.1 | 22.0 | 3,689 | 1.68 |
| | 2-C | 75.4 | 2.9 | 6.1 | 17.7 | 2,501 | 1.41 |
| 5 | 3-C | 76.2 | 3.0 | 6.2 | 18.6 | 3,181 | 1.71 |
| | 4-C | 78.4 | 3.3 | 12.3 | - | - | - |
| | 1-C | 74.9 | 2.5 | 6.4 | 16.0 | 3,488 | 2.18 |
| | 2-C | 75.5 | 2.9 | 7.4 | 21.5 | 4,356 | 2.03 |
| 10 | 3-C | 75.5 | 2.5 | 6.1 | 15.3 | 3,385 | 2.21 |
| | 4-C | 75.7 | 3.9 | 7.1 | 27.7 | 5,525 | 1.99 |
| | 1-C | 74.8 | 2.5 | 7.2 | 18.0 | 3,724 | 2.07 |
| | 2-C | 76.4 | 3.6 | 7.1 | 25.6 | 7,654 | 2.99 |
| 20 | 3-C | 75.5 | 2.4 | 8.5 | 20.4 | 4,258 | 2.09 |
| | 4-C | 75.5 | 2.8 | 6.2 | 17.4 | 4,302 | 2.47 |
| | 1-C | 75.7 | 2.2 | 8.4 | 18.5 | 5,661 | 3.06 |
| | 2-C | 74.8 | 2.9 | 7.1 | 20.6 | 4,933 | 2.39 |
| 40 | 3-C | 75.4 | 2.9 | 6.3 | 18.3 | 5,196 | 2.84 |
| | 4-C | 75.2 | 2.5 | 9.9 | 24.8 | 6,746 | 2.72 |
| | 1-C | 75.4 | 2.6 | 6.6 | 17.2 | 5,258 | 3.06 |
| | 2-C | 74.2 | 1.8 | 6.0 | 10.8 | 4,012 | 3.71 |
| 90 | 3-C | 76.3 | 3.9 | 7.1 | 27.7 | 5,100 | 2.66 |
| | 4-C | 69.3 | 2.1 | 11.6 | - | - | - |

TABLE XXIV

Calculation of Bath Specific Activity

| | |
|---|---|
| Counts from 1 ml bath sample | $21.1743 \times 10^5$ |
| Sodium concentration of sample | $0.450 M/_{liter}$ |
| Sodium content of sample | $4.5 \times 10^{-4}$ M |
| Specific activity of bath | $\frac{21.1743 \times 10^5}{4.5 \times 10^{-4}}$ |
| | $= 4.71 \times 10^9$ counts/mole |

TABLE XXV

Influx Analysis

| Time (Mins.) | Fiber No. | Fiber Specific Activity (Counts/ Mole. x $10^9$) | Bath Specific Activity (Counts/ Mole. x $10^9$) | % Labelling |
|---|---|---|---|---|
| | 1-A | 1.77 | | 37.6 |
| | 2-A | 1.32 | | 28.0 |
| | 3-A | 1.36 | | 28.9 |
| | 4-A | 0.82 | | 17.4 |
| 5 | 1-B | 1.12 | 4.71 | 23.9 |
| | 2-B | 1.62 | | 34.5 |
| | 3-B | 1.79 | | 38.0 |
| | 1-C | 1.68 | | 35.6 |
| | 2-C | 1.41 | | 30.0 |
| | 3-C | 1.71 | | 37.0 |
| Mean and Standard Error | | | | 31.1 ± 2.0 |
| | 1-A | 2.39 | | 50.8 |
| | 2-A | 2.51 | | 53.3 |
| | 3-A | 2.03 | | 43.1 |
| | 4-A | 2.09 | | 44.4 |
| | 1-B | 2.52 | | 53.5 |
| 10 | 2-B | 2.19 | 4.71 | 46.6 |
| | 3-B | 1.99 | | 42.4 |
| | 4-B | 1.81 | | 38.3 |
| | 1-C | 2.18 | | 46.3 |
| | 2-C | 2.03 | | 43.1 |
| | 3-C | 2.21 | | 47.0 |
| | 4-C | 1.99 | | 42.4 |
| Mean and Standard Error | | | | 45.9 ± 1.3 |

TABLE XXV cont'd

Influx Analysis

| Time (Mins.) | Fiber No. | Fiber Specific Activity (Counts/ Mole. x $10^9$ | Bath Specific Activity (Counts/ Mole. x $10^9$ | % Labelling |
|---|---|---|---|---|
| | 1-A | 1.94 | | 41.3 |
| | 2-A | 2.96 | | 63.0 |
| | 1-B | 3.04 | | 64.6 |
| | 2-B | 2.15 | | 45.8 |
| 20 | 3-B | 1.79 | 4.71 | 38.0 |
| | 4-B | 2.85 | | 60.5 |
| | 1-C | 2.07 | | 44.0 |
| | 2-C | 2.99 | | 63.5 |
| | 3-C | 2.09 | | 44.4 |
| | 4-C | 2.47 | | 52.5 |
| Mean and Standard Error | | | | 51.8 ± 3.1 |
| | 1-A | 3.20 | | 68.1 |
| | 2-A | 2.75 | | 58.5 |
| | 3-A | 2.89 | | 61.6 |
| | 1-B | 2.92 | | 62.0 |
| 40 | 2-B | 2.66 | 4.71 | 56.7 |
| | 3-B | 2.73 | | 57.9 |
| | 1-C | 3.06 | | 65.0 |
| | 2-C | 2.39 | | 50.9 |
| | 3-C | 2.84 | | 60.3 |
| | 4-C | 2.72 | | 57.8 |
| Mean and Standard Error | | | | 59.9 ± 1.4 |
| | 1-A | 3.38 | | 71.8 |
| | 2-A | 4.13 | | 87.8 |
| | 3-A | 3.17 | | 67.4 |
| | 1-B | 3.45 | | 73.3 |
| 90 | 2-B | 3.78 | 4.71 | 80.4 |
| | 3-B | 2.89 | | 61.4 |
| | 1-C | 3.06 | | 64.9 |
| | 2-C | 3.71 | | 78.8 |
| | 3-C | 2.66 | | 56.4 |
| Mean and Standard Error | | | | 71.4 ± 3.1 |

Figure 8

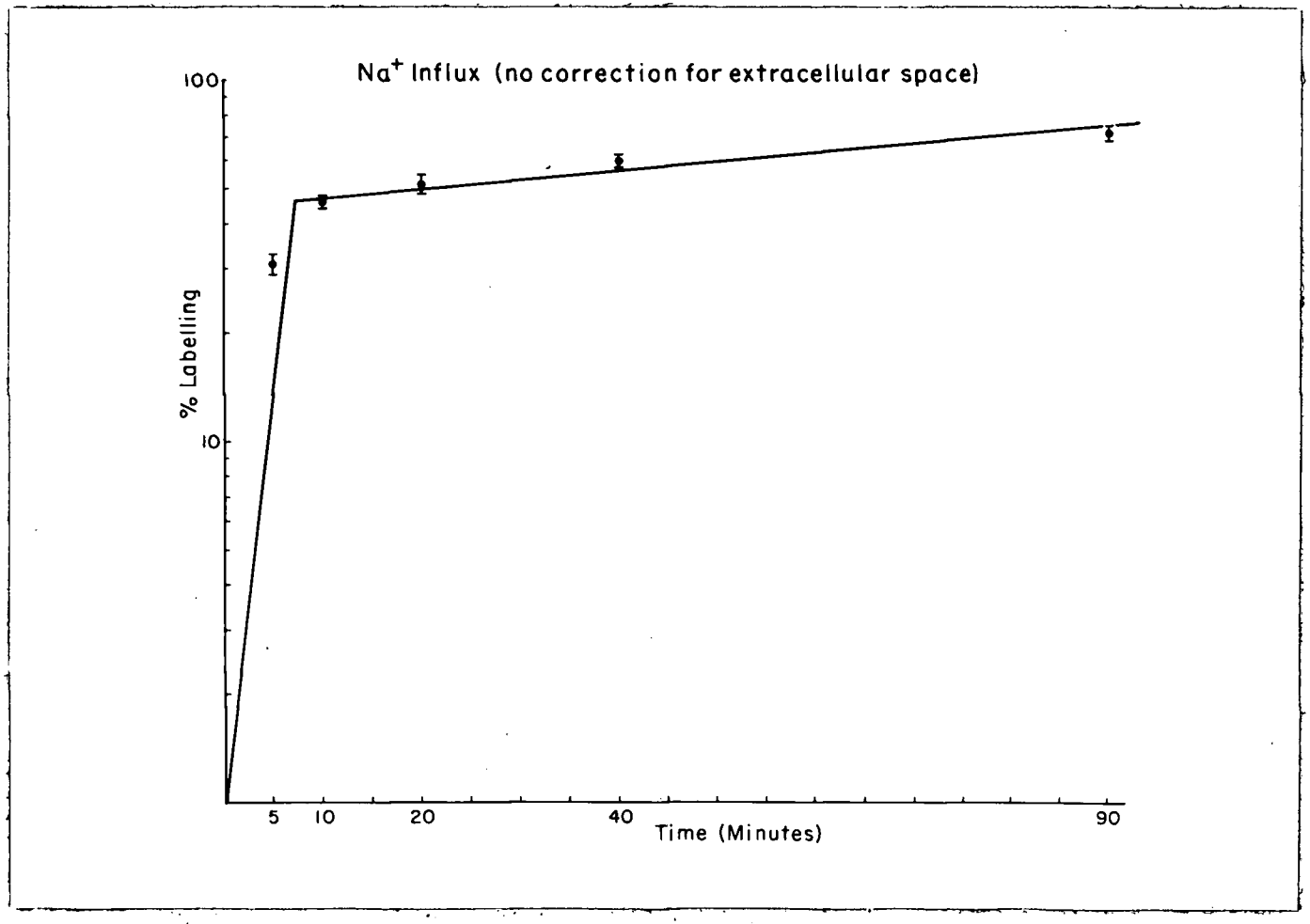
Na+ Influx (no correction for extracellular space)
100
10
% Labelling
5
10
20
40
90
Time (Minutes)

# CHAPTER VI

## General Conclusion

A useful technique for the radioautography of soluble substances was developed. This technique was simpler than many reported in the literature. The resolution achieved with the technique (15 - 17.5μ) was comparable to that reported for $^{22}Na^{+}$ with other types of tissue. These low resolution values imply no significant translocation of the label occurred throughout the technique. The background levels were equivalent to the values of Appleton (61) for the same isotope and emulsion. The efficiency of these radioautographs compared favourably with the theoretical efficiency for the particular emulsion, isotope and tissue utilized.

Useful information on the size and complexity of the extracellular space of a single muscle fiber from the giant barnacle was obtained. The extracellular space (cleft and tubular system) is more extensive than has been reported. The light photomicrographs revealed no part of the myoplasm was more than 2 - 3μ from a 0.3μ cleft. The electron microscopic photographs indicated no part of the myoplasm was more than 1 - 2μ from a triad or diad contact of a tubule with the sarcoplasmic reticulum. These tubules were patent up to the diad (and triad) as revealed by ferritin and horse radish peroxidase uptake studies. The final picture of the cleft system was an invagination of the plasma membrane, dividing extensively in three dimensions and reducing in size down to

T tubules. The latter make contact with the sarcoplasmic reticulum to form both diad and triad junctions. The tubular system is sufficiently extensive so that no part of the myoplasm is more than 2μ from extracellular space.

Valuable information on $^{22}Na^{+}$ entry into the extracellular space was provided by the short term radioautographic study. The path of entry for $^{22}Na^{+}$ is the cleft system which theoretically occupies over 50% of the fiber surface area. The radius of the fiber is a reasonable approximation of the $^{22}Na^{+}$ diffusion pathway. The rate of diffusion of $^{22}Na^{+}$ along this pathway is as rapid in the extracellular space as in dilute solutions. The time required for the $^{22}Na^{+}$ concentration of the fiber center to reach half the concentration of the fiber edge by diffusion along this pathway is approximately six minutes.

The sucrose rinse data provided extra information on the complexity of the extracellular space. The sucrose rinse washed at least half the extracellular $^{22}Na^{+}$ from the 1.5 minute fibers. This $^{22}Na^{+}$ was thought to be washed from the larger clefts. It was postulated that the agitation of the fiber which accompanied the rinse destroyed whatever $^{22}Na^{+}$ gradient the rinse created in the fiber. The $^{22}Na^{+}$ left in the smaller terminal clefts following the rinse would explain the reduced but homogeneous grain distribution of the 1.5 minute fibers with sucrose rinse. The fine terminal clefts involved may also include the T tubules. The loading of the extracellular space in the long term

radioautographic study reflected increasing $^{22}Na^{+}$ entry into these smaller clefts inaccessible to the sucrose rinse.

The fine divisions of the cleft system prevented consistent radioautographic visualization of discrete clefts. The distance from the termination of the clefts to the center of the myoplasm (1 - 2μ) was much less than the resolution of the technique (15 - 17.5μ). Therefore, grains over the myoplasm caused by isotope present in the clefts resulted in a homogeneous distribution of grains over myoplasm and cleft. The use of a lower energy isotope would not have helped appreciably (e.g. resolutions obtained with tritium are in the vicinity of 2 - 4μ). Radioautography at the electron microscope level is required to visualize the clefts consistently as discretely labelled structures.

The sodium content of the extracellular space was demonstrated by both the long term radioautographic study and the conventional influx study. Both techniques revealed that the extracellular space contained approximately half the fiber sodium. The half time for exchange of this $Na^{+}$ compartment was 6 - 10 minutes. Both studies also detected the same myoplasmic compartment which was still exchanging when the experiments were terminated. The calculated rate constant for myoplasmic exchange was in good agreement with the value of Allen and Hinke (31). This myoplasmic exchange is intimately related to the extracellular space. The myoplasmic exchange probably commences immediately when $^{22}Na$ enters the cleft system and it probably makes use

of the full area of the cleft surface. This myoplasmic loading is masked by the filling of the extracellular space and does not become apparent until the latter is saturated (20 minutes).

From these studies emerges a more comprehensive picture of the extracellular space as a pathway for diffusion. A study of the morphology of the extracellular space reveals an extensive cleft system with diffuse ramifications penetrating within 1 - 2$\mu$ of the myoplasm. This is the morphological pathway for diffusion. The data from the short term radioautographic study of $^{22}Na^{+}$ influx gave a picture of the physiological pathway for diffusion. The path of entry for $^{22}Na^{+}$ is the cleft system which theoretically occupies over 50% of the fiber surface area. The radius of the fiber is an approximation of the length of the pathway. Diffusion of $^{22}Na^{+}$ along the length of the pathway is as rapid as self-diffusion of $^{22}Na^{+}$ in dilute solutions.

The literature review summarized evidence for a heterogeneous sodium distribution in muscle. Perhaps the extracellular space is the most important single $Na^{+}$ compartment of the single muscle since it contains over half the fiber sodium at a concentration of 10 times the myoplasm in only 5 - 6% of fiber volume. In experiments reported here it was concluded that the sucrose rinse removed half of the $^{22}Na^{+}$ from the extracellular space. This is in good agreement with data obtained by Hinke (67). However, McLaughlin and Hinke's (26) calculation of the sodium content of the

extracellular space (43% of total fiber sodium) was based on fibers which had a sucrose rinse. This implies the extracellular space before the 0.5 minute sucrose rinse contains about 60% of the total fiber sodium. These conclusions correlate well with the work of Shaw (33) on Carcinus. He found over 70% of the fiber sodium was in an extrasarcoplasmic region and exchanged rapidly. The experiments reported here provide no evidence as to the nature or location of the "bound" fraction of sodium in Balanus.

With this knowledge of the extracellular space, it is apparent that microinjections or flux studies which do not allow for this compartment could be erroneous. Bunch and Kallsen (69) in a recent paper concluded the diffusion rates of water, urea and glycerol were similar for barnacle myoplasm and dilute solutions. Fibers were coated with oil and the base plate rock was removed. This cut end of the fiber was immersed in the isotope bath.

Allen (40) has shown that oil does not effectively enter the extracellular space. Thus, this procedure exposes both myoplasm and extracellular space to the tracer bath. No separate consideration was made of the extracellular space. Therefore, this experiment assumes diffusion in both the extracellular space and the myoplasm is equivalent to diffusion in dilute solutions, although the authors do not state this.

In experiments reported here it was concluded that the rate of diffusion of $^{22}Na^{+}$ in the extracellular space was equivalent to the rate of self diffusion in dilute solutions. The same should be true of larger non ionic molecules. Thus, failure to consider the extracellular space allows no clear conclusion of the rate of myoplasmic diffusion to be made.

In another paper, Bunch and Edwards (70) examined the efflux of glycerol, urea, ASA and DMSO from barnacle muscle fibers following microinjection. The label was injected as a 5µl bolus through a 1300µ needle. A needle this size would puncture both the extracellular space and the myoplasm.

Bunch compared the course of efflux from the fiber to the efflux that would be expected from an idealized cylinder. He concluded the fiber membrane exerted a retarding effect on the diffusion of DMSO. No compensation for the extracellular space was made. For label to diffuse out of the myoplasm it would probably cross at least one cleft. Thus, the label may leave the fiber by diffusing from the myoplasm adjacent to the fiber periphery or by diffusing out along the extracellular space pathway. Thus, Bunch and Edwards attributed part of the retarding effect on DMSO to the membrane when it may be due to the extracellular space.

# BIBLIOGRAPHY


1. J. A. M. Hinke. Nature. 184, 1257 (1959).
2. S. G. A. McLaughlin and J. A. M. Hinke. Can. J. of Physiol. and Pharm. 44, 837 (1966).
3. A. A. Lev. Nature, 201, 1132 (1964).
4. J. D. Robertson. J. Exp. Biol. 38, 707 (1961).
5. F. W. Cope. J. Gen. Physiol. 50, 1353 (1967).
6. E. J. Conway. Symp. Soc. Exp. Biol. 8, 297 (1954).
7. E. J. Conway and M. J. Carey. J. Physiol. (London) 125, 232 (1954).
8. E. J. Harris. J. Physiol. 166, 87 (1963).
9. P. B. Dunham and H. Gainer. Biochimica et Biophysica Acta. 150, 488 (1968).
10. H. E. Huxley. Nature, 202, 1067 (1964).
11. S. Page. J. Physiol. 10, 175 (1964).
12. G. Falk and P. Flatt. Proc. Roy. Soc. London. 160, 69 (1969).
13. R. S. Eisenberg and P. W. Gage. Science. 158, 1701 (1967).
14. J. A. Zadunaisky. J. Cell. Biol. 31, C11 (1966).
15. L. D. Peachey. J. Cell Biol. 25, 209 (1965).
16. R. I. Birks and D. F. Davey. J. Physiol. 202, 171 (1969).
17. R. I. Birks. In Muscle. Edited by P. W. Daniel, E. E. Kay and C. M. Monckton, Permagon Press Inc., Oxford. (1965).
18. E. Herlihy, E. J. Conway and M. G. Harrington. Biochem. J. 103, 46 p. (1967).
19. R. D. Keynes and R. A. Steinhardt. J. Physiol. 198, 551 (1968).
20. F. W. Cope. Bull. of Math. Biophy. 29, 691 (1967).
21. W. Hasselbach. Ann. N. Y. Acad. of Sci. 137, 1401 (1966).

22. J. A. M. Hinke. In Experiments in Physiology and Biochemistry. Edited by G. A. Kerkut. Academic Press Inc., New York and London. 1969.

23. A. Szent-Györgyi. In Chemistry of Muscular Contraction, Academic Press Inc., New York. 1951.

24. M. S. Lewis and H. A. Saroff. J. Am. Chem. Soc. 79, 2112 (1957).

25. W. O. Fenn. Proc. Soc. Exptl. Biol. Med. 96, 783 (1957).

26. S. G. A. McLaughlin and J. A. M. Hinke. Can. J. of Physiol. and Pharm. 46, 247 (1968).

27. S. Itoh and I. L. Schwartz. Am. J. Physiol. 188, 490 (1957).

28. I. A. Utina and A. L. Byzlov. Biofisika. 10, 1087 (1965).

29. R. E. Thiers, E. S. Reynolds and B. L. Vallee. J. Biol. Chem. 235, 2130 (1960).

30. H. Nora, M. Jarwa, W. C. Alfrey and A. E. Mirsky. Proc. U. S. Nat. Acad. Sci. 48, 583 (1962).

31. R. Allen and J. A. M. Hinke. In publication.

32. J. A. M. Hinke and S. G. A. McLaughlin. Can. J. of Physiol. and Pharm. 45, 655 (1967).

33. J. Shaw. J. Exp. Biol. 35, 902 (1958).

34. P. C. Caldwell. Physiol. Rev. 48, 15 (1968).

35. G. Hoyle and T. Smith. Science, 139, 49 (1963).

36. G. Hoyle and T. Smith. Comp. Biochem. Physiol. 10, 291 (1963).

37. A. Selverston. Am. Zoologist. 7, 515 (1967).

38. G. Hoyle. Ann. Rev. of Physiol. 31, 1019 (1969).

39. A. Spira. Personal communication.

40. R. Allen. Personal communication.

41. W. Bloom and D. W. Fawcett. In A Text of Histology. W. B. Saunders, New York. 1968.

42. A. W. Rogers. Personal communication.

43. S. R. Pelc. Biochem. J. 85, 189 (1962).

44. R. H. Herz. Lab. Invest. 8, 71 (1959).

45. R. W. Hendler. Science, 130, 772 (1959).

46. A. W. Rogers. In Techniques of Radioautography. Elsenier Publishing Co., New York. 1967.

47. W. E. Stumpf and L. J. Roth. J. Histo. Cytochem. 14, 274 (1966).

48. E. J. Kaminski. J. Stain Technol. 30, 139 (1955).

49. R. W. Merriam. J. Histochem. Cytochem. 5, 43 (1957).

50. T. C. Appleton. J. of Cell Sci. 4, 265 (1969).

51. B. F. Trump, P. J. Goldblatt, C. C. Griffin, V. S. Wavardekar and R. E. Stowell. Lab. Invest. 13, 967 (1964).

52. A. U. Smith. In Biological Effects of Freezing and Supercooling. Arnold Publishing Co. London. 1961.

53. K. R. Wilske and R. Ross. J. Histochem. Cytochem. 13, 38 (1965).

54. S. Ullberg, L. Hammarstrom and L. E. Appelgrew. Exptl. Cell. Res. 37, 608 (1965).

55. L. Rabinow and P. Barry. J. Applied Physiol. 24, 106 (1968).

56. W. B. Kinter, L. Leape and J. J. Cohen. Am. J. Physiol. 199, 931 (1960).

57. W. B. Kinter and T. H. Wilson. J. Cell Biol. 25, 19 (1965).

58. S. B. Horowitz and I. R. Finichel. J. Gen. Physiol. 51, 703 (1968).

59. M. L. Roberts, L. Ciofalo and L. Martin. J. Stain. Technol. 39, 47 (1964).

60. W. E. Stumpf, L. J. Roth and D. A. Brown. J. of Cell Sci. 4, 265 (1969).

61. T. C. Appleton. J. of the Royal Micros. Soc. 83, 277 (1964).

62. T. C. Appleton. J. Histochem. Cytochem. 14, 414 (1966).

63. T. C. Appleton. Personal communication.

64. Z. Darzynkiewicz and J. Komender. J. Histochem. Cytochem. 15, 605 (1967).

65. J. Crank. In The Mathematics of Diffusion. Oxford Press, London. 1964.

66. H. B. Bull. In An Introduction to Physical Biochemistry. F. A. Davis Company, Philadelphia. (1964).

67. J. A. M. Hinke. Personal communication.

68. J. A. M. Hinke. In Glass Microelectrodes. Edited by M. Lavalle, O. F. Schanne and N. C. Hebert. John Wiley and Sons Inc., New York. 1967.

69. W. H. Bunch and G. Kallsen. Science. 164, 1179 (1969).

70. W. H. Bunch and C. Edwards. J. of Physiol. 202, 683 (1969).